

CONFIDENTIAL

Copy

5

RM A55CO8

NACA RM A55CO8



RESEARCH MEMORANDUM

A CORRELATION OF AIRFOIL SECTION DATA WITH THE
AERODYNAMIC LOADS MEASURED ON A 45°
SWEPTBACK WING MODEL AT SUBSONIC
MACH NUMBERS

By Harold J. Walker and William C. Maillard

Ames Aeronautical Laboratory

Moffett Field, Calif.

CLASSIFICATION CHANGED

UNCLASSIFIED

LIBRARY COPY

JUN 1 1955

By authority of *NACA Res. abs. effective*
4 RN-113 Date *3-14-57*
N13 4-4-57 CLASSIFIED DOCUMENT

LANGLEY AERONAUTICAL LABORATORY
LIBRARY, NACA
LANGLEY FIELD, VIRGINIA

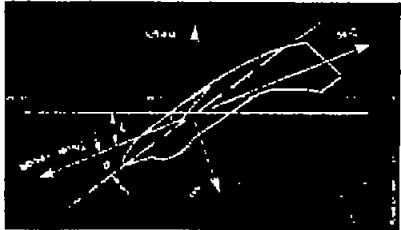
This material contains information affecting the National Defense of the United States within the meaning of the espionage laws, Title 18, U.S.C., Secs. 793 and 794, the transmission or revelation of which in any manner to an unauthorized person is prohibited by law.

NATIONAL ADVISORY COMMITTEE FOR AERONAUTICS

WASHINGTON

May 27, 1955

CONFIDENTIAL



Aircraft performance analysis determines how far, how fast, and how high an airplane can fly, and how much fuel it uses in the process. It also determines the maneuvering performance of an aircraft throughout its flight envelope as well as its takeoff and landing capabilities.

BASIC Aircraft Performance is a system of 8 microcomputer programs that can be used to estimate the performance of aircraft, both on prescribed missions and in maneuvering flight at prescribed conditions. Included are a sophisticated state-of-the-art drag prediction program, a thrust/fuel input and evaluation program, and a simple method of describing complex missions.

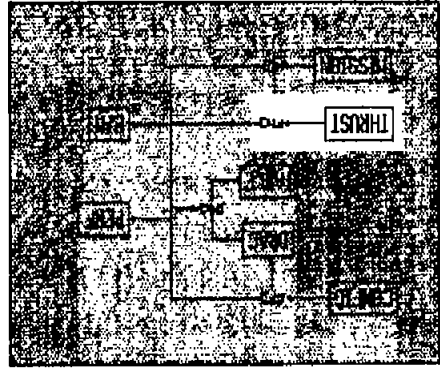


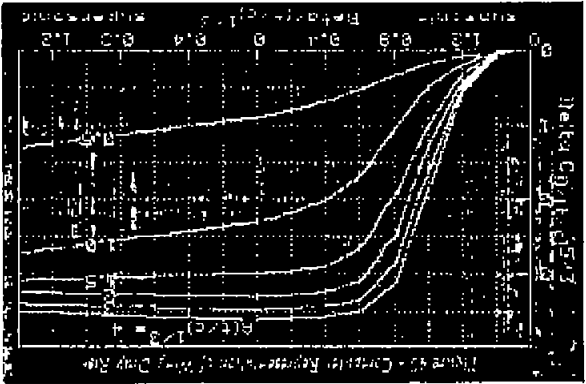
Figure 44 - Logic Flow Chart for Program THRUST

These 8 programs will take you from a three-view drawing of an aircraft with a table of thrust/fuel flow data for the engine to a completed performance envelope and a mission performance description.

They have not been specialized with regard to powerplant type. The use of thrust/fuel flow tables allows the user to calculate the performance of propeller/piston engine, turboprop, turbojet and turbofan aircraft with equivalent ease. The programs provide a logical and simple method for generating the data needed to calculate aircraft performance. The input process has been broken down into several elements, each handled by a separate program so that alternate solutions can be run with little additional

work. You can build up a library of aircraft and engine data files and store them on disk. Then recall and process at any time.

The programs are written in BASIC in a clear, easy to follow style. The package includes a 240 page manual which contains a review of the underlying theory, operating instructions and program descriptions. The disk contains the program source code in BASIC. You can modify or customize the programs for special applications.



$$C_{L\alpha} = \frac{2 \cdot \pi \cdot \rho \cdot V \cdot c \cdot \alpha}{4}$$

BASIC Aircraft Performance will be of interest to aircraft designers, experimental aircraft builders, and teachers of aeronautical and aerospace engineering. They will also be of interest to mechanical engineering educators since they illustrate how fundamental engineering principles combined with modern microcomputers can be combined and used in a practical and exciting application.

BASIC Aircraft Performance was written by Sidney A. Powers, a Project Manager at the Fairchild Republic Company. These programs are the culmination of several years work at Fairchild.

Other Titles of Interest

We have many other microcomputer programs of interest to engineers for structural analysis, computer-aided design, statistics, computer graphics, dynamics and stress analysis. All are in BASIC, accompanied by a detailed user's manual with program source code in BASIC, and written by highly experienced professionals. Call or write for a free catalog.

Custom Programming

Our staff of engineers and programmers can customize any of our programs for your specific applications. Call or write for details.

TO ORDER

Call (617) 934-0445 or -0448 or send this form

Please send **BASIC Aircraft Performance** for the
☐ IBMpc ☐ Apple II, IIe ☐ Send Free Catalog
☐ check enclosed ☐ money order enclosed ☐ charge my credit card

Name _____
 Address _____

VISA/MASTERCARD number _____
 Expiration Date _____

Be sure to include shipping charges (see below for details).
 Massachusetts residents add 5% sales tax.

Shipping: Please add \$4 for the first book and \$2 for each additional book for U.S. shipping in the US; \$12 for the first book and \$6 for each additional book for shipping in the US; \$12 for the first book and \$6 for each additional book for the first book at Canada, Central America and South America; \$3 for each additional book for the first book at Europe; \$6 for each additional book for the first book at Japan; \$12 for the first book and \$6 for each additional book for the first book at elsewhere; \$7 for each additional book. Make shipping free in the US. Add \$3 for air shipping of disks outside US.

Payment: Payment is required on all orders from individuals. Please use check drawn on a US bank in US funds; international money order; VISA or MASTERCARD number with expiration date. Recognized corporations and institutions may use purchase orders. **Bridge Decks are 5% "single-sided, double density. They will run on all IBM PCs including the XT and compatible systems such as the Concept. Your system must be capable of high resolution graphics which means it must be fitted with a Color Graphics Adapter Card. Most compatibles, such as the Compat, do not require this card. Apple Decks are 5% "single-sided, double density. They will run on all Apple II's including the IIe. They will also run on the Apple III in the emulation mode. Systems Requirements:** All packages that do graphics will produce a picture on the screen of your monitor. You may need a separate screen during program (available from your computer dealer) to get hard copy output. IBM's with DOS 2.0 or higher can use the SCREEN/IMP key. With the exception of disks, is allowed within 30 days of purchase. Call or write for return authorization. Shipping must be prepaid.

KERN INTERNATIONAL, INC
 433 Washington Street, PO Box 1029
 Duxbury, MA 02331
 Fold, seal and mail - no postage required

KERN
INTERNATIONAL, INC
433 Washington Street, Po Box 1029
Duxbury, MA 02331 (617)934-0445

BASIC Aircraft Performance

Microcomputer Software
for Aircraft Designers



KERN INTERNATIONAL, INC
433 Washington Street, PO Box 1029
Duxbury, MA 02332 (617)934-0445

Bulk Rate
U.S. Postage
PAID
Duxbury, MA 02331
PERMIT No. 36

#671-0172 HT E
DR JENN-LOUH PAO
VIGYAN RES ASSOCS INC
28 RESEARCH DR
HAMPTON VA 23665



NO POSTAGE
NECESSARY
IF MAILED
IN THE
UNITED STATES

BUSINESS REPLY CARD

FIRST CLASS PERMIT NO. 36 DUXBURY, MA 02331

POSTAGE WILL BE PAID BY ADDRESSEE

KERN INTERNATIONAL, INC
433 Washington Street
PO Box 1029
Duxbury, MA 02331



NATIONAL ADVISORY COMMITTEE FOR AERONAUTICS

RESEARCH MEMORANDUM

A CORRELATION OF AIRFOIL SECTION DATA WITH THE

AERODYNAMIC LOADS MEASURED ON A 45°

SWEEPBACK WING MODEL AT SUBSONIC

MACH NUMBERS

By Harold J. Walker and William C. Maillard

SUMMARY

An investigation has been made of the possibility of correlating airfoil section data with measured pressure distributions over a 45° sweptback wing in the Mach number range from 0.50 to 0.95 at a free-stream Reynolds number of approximately 2 million. The wing had an aspect ratio of 5.5, a taper ratio of 0.53, NACA 64A010 sections normal to the quarter-chord line, and was mounted on a slender body of revolution.

At Mach numbers of 0.85 and below, and for wing normal-force coefficients below the maximum normal-force coefficient for an infinite-aspect-ratio wing yawed 45° to the flow (derived from airfoil section data by simple sweep relations), good correlation was obtained over most of the wing between wing-section and two-dimensional-airfoil pressure distributions. For greater normal-force coefficients lateral boundary-layer flow permitted the inboard wing sections to rise to high maximum section normal-force coefficients. The effectiveness of this lateral boundary-layer flow disappeared towards the tip. For all Mach numbers, the influence of plan-form effects on the pressure distributions limited the quality of the correlation at the 20- and 95-percent-semispan stations. Above a Mach number of about 0.85 the shock waves originating at the juncture of the body and the wing trailing edge spread over the span, preventing further application of two-dimensional data.

The spanwise load distributions at moderate normal-force coefficients could be predicted from span-loading theory for the entire Mach number range of the tests.

INTRODUCTION

It is commonly assumed in the prediction of wing loading that the sections of finite-span wings have essentially the same chordwise load distributions as the corresponding profile in two-dimensional flow, and that the spanwise and chordwise load distributions may be treated independently. The validity of these assumptions has been amply confirmed in applications to unswept wings at low speeds (see, e.g., ref. 1). In reference 2, span-loading theory and experimental two-dimensional section data are shown to be applicable to a limited extent at low speeds in predicting the spanwise and chordwise load distributions on a 45° swept wing of aspect ratio 6. It was thought that this method could be used in the prediction of load distributions at high subsonic speed.

In the present investigation of a model similar in configuration to that of reference 2, comparisons are made between the chordwise pressure distributions for a two-dimensional airfoil section and those for several stations on a 45° sweptback wing to establish limits of Mach number and lift coefficient for which satisfactory correlations can be obtained. The profile of the two-dimensional airfoil section employed and the profile of the swept wing in planes normal to its quarter-chord line are the same. The extent to which present theoretical methods permit the calculation of the effects of finite span on the magnitudes of the section loads is also shown. The variations of the chordwise and spanwise load distributions with lift coefficient and Mach number beyond the limits for good correlation are discussed with regard to the effects of flow separation.

NOTATION

- A aspect ratio
- c local chord parallel to plane of symmetry
- \bar{c} wing mean aerodynamic chord, $\frac{\int_0^1 c^2 d\eta}{\int_0^1 c d\eta}$
- c_{av} average wing chord, $\int_0^1 c d\eta$
- c_l section lift coefficient, $\frac{\text{section lift}}{qc}$

- $c_{l\alpha}$ section lift-curve slope
- c_n section normal-force coefficient, $\frac{\text{normal force}}{qc}$
- $\Delta c_{l\alpha}$ body-induced increment of section lift-curve slope
- c.p. local center of pressure
- C_D drag coefficient, $\frac{\text{drag}}{qS}$
- C_L lift coefficient, $\frac{\text{lift}}{qS}$
- $C_{L\alpha}$ lift-curve slope
- C_m pitching-moment coefficient about quarter-chord point of mean aerodynamic chord, $\frac{\text{pitching moment}}{qSc}$
- C_N normal-force coefficient, $\frac{\text{normal force}}{qS}$
- $C_{N\alpha}$ normal-force-curve slope
- M free-stream Mach number
- p free-stream static pressure
- p_l local static pressure
- P pressure coefficient, $\frac{p_l - p}{q}$
- ΔP lower-surface pressure coefficient minus upper-surface pressure coefficient
- P_{cr} local critical pressure coefficient
- q free-stream dynamic pressure

r	body radius
R	Reynolds number
s	wing semispan
S	wing area
x	longitudinal coordinate
y	lateral coordinate
α	angle of attack
α_z	local section angle of attack, measured parallel to plane of symmetry
α_u	uncorrected angle of attack
η	fraction of semispan, $\frac{y}{s}$
Λ	sweep angle of wing quarter-chord line

Subscript

Λ	yawed flow
-----------	------------

APPARATUS, TESTS, AND CORRECTIONS

The model used in this investigation consisted of a steel sweptback wing mounted on a slender body of revolution as shown in figures 1 and 2. The wing had 45° of sweepback at the quarter-chord line, was untwisted, and had an aspect ratio of 5.5, a taper ratio of 0.53, and NACA 64A010 airfoil sections in planes perpendicular to the quarter-chord line. Five rows of upper- and lower-surface static-pressure orifices (identified in figure 1 by the location of their intersections with the quarter-chord line) were employed to measure the loads on the wing. The three rows of

orifices near the wing mid-semispan were placed perpendicular to the quarter-chord line (as in ref. 2) with the expectation that this region of the wing, in accordance with the theory of sweep (refs. 3 and 4), would behave as a yawed infinite wing.

In order to show more clearly the three-dimensional influence on the loadings near the root and tip, the rows of orifices in these regions were oriented parallel to the free-stream direction.¹ The body contained a row of upper- and lower-surface orifices which extended a short distance beyond the region of the wing-body juncture in the vertical plane of symmetry of the model.

The pressure distribution and the lift, drag, and pitching moment for this swept-wing model were measured in the Ames 16-foot high-speed wind tunnel at Mach numbers from 0.50 to 0.95 and angles of attack from -1° to a maximum of approximately 20° . For these tests the Reynolds numbers based on the mean aerodynamic chord and the free-stream Mach number varied from 1.9 to 2.5 million, as shown in figure 3(a). Also shown in figure 3(a) is a plot of the variation with free-stream Mach number of the Reynolds number based on the component of the free-stream velocity perpendicular to the quarter-chord line and on the chord perpendicular to the quarter-chord line at the intersection of the mean aerodynamic chord and the quarter-chord line.

Two-dimensional pressure-distribution data for use in the correlations were obtained in the Ames 1- by 3-1/2-foot high-speed wind tunnel at Mach numbers from 0.30 to 0.70. These tests were made at three Reynolds numbers to encompass the variation in Reynolds number from root to tip of the tapered swept wing. Two of the models were of constant 3- and 6-inch chord and NACA 64A010 profile. The third model consisted of one panel of the swept wing mounted with its quarter-chord line perpendicular to the free stream. Only the orifices at the 60-percent-semispan station (4.40-inch chord) were used in this test. All three models spanned the 1-foot dimension of the tunnel. The variation of Reynolds number with Mach number for these models is shown in figure 3(b). Examination of the pressure distributions for these three models indicated no significant variation with Reynolds number; hence, only the distributions for the 6-inch-chord model (reported in ref. 5) are used in the comparisons which follow.

All the data presented have been corrected for the effects of wind-tunnel-wall interference by the methods of references 6, 7, and 8.

¹On a yawed infinite wing the orientation of the reference chord along which the orifices are located has no effect on the pressure distribution. Taper, however, introduces a small percentagewise variation in the location of the pressure orifices depending on the reference chord used. This variation has been neglected in the following discussion.

METHOD OF ANALYSIS

In studying wing loadings it is convenient to consider separately the chordwise distribution of load and the magnitude of the section loads. Accordingly, the measured chordwise pressure distributions for the wing are compared at equal normal-force coefficients with the pressure distributions obtained from two-dimensional tests so as to show the correlation between the two- and three-dimensional pressure distributions without involving the accuracy of a span-loading theory. Following this chordwise-loading phase of the analysis, comparisons are made between measured section normal-force-curve slopes and calculated section lift-curve slopes, between measured and calculated span load distributions, and between measured and calculated wing-plus-body lift-curve slopes, to determine the extent to which the magnitudes of the section loads can be calculated.

According to the theory of sweep for the flow over a yawed infinite wing, only the component of the free-stream velocity in a plane perpendicular to the leading edge is effective in producing lift (see ref. 3). Thus, the yawed infinite wing should have a pressure distribution like that of an unyawed infinite wing, provided that the Mach number, Reynolds number, airfoil section, and normal-force coefficient all perpendicular to the leading edge are the same in both cases. The pressure coefficients and normal-force coefficients for a yawed wing, however, are usually based on the free-stream velocity and consequently differ from the corresponding coefficients for an unyawed wing for which the coefficients are based on the velocity perpendicular to the leading edge. Accordingly, in the correlations which follow, two-dimensional pressure distributions (infinite-aspect-ratio, zero-sweep wing) are converted to those expected on a yawed infinite-aspect-ratio wing. The steps employed in this conversion are as follows: First, the section normal-force coefficient for the yawed wing, $c_{n\Lambda}$, is used in the following expression to find the appropriate two-dimensional normal-force coefficient, $c_{n\Lambda=0}$

$$c_{n\Lambda=0} = \frac{c_{n\Lambda}}{\cos^2 \Lambda}$$

Then the two-dimensional pressure coefficients, $P_{\Lambda=0}$, for this normal-force coefficient are determined for a Mach number governed by

$$M_{\Lambda=0} = M_{\Lambda} \cos \Lambda$$

These pressure-coefficient values then must be converted to the reference dynamic pressure for the yawed wing by the relation

$$P_{\Lambda} = P_{\Lambda=0} \cos^2 \Lambda$$

The above expression indicates that a yawed infinite wing should reach a maximum normal-force coefficient given by

$$(c_{n_{\max}})_{\Lambda=0} \cos^2 \Lambda$$

In the subsequent comparisons, pressure distributions for the yawed infinite wing are obtained from two-dimensional-airfoil section data (designated experimental infinite wing) and from theoretical two-dimensional-airfoil pressure distributions (designated theoretical infinite wing). The theoretical pressure distributions were obtained by the method of velocity superposition described in reference 9, using the values from reference 10 and including the Prandtl-Glauert correction for the effect of compressibility.

Even at those stations where the orifices were located streamwise, both the theoretical and experimental two-dimensional pressure distributions were converted to yawed flow before comparison with the values for the finite wing.²

The section lift curves expected for a yawed infinite wing are obtained from two-dimensional section lift curves by suitably adjusting the lift-coefficient and angle-of-attack scales. The lift-coefficient scale is changed to account for the difference between the velocity in the free-stream direction and in the plane normal to the leading edge. The angle-of-attack scale is changed to account for the difference between the angle of attack measured from the free-stream direction and the angle of attack measured from the direction of the component of the free-stream velocity perpendicular to the leading edge. The changes are made by means of the following expressions:

$$\alpha_{\Lambda} = \alpha_{\Lambda=0} \cos \Lambda$$

$$c_{l_{\Lambda}} = c_{l_{\Lambda=0}} \cos^2 \Lambda$$

Finally, in order to account for the effects of finite aspect ratio, the angle-of-attack scales of the section lift curves for the yawed infinite-aspect-ratio wing were stretched slightly so that these lift-curve slopes

²As was pointed out earlier, in the absence of end effects, on a swept wing with only slight taper it makes little difference whether the orifices are located along a streamwise section or along one perpendicular to the quarter-chord line. However, the predicted yawed-infinite-wing pressure distributions obtained from two-dimensional data must be taken for the section, Mach number, and normal-force coefficient perpendicular to the quarter-chord line or they are of little value.

at zero lift matched the local slopes calculated from span-loading theory for the finite-aspect-ratio swept wing. The section lift-curve slopes for the finite-aspect-ratio swept wing, $c_{l\alpha}$, were obtained from the calculated values of span loading coefficient, $(c_l c)/(C_{l\alpha} c_{av})$, and wing-body lift-curve slope, $C_{l\alpha}$, using the following expression:

$$c_{l\alpha} = C_{l\alpha} \left(\frac{c_{av}}{c} \right) \left(\frac{c_l c}{C_{l\alpha} c_{av}} \right)$$

Both the lift-curve slope and the span loading coefficients for the wing alone were calculated by the method of reference 11. Appendixes A and B give the details of how these calculated values were modified to include the effects of the presence of the body and of aeroelasticity on the wing loading.

RESULTS AND DISCUSSION

The discussion of the results of this investigation is divided into three parts. The first part is concerned with the correlation between the distributions of chordwise pressure obtained on the swept-wing model and those expected on an infinite-aspect-ratio wing yawed at the sweep angle of the finite wing and operating at the same section lift coefficient. The second part of the discussion treats the accuracy with which the magnitudes of the section loads can be predicted. This involves predicting the section lift-curve slopes, the spanwise load distribution, and the wing-plus-body lift-curve slope. The third part of the discussion deals with the wing-plus-body lift, drag, and pitching-moment characteristics.

The measured surface pressures are presented in tabular form as pressure coefficients. Table I is an index to these data which are presented in tables II through VIII. The pressure coefficients for the orifices along the body are included in these tables but are not used in the discussion that follows.

Correlation of Chordwise Pressure Distributions

Subcritical Mach number range. - In figure 4 the pressure distributions for five semispan stations of the swept wing are compared with those for a yawed infinite wing at a representative subcritical Mach number of 0.70 and for normal-force coefficients between 0.2 and 0.8. The pressure distributions designated finite wing are those which were measured on the

swept wing, while those designated infinite-wing experiment or infinite-wing theory are those to be expected on a yawed infinite-aspect-ratio wing using, respectively, experimental two-dimensional or theoretical two-dimensional pressure distributions as described previously in the Method of Analysis section. The critical pressure coefficients shown in figure 4 (as well as the calculated stagnation pressure coefficients used to aid in fairing the finite-wing pressure distributions) were obtained from expressions given in reference 4, assuming that the isobars are swept 45° . Also included in figure 4 are sketches of the upper-surface isobars to aid in visualizing the pressure distribution over the wing.

At normal-force coefficients of 0.203 (fig. 4(a)) and 0.363 (fig. 4(b)), the correlation between the pressure distributions for the finite- and infinite-span wings at the 40-, 60-, and 80-percent-semispan stations is good. At the 20-percent-semispan station the loading is shifted slightly rearward with respect to that for the infinite wing, while at the 95-percent-semispan station the loading is shifted forward. These shifts in loading, sometimes referred to as induced camber, are typical of swept wings and have been treated by Kuchemann (ref. 12) and Falkner (ref. 13).

For normal-force coefficients slightly greater than 0.36, the finite-wing pressure distributions begin to show evidence of local flow separation (starting near the leading edge) which prevents further good correlation. However, at the 20-percent-semispan station the measured pressure distributions for normal-force coefficients of 0.495 (fig. 4(c)), 0.564 (fig. 4(d)), and 0.639 (fig. 4(e)) are in fair agreement with theoretical yawed-infinite-wing pressure distributions. The experimental (but not the theoretical) infinite wing reaches a maximum section normal-force coefficient of about 0.38. Thus, there are no experimental infinite-wing pressure distributions available for the swept-wing section normal-force coefficients shown in figures 4(c) through 4(h). Here the experimental infinite-wing pressure distributions shown are for an angle of attack slightly greater than the angle for maximum normal-force coefficient.

The NACA 64A010 airfoil section was described in reference 14 as the type in which the flow separated near the leading edge but reattached farther back, causing partial recovery of the free-stream pressure beyond the point of reattachment. It is expected that on a yawed infinite wing the flow would separate in the same manner, leaving a tube of secondary flow in which the air moves spanwise. At the tip of a finite-aspect-ratio wing this tube of secondary flow would spread out chordwise and spill off the trailing edge of the wing. Such an effect has been frequently observed experimentally on swept wings with relatively sharp leading edges, and is sometimes designated leading-edge-vortex flow (see ref. 15).

The pressure distributions for a normal-force coefficient of 0.495 which is above the experimental infinite wing $c_{l_{max}}$, (fig. 4(c)) indicate

that there is one leading-edge vortex, originating at the inboard sections and sweeping off the wing beyond the 60-percent-semispan station, followed by a second leading-edge vortex beginning near the 60-percent-semispan station. At higher normal-force coefficients there is also evidence of two leading-edge vortices. The possibility of more than one leading-edge vortex on the same wing panel is strongly indicated in boundary-layer studies reported in reference 16.

The pressure distributions for the finite wing at Mach number 0.70 are summarized in figure 5 (including several angles of attack not shown in figure 4). Those designated by N show no evidence of flow separation, those designated S show evidence of extensive flow separation, whereas the undesignated intermediate distributions in general show evidence of leading-edge-vortex-type flow. The heavy solid line is the boundary below which all the local normal-force coefficients are less than the maximum normal-force coefficient for the experimental yawed infinite wing. Beyond this line, of course, experimental two-dimensional loadings cannot be used to predict the loading on the finite wing. However, in some cases, the theoretical infinite-wing pressure distributions give good correlation to higher normal-force coefficients, as was shown in figure 4. The heavy dotted line in figure 5 gives the limit of good correlation (provided that theoretical infinite-wing pressure distributions are used for normal-force coefficients at which the experimental infinite-wing pressure distributions do not exist). It should be noted that the above boundaries indicated by the two heavy lines nearly coincide with the first indications of flow separation at the 40-, 60-, and 80-percent-semispan stations.

Critical Mach number range.- Correlation of the pressure distributions at a Mach number of 0.85 is shown in figure 6 for normal-force coefficients between 0.18 and 0.72. It can be seen that the critical pressure coefficient is attained at a wing normal-force coefficient of about 0.18. The pressure distributions at this Mach number still show the same trends as those at Mach number 0.70. For normal-force coefficients of 0.184 and 0.339, the correlation between the infinite- and finite-span distributions at the 40-, 60-, and 80-percent-semispan stations is good. The isobars and finite-wing pressure distributions at normal-force coefficients of 0.605, 0.691, and 0.724 show evidence of one or two leading-edge vortices. The correlation at the 20- and 95-percent-semispan stations is poor at all the normal-force coefficients shown in figure 6. In terms of pressure distribution, the prime reason for the poor correlation at the 20-percent-semispan station is the presence of a hump in the pressure distribution over the rear portion of the section (not present at the lower Mach numbers). For lift coefficients low enough so that shock waves are not present over the rear part of the chord, the existence of this hump is qualitatively explained by a combination of two effects: first, the variation of the zero-lift pressure distribution with Mach number as discussed by R. T. Jones in reference 17 for sharp-edged airfoils and, second, the rearward shift in the distribution of additional lift due to the increase in induced camber with Mach number.

Since the isobars curve considerably in some areas, the value shown for the critical pressure coefficient is only approximate. At the 20-percent-semispan station for normal-force coefficients of 0.605, 0.691, and 0.724, the sweep of the isobars near the leading edge is greater than 45° ; thus, the critical pressure coefficient should be more negative than shown, whereas over the rear of the chord the reverse is true. Therefore, the upper-surface pressure rises through the critical value twice.

The pressure distributions for Mach number 0.85 are summarized in figure 7 (including several angles of attack not shown in figure 6). It is seen that correlation (broken line) is never good at the 20- and 95-percent-semispan stations, while correlation is good up to the limit of the experimental two-dimensional data (solid line) at the intermediate stations.

Supercritical Mach number range.- Figure 8 shows the isobars and the correlation of the pressure distributions for the extensive supercritical flow at Mach number 0.95. There is no correlation at any of the stations between the pressure distributions for the finite wing and those measured for the infinite wing. The humping of the pressure distribution at the 20-percent-semispan station has increased with Mach number and has spread outboard to approximately the 60-percent-semispan station. The close grouping of the isobars at all the normal-force coefficients shown in figure 8 indicates that a shock extends out from the juncture of the body with the wing trailing edge. The finite-wing pressure distributions shown in figure 8, together with those for several intermediate values of angles of attack, are summarized in figure 9. This summary of pressure distributions at Mach number 0.95 shows no region of good correlation in contrast to the corresponding summaries at Mach numbers 0.70 and 0.85 (figs. 5 and 7).

Limits for good correlation.- The experimental pressure distributions are summarized in figure 10 for each of the five stations on the wing at seven Mach numbers between 0.50 and 0.95 to show the variation with Mach number of the boundaries shown previously in the summary plots for Mach numbers 0.70, 0.85, and 0.95. It is of interest to note in figure 10 that the limit of good prediction, the yawed infinite wing $c_{n_{max}}$, and the first indications of flow separation nearly coincide at the 40-, 60-, and 80-percent-semispan stations. That is, the swept-wing pressure distributions for normal-force coefficients below the maximum for the experimental yawed infinite wing are in good agreement with the two-dimensional distributions except near the root and tips. In general, above this maximum the pressure distributions show evidence of leading-edge vortices. Since the leading-edge vortex is small in extent at the inboard stations, the limit for good correlation (with the theoretical pressure distributions) at the 20-percent-semispan station extends well above the maximum normal-force coefficient for the experimental yawed infinite wing at Mach numbers below 0.80. However, the root and tip effects spread rapidly with

increasing Mach number; hence, the limits for good correlation at the 20- and 95-percent-semispan stations occur at lower Mach numbers than at the intermediate stations.

At the higher subsonic Mach numbers, a shock wave originating at the juncture of the wing trailing edge and the body spreads over most of the wing, thus precluding further use of two-dimensional-airfoil section data. Since this shock wave will be present until the trailing edge becomes supersonic (this occurs at a Mach number of 1.30 for the configuration of the present report), it is expected that its initial appearance marks the Mach number limit at which two-dimensional data can be expected to give good correlation.

Correlation of Magnitudes of Section Loads

The magnitudes of the section loads for the swept wing as given by the experimental section normal-force curves obtained from integrated pressure distributions are shown by the solid line in figure 11. The dashed curves are the section lift curves³ obtained using experimental two-dimensional lift curves and the calculated section lift-curve slopes in the manner described in the Method of Analysis section. The peaks of the dashed lift curves do not match those of the experimental normal-force curves, but the calculated and experimental slopes at zero lift match quite well for Mach numbers below 0.85. For a Mach number of 0.85, the calculated slopes underestimate the measured slopes at zero lift by an amount which is approximately the same for all stations. With increasing Mach number, this difference between calculated and measured slopes becomes greater, but at a given Mach number it remains nearly constant across the span. This means that in terms of wing-body lift coefficient the magnitude of the section loads can be predicted quite well, as will be seen again in the plots of span load distribution. However, the prediction of wing-body lift-curve slope will be poor at the higher Mach numbers.

The maximum lift coefficients of the two-dimensional data are of value in determining the maximum section normal-force coefficients near the tip as well as the limiting normal-force coefficient for good correlation of chordwise pressure distributions. This was shown previously in the present report and in reference 2. The considerable increase in maximum normal-force coefficient toward the wing root is attributed mainly to the lateral flow in the boundary layer both inside and outside of the leading-edge vortex which acts to remove the low-energy air from the inboard wing sections. The influence of this lateral flow decreases from root to tip.

³The measured curves in figure 11 are normal-force curves rather than lift curves. For the angles of attack involved, it is believed that the difference between normal force and lift is insignificant.

In figure 11 the experimental swept-wing section centers of pressure are also compared with the experimental yawed-infinite-wing centers of pressure.⁴ The magnitude of the induced camber effect near the root and tips is indicated by the differences shown in the center-of-pressure curves.

In obtaining the span loading coefficients, the method of reference 11 was used to get the coefficients for the wing alone. The effects of the presence of the body and of elastic deformation on the span loading for the wing were determined by the methods described in Appendixes A and B and are illustrated in figures 12 and 13. The resultant span-loading coefficients are seen in figure 14 to be in good agreement with the experimental results until the loading coefficients at the outer sections begin to diminish with increasing angle of attack. This relative loss in loading at the outer sections occurs at a wing-body lift coefficient slightly greater than the yawed-infinite-wing maximum lift coefficient. It is accompanied by an inboard shift of the lateral center of load. Thus, for this wing at high lift coefficients, theory would underestimate the inboard section loads and overestimate the root bending moment.

Wing-Body Characteristics

The lift, pitching-moment, and drag characteristics for the wing-body model as measured by force tests are shown in figure 15. For all the Mach numbers tested, the lift curves rise to values well above the yawed-infinite-wing maximum lift coefficient of approximately 0.38. The section normal-force curves of figure 11 indicate that the maximum normal-force coefficient for the 95-percent-semispan station is only slightly above that for the yawed infinite wing. The normal-force curves for the inboard sections rise to higher maximums, and have slopes which increase with increasing angle of attack. The increase in slope tends to compensate for the relative loss in lift at the outboard sections, so that the wing-body lift curves of figure 15(a) remain nearly linear to lift coefficients considerably above the maximum for the yawed infinite wing. The bending over of the wing-body lift curves, where shown, is gradual, as would be expected from the slow rate at which the stall progresses inboard with increasing angle of attack.

Calculated lift-curve slopes for the wing-body combination are shown as dashed lines in figure 15(a), and the variation with Mach number of the calculated lift-curve slopes is compared with the experimental values in figure 16. The method of reference 11 was employed to calculate the

⁴These infinite-wing center-of-pressure curves were obtained by adjusting the lift-coefficient scales of these data, using the expression given in the Method of Analysis section.

lift-curve slope for the wing alone. The methods described in Appendixes A and B were utilized to include the effects of wing-body interference and elastic deformation of the wing. For Mach numbers below 0.80, these calculations give a fairly good, although low, estimate of the lift-curve slope. For Mach numbers above 0.85, however, the calculations underestimate the lift-curve slope by an increasingly large amount. This was indicated previously in figure 11, where at any one of the higher Mach numbers the lift-curve slopes for all the sections were underestimated by about the same percentage.

The wing-body pitching-moment curves of figure 15(a), in general, are linear up to the yawed-infinite-wing maximum lift coefficient. Above this lift coefficient, the pitching-moment curves for the three lowest Mach numbers show unstable breaks even though the lift curves are linear to higher lift coefficients. This results because both the increase in normal-force-curve slope with angle of attack at the inboard sections and the approach to the maximum section normal-force coefficient at the outboard sections tend to produce more positive pitching moments, rather than to compensate for each other as in the lift case.

For Mach numbers of 0.85 and over, the unstable break in the pitching-moment curves of figure 15(a) is delayed to a higher value of lift coefficient than for the lower Mach numbers. This behavior may be explained by referring back to figure 11, where the normal-force curves for the 80-percent-semispan station reach higher maximum values for Mach numbers of 0.85 and over than for Mach numbers below 0.85. The abrupt increase in the slopes of the normal-force curves near their maximums for the 80- and 90-percent-semispan stations at the three highest Mach numbers tends to produce the negative shifts seen in the pitching-moment curves.

The measured wing-body drag characteristics are shown by the solid line in figure 15(b). A lower bound for the drag, given by the sum of the measured drag at zero lift and the calculated induced drag for an elliptical span load distribution, is shown by the short dashed line. The long dashed line shows the drag expected in the absence of leading-edge suction (actually in the absence of any chord force). Below the yawed-infinite-wing maximum lift coefficient, about 60 percent of the possible leading-edge suction is realized. Above this lift coefficient, the drag coefficient increases rapidly as expected since this is approximately the lift coefficient at which the first indications of flow separation appear.

CONCLUSIONS

From the foregoing comparisons of the experimental chordwise and spanwise load distributions for the 45° sweptback wing model with those predicted from two-dimensional data and span-loading theory, the following conclusions may be drawn:

1. Airfoil section data are in reasonable agreement with measured chordwise load distributions for lift coefficients below a limiting value approximately equal to the maximum lift coefficient for the yawed infinite-aspect-ratio wing and for Mach numbers at which shock waves from the wing-body juncture do not greatly influence the flow. For the configuration of the present report, these shock waves preclude the use of two-dimensional data for Mach numbers greater than 0.85.

2. End effects limit to some extent the applicability of airfoil section data for sections in the immediate vicinity of the root and tips.

3. For wing lift coefficients above the maximum lift coefficient for the yawed infinite-aspect-ratio wing, a lateral flow in the boundary layer occurs, which relieves the tendency for the flow to separate and greatly increases the lifting capacity of the inboard sections.

4. The distribution of loading along the span for the range of Mach numbers investigated may be predicted with good accuracy for lift coefficients not exceeding the maximum lift coefficient for the yawed infinite-aspect-ratio wing.

Ames Aeronautical Laboratory
National Advisory Committee for Aeronautics
Moffett Field, Calif., Mar. 8, 1955

APPENDIX A

CALCULATION OF EFFECT OF WING-BODY INTERFERENCE

ON THE SPAN LOAD DISTRIBUTION

The effect of the interference between the wing and body on the span load distribution may be calculated to a first approximation by treating independently the effect of the body on the wing loading by the method of reference 18, and the effect of the wing-body combination on the loading over the center section of the wing by the method of Lennertz (ref. 19).

The body is considered to be replaced by an infinitely long cylinder having a radius equal to the average body radius at the wing-body juncture. Increments of loading due to the upwash induced by the body along the wing span are calculated by a modified Falkner method (see ref. 18). Values for these increments, which are additive to the loading coefficients for the wing alone, are shown in figure 12 where the loading increment is represented by the term $(\Delta c_{l_\alpha c})/(c_{av})$. The corresponding increment in wing lift-curve slope (ΔC_{L_α}) is 0.0043 (from mechanical integration of fig. 12).

In calculating the loading over the portion of the wing covered by the body by the method of Lennertz, a uniform distribution of lift across the span is assumed. The ratio of the lift coefficients for the sections within the body c_{l_b} to that for the uniformly loaded sections c_{l_u} is given (for the case of coplanar wing and body axes) by the expression

$$\frac{c_{l_b}}{c_{l_u}} = 1 - \frac{1}{\pi} \tan^{-1} \left[\frac{4(1 - \sigma^2) \sqrt{\sigma^2 - \eta^2}}{1 + \sigma^4 - 2\sigma^2 - 4(\sigma^2 - \eta^2)} \right], \quad -\sigma \leq \eta \leq \sigma \quad (A1)$$

where the symbol σ represents the ratio of the average body radius to the wing semispan. For the present model σ is approximately equal to 0.081, and the ratio of lift coefficient at the wing center section ($\eta = 0$) becomes

$$\frac{c_{l_b}}{c_{l_u}} = 0.900 \quad (A2)$$

The lift-curve slope of the wing corrected for interference effects is related to that for the wing alone by the relation

$$\frac{(C_{L\alpha})_{W+I}}{[(C_{L\alpha})_W + 0.0043]} = 1 - \sigma^2$$

$$= 0.993 \quad (A3)$$

where subscripts W and W+I designate, respectively, values for the wing alone and the wing-plus-interference effects. The right side of the above expression was obtained by integration of equation (A1) over the region of the wing enclosed in the body and the assumption of a uniform load over the remainder of the span. The value 0.0043 appearing in the denominator on the left side of the above expression is the increment of lift-curve slope due to the effect of the upwash of the body on the wing.

The span load distribution corrected for interference effects may then be written in terms of the corresponding quantities for the wing alone as follows:

$$\left(\frac{c_{lc}}{C_{Lcav}}\right)_{W+I} = \frac{(C_{L\alpha})_W}{(C_{L\alpha})_{W+I}} \left(\frac{c_{lc}}{C_{Lcav}}\right)_W + \frac{\left(\frac{\Delta c_{l\alpha}^c}{c_{av}}\right)}{(C_{L\alpha})_{W+I}} \quad \text{for } \eta \neq 0 \quad (A4)$$

$$\left(\frac{c_{lc}}{C_{Lcav}}\right)_{W+I} = 0.900 \frac{(C_{L\alpha})_W}{(C_{L\alpha})_{W+I}} \left(\frac{c_{lc}}{C_{Lcav}}\right)_W + \frac{\left(\frac{\Delta c_{l\alpha}^c}{c_{av}}\right)}{(C_{L\alpha})_{W+I}} \quad \text{for } \eta = 0 \quad (A5)$$

For purposes of this analysis, the loading carried by the fuselage fore and aft of the wing-root region has been ignored.

APPENDIX B

CALCULATION OF EFFECT OF ELASTIC DEFORMATION ON
THE SPAN LOAD DISTRIBUTION

It is assumed that the wing is deformed by bending only (the torsional stiffness of the wing being relatively large), and that the ratio of bending moment to moment of inertia of any wing section is nearly constant across the span. The deflection curve is then parabolic and the twist varies linearly across the span (see ref. 20).

As shown in reference 20, the change in angle of attack of any streamwise section due to the wing loading is given by

$$\epsilon = \frac{-M'y}{EI} \tan \Lambda_f \quad (B1)$$

where

- ϵ change in local angle of attack due to aeroelasticity
- M' bending moment at any point on the flexural axis
- I moment of inertia of any section normal to the flexural axis
- E modulus of elasticity of wing material
- Λ_f sweep angle of flexural axis
- y spanwise distance perpendicular to wing root section

The term $\frac{M'}{EI}$ (assumed to be a constant), when calculated for the root section, gives

$$\frac{M'}{EI} = \frac{M_r}{EI_r} = \frac{\frac{1}{2} q S C_{L_f}}{EI_r \cos \Lambda_f} \quad (B2)$$

where

- M_r bending moment at root section
- I_r moment of inertia of root section

q dynamic pressure

S wing area

\bar{y} perpendicular distance from wing root section to spanwise center of loading

Substituting equation (B2) in (B1) and replacing $\frac{y}{S}$ and $\frac{\bar{y}}{S}$ by η and $\bar{\eta}$ gives

$$\epsilon = \frac{-q \frac{S}{2} C_L \bar{\eta} s^2 \tan \Lambda_f}{EI_R \cos \Lambda_f} \eta \quad (B3)$$

For the wing of the present investigation

$$\begin{aligned} S &= 2.02 \text{ ft}^2 \\ s &= 1.667 \text{ ft} \\ EI_R &= 25,100 \text{ lb-ft}^2 \text{ (from static load tests)} \\ \bar{\eta} &= 0.462 \text{ (from ref. 11)} \\ \tan \Lambda_f &= 0.9657 \\ \cos \Lambda_f &= 0.7193 \end{aligned}$$

Thus equation (B3) becomes

$$\frac{\epsilon}{C_L} = - \frac{3.96}{1000} q \eta \quad (\text{deg}) \quad (B4)$$

where q is in pounds per square foot.

The effect of bending on the span load distribution of the wing (corrected for interference effects, Appendix A) may be determined by considering the change in loading due to elastic twist as a basic-type loading (ref. 11) to be superimposed on the additional loading for the rigid wing. Thus,

$$\left(\frac{c_{lc}}{C_{Lcav}} \right)_E = \left(\frac{c_{lc}}{C_{Lcav}} \right)_R + \left(\frac{c_{lb}}{e_t c_{av}} \right) \frac{\epsilon_t}{C_L} \quad (B5)$$

where $(c_{lb})/(e_t c_{av})$ represents the basic load distribution per unit twist, and e_t the twist of tip section ($\eta = 1$) mean line relative to wing root.

Subscripts E and R refer to the elastic and rigid wing values, respectively. Substitution for ϵ_t/C_L from equation (B4) allows equation (B5) to be written

$$\left(\frac{c_{lc}}{C_{Lcav}}\right)_E = \left(\frac{c_{lc}}{C_{Lcav}}\right)_R \left[1 - \frac{3.96}{1000} q \frac{\left(\frac{c_{lb}c}{\epsilon_t c_{av}}\right)}{\left(\frac{c_{lc}}{C_{Lcav}}\right)_R} \right] \quad (B6)$$

The terms $(c_{lb}c)/(\epsilon_t c_{av})$ and $[(c_{lc})/(C_{Lcav})]_R$ may be obtained from reference 11 for the particular wing plan form and assumed twist distribution (wing-body interference effects neglected). Values of these parameters for the present model are listed in the following table:

η	$\left(\frac{c_{lc}}{C_{Lcav}}\right)_R$	$\left(\frac{c_{lb}c}{\epsilon_t c_{av}}\right)$	$\left[1 - \frac{3.96}{1000} q \frac{\left(\frac{c_{lb}c}{\epsilon_t c_{av}}\right)}{\left(\frac{c_{lc}}{C_{Lcav}}\right)_R} \right]$
0	1.045	-0.0168	$1 + 0.0637 (q/1000)$
.1	1.062	-.0155	$1 + .0578 (q/1000)$
.2	1.100	-.0123	$1 + .0443 (q/1000)$
.4	1.133	-.0035	$1 + .0122 (q/1000)$
.6	1.090	.0060	$1 - .0218 (q/1000)$
.8	.925	.0129	$1 - .0552 (q/1000)$
.95	.540	.0115	$1 - .0843 (q/1000)$
1.0	0	0	1

The effect of elastic deformation on the ratio of wing-section angle of attack to body angle of attack at various Mach numbers and on the span load distribution at a Mach number of 0.95 is shown in figure 13.

The over-all reduction in lift-curve slope due to bending may be calculated in terms of the lift-curve slope of the rigid wing, and the change in angle of attack of the root section due to twist. Thus,

$$(C_L)_E = (C_{L\alpha})_R (\alpha - \Delta\alpha)$$

~~CONFIDENTIAL~~

or

$$(C_{L\alpha})_E = (C_{L\alpha})_R \left(1 - \frac{\Delta\alpha}{\alpha}\right) \quad (B7)$$

where

α angle of attack of root-section mean line for elastic wing corresponding to $(C_L)_E$

$\Delta\alpha$ zero-lift angle of attack of the root-section mean line for the twist distribution corresponding to $(C_L)_E$

The term $\Delta\alpha$ is determined by the method of reference 11 in terms of root-section angle of attack per unit of twist corresponding to the basic-type loading; that is,

$$\Delta\alpha = -\alpha_{r0} \epsilon_t$$

where α_{r0} is the angle of attack of the root-section mean line per unit of twist and ϵ_t is obtained from equation (B4). Hence,

$$\Delta\alpha = \alpha_{r0} \frac{3.96}{1000} q (C_{L\alpha})_R (\alpha - \Delta\alpha)$$

or

$$\frac{\Delta\alpha}{\alpha} = \frac{\alpha_{r0} \frac{3.96}{1000} q (C_{L\alpha})_R}{1 + \alpha_{r0} \frac{3.96}{1000} q (C_{L\alpha})_R}$$

Substitution of this equation in equation (B7) gives

$$(C_{L\alpha})_E = \frac{(C_{L\alpha})_R}{1 + \alpha_{r0} \frac{3.96}{1000} q (C_{L\alpha})_R}$$

where for the 45° swept wing $\alpha_{r0} = 0.385$ degree per degree (ref. 11).

~~CONFIDENTIAL~~

REFERENCES

1. Sivells, James C., and Neely, Robert H.: Method for Calculating Wing Characteristics by Lifting-Line Theory Using Nonlinear Section Lift Data. NACA Rep. 865, 1947.
2. Hunton, Lynn W.: Effects of Finite Span on the Section Characteristics of Two 45° Sweptback Wings of Aspect Ratio 6. NACA TN 3008, 1953. (Formerly NACA RM A52A10)
3. Jones, Robert T.: The Effects of Sweepback on Boundary Layer and Separation. NACA Rep. 884, 1947.
4. Lippisch, A., and Beuschausen, W.: Pressure Distribution Measurements at High Speed and Oblique Incidence of Flow. NACA TM 1115, 1947.
5. Stivers, Louis S., Jr.: Effects of Subsonic Mach Number on the Forces and Pressure Distributions on Four NACA 64A-Series Airfoil Sections at Angles of Attack as High as 28° . NACA TN 3162, 1954. (Formerly NACA RM A53K06)
6. Silverstein, Abe, and White, James Aubrey: Wind Tunnel Interference With Particular Reference to Off-Center Positions of the Wing and to the Downwash at the Tail. NACA Rep. 547, 1935.
7. Herriot, John G.: Blockage Corrections for Three-Dimensional-Flow Closed-Throat Wind Tunnels, With Consideration of the Effect of Compressibility. NACA Rep. 995, 1950. (Formerly NACA RM A7B28)
8. Allen, H. Julian, and Vincenti, Walter G.: Wall Interference in a Two-Dimensional-Flow Wind Tunnel, With Consideration of the Effect of Compressibility. NACA Rep. 782, 1944.
9. Abbott, Ira H., von Doenhoff, Albert E., and Stivers, Louis S., Jr.: Summary of Airfoil Data. NACA Rep. 824, 1945.
10. Loftin, Lawrence K., Jr.: Theoretical and Experimental Data for a Number of NACA 6A-Series Airfoil Sections. NACA Rep. 903, 1948.
11. DeYoung, John, and Harper, Charles W.: Theoretical Symmetric Span Loading at Subsonic Speeds for Wings Having Arbitrary Plan Form. NACA Rep. 921, 1948.
12. Kuchemann, Dietrich: A Simple Method for Calculating the Span and Chordwise Loadings on Thin Wings. Rep. No. Aero. 2392, British R.A.E., Aug. 1950.

13. Falkner, V. M.: Comparison of the Simple Calculated Characteristics of Four Sweptback Wings. Rep. No. 7446, British A.R.C., Feb. 9, 1944.
14. Peterson, Robert F.: The Boundary-Layer and Stalling Characteristics of the NACA 64A010 Airfoil Section. NACA TN 2235, 1950.
15. Furlong, G. Chester, and McHugh, James Gorman: A Summary and Analysis of the Low-Speed Longitudinal Characteristics of Swept Wings at High Reynolds Number. NACA RM L52D16, 1952.
16. Black, Joseph: A Note on the Vortex Patterns in the Boundary Layer Flow of a Sweptback Wing. Jour. of Royal Aero. Soc., April 1952, pp. 279-285.
17. Jones, Robert T.: Subsonic Flow Over Thin Oblique Airfoils at Zero Lift. NACA Rep. 902, 1948. (Formerly NACA TN 1340)
18. Martina, Albert P.: The Interference Effects of a Body on the Spanwise Load Distributions of Two 45° Swept-Back Wings of Aspect Ratio 8 From Low-Speed Tests at a Reynolds Number of 4×10^6 . NACA RM L51K23, 1952.
19. Durand, William Frederick: Aerodynamic Theory. Vol. IV, 1943, pp. 152-154.
20. Frick, Charles W., and Chubb, Robert S.: The Longitudinal Stability of Elastic Swept Wings at Supersonic Speed. Jour. Aero. Sci., vol. 17, Nov. 1950, pp. 691-704.

~~CONFIDENTIAL~~

NACA RM A55C08

TABLE I.- INDEX OF TABULATED PRESSURE COEFFICIENTS

Table no.	M	α range
II	0.50	-1.18° to 19.82°
III	.70	-1.22° to 15.16°
IV	.75	-1.24° to 13.15°
V	.80	-1.13° to 9.98°
VI	.85	-1.25° to 10.09°
VII	.90	-1.30° to 9.15°
VIII	.95	-1.27° to 9.19°

~~CONFIDENTIAL~~

TABLE II.- PRESSURE COEFFICIENTS AT SIX SPANWISE STATIONS; $M = 0.50$
 (a) $\alpha = -1.18^\circ$ to 9.46°

η	Per- cent chord	Upper surface										Lower surface									
		Angle of attack, deg										Angle of attack, deg									
		-1.18	0.89	2.01	3.15	4.20	5.24	6.29	7.33	8.40	9.46	-1.18	0.89	2.01	3.15	4.20	5.24	6.29	7.33	8.40	9.46
0	5.58	0.03	0.01	0	-0.02	-0.02	-0.03	-0.04	-0.06	-0.08	-0.09	0	0.01	0.03	0.04	0.07	0.08	0.08	0.12	0.14	0.15
	26.6	-.01	-.05	-.06	-.08	-.10	-.12	-.14	-.18	-.20	-.23	-.03	-.02	-.02	-.06	-.06	-.08	-.10	-.14	-.16	-.17
	37.2	-.01	-.05	-.06	-.08	-.10	-.12	-.14	-.18	-.20	-.23	-.05	-.03	-.01	-.02	-.07	-.08	-.11	-.13	-.17	-.18
	47.7	-.02	-.06	-.07	-.09	-.12	-.13	-.16	-.20	-.22	-.25	-.06	-.04	0	-.01	-.05	-.06	-.10	-.12	-.16	-.17
	58.2	-.03	-.07	-.10	-.13	-.14	-.15	-.17	-.21	-.23	-.26	-.08	-.06	-.02	-.01	-.03	-.05	-.08	-.09	-.13	-.15
	68.8	-.03	-.08	-.09	-.13	-.14	-.14	-.16	-.20	-.21	-.25	-.09	-.06	-.04	-.01	-.02	-.04	-.06	-.07	-.12	-.13
	79.3	-.05	-.07	-.09	-.12	-.13	-.14	-.15	-.19	-.20	-.23	-.08	-.06	-.03	-.02	-.01	-.04	-.04	-.06	-.10	-.11
	89.3	-.03	-.06	-.07	-.09	-.10	-.10	-.11	-.13	-.15	-.16	-.07	-.06	-.03	-.03	-.01	-.03	-.04	-.04	-.09	-.09
	100.2	-.03	-.06	-.07	-.09	-.10	-.10	-.11	-.13	-.15	-.16	-.06	-.05	-.03	-.02	0	-.03	-.04	-.03	-.08	-.08
	110.9	-.01	-.03	-.03	-.05	-.05	-.05	-.05	-.07	-.07	-.08	-.05	-.04	-.02	-.02	0	-.03	-.04	-.03	-.07	-.08
	121.3	-.02	-.02	-.01	-.04	-.02	-.02	-.01	-.03	-.03	-.04	-.02	-.03	-.01	-.01	-.01	-.03	-.04	-.03	-.07	-.07
	147.8	0	-.02	-.01	0	0	0	0	0	0	0	-.01	-.01	-.01	0	-.02	-.02	-.04	-.01	-.03	-.04
0.20	0	.34	.41	.36	.24	.04	-.16	-.42	-.72	-.90	-.93	-.17	.03	.14	.25	.29	.34	.39	.42	.44	.46
	1.25	.09	-.15	-.37	-.59	-.81	-1.18	-1.66	-2.13	-2.38	-2.40	-.17	.03	.14	.25	.29	.34	.39	.42	.44	.46
	2.5	.06	-.14	-.29	-.48	-.74	-.97	-1.27	-1.68	-1.94	-1.94	-.17	.03	.14	.25	.29	.34	.39	.42	.44	.46
	5	.01	-.13	-.24	-.34	-.43	-.54	-.66	-.75	-.78	-.93	-.18	-.04	.06	.16	.20	.26	.31	.36	.41	.44
	10	-.05	-.14	-.22	-.29	-.36	-.43	-.53	-.57	-.66	-.84	-.16	-.06	.01	.08	.12	.16	.22	.25	.30	.34
	20	-.07	-.15	-.19	-.25	-.30	-.34	-.42	-.45	-.55	-.66	-.18	-.11	-.05	.01	.04	.07	.12	.15	.19	.23
	30	-.12	-.17	-.20	-.23	-.27	-.30	-.34	-.35	-.42	-.47	-.17	-.15	-.12	-.06	-.05	-.04	-.01	.01	.06	.08
	40	-.13	-.17	-.18	-.22	-.24	-.26	-.30	-.31	-.36	-.39	-.17	-.15	-.12	-.06	-.05	-.04	-.03	0	.04	.05
	50	-.10	-.14	-.15	-.17	-.19	-.20	-.24	-.25	-.28	-.31	-.15	-.12	-.10	-.05	-.04	-.03	0	.02	.05	.05
	60	-.06	-.10	-.08	-.11	-.13	-.13	-.16	-.17	-.21	-.23	-.09	-.10	-.06	-.02	-.02	-.01	.01	.02	.04	.05
	70	-.02	-.03	-.03	-.05	-.06	-.06	-.09	-.09	-.12	-.14	-.04	-.04	-.03	-.01	-.01	.01	.01	.01	.03	.04
	80	-.02	-.02	-.04	-.05	-.06	-.06	-.09	-.09	-.12	-.14	-.04	-.04	-.03	-.01	-.01	.01	.01	.01	.03	.04
90	.02	.03	.04	.02	.02	.01	-.01	-.02	-.04	-.04	.02	.01	.02	.03	.02	.02	.02	.03	.04	.05	
0.40	0	.37	.41	.24	.04	-.42	-.82	-1.22	-.95	-1.05	-1.15	-.17	.03	.14	.25	.29	.34	.39	.42	.44	.46
	1.25	.16	-.12	-.37	-.64	-.96	-1.36	-1.84	-1.33	-1.15	-1.24	-.26	-.02	.12	.24	.32	.37	.42	.45	.48	.48
	2.5	.05	-.19	-.39	-.59	-.83	-.93	-1.12	-.90	-.98	-.97	-.26	-.02	.12	.24	.32	.37	.42	.45	.48	.48
	5	-.03	-.18	-.33	-.47	-.59	-.71	-.87	-.89	-.89	-.94	-.22	-.09	.05	.16	.22	.27	.32	.34	.38	.42
	10	-.06	-.17	-.26	-.35	-.45	-.51	-.63	-.63	-.62	-.66	-.20	-.07	-.01	.08	.13	.18	.23	.25	.29	.33
	20	-.12	-.18	-.22	-.27	-.33	-.33	-.39	-.48	-.51	-.54	-.18	-.12	-.05	.01	.05	.08	.11	.14	.18	.22
	30	-.13	-.18	-.22	-.27	-.33	-.33	-.39	-.48	-.51	-.54	-.18	-.12	-.05	.01	.05	.08	.11	.14	.18	.22
	40	-.12	-.15	-.18	-.19	-.23	-.24	-.28	-.26	-.24	-.19	-.18	-.16	-.12	-.06	-.04	-.02	0	.03	.07	.09
	50	-.07	-.12	-.13	-.14	-.17	-.16	-.20	-.18	-.15	-.12	-.10	-.07	-.04	-.04	-.02	-.01	.01	.02	.04	.06
	60	-.06	-.06	-.06	-.07	-.11	-.10	-.13	-.11	-.12	-.11	-.04	-.05	-.05	-.03	-.03	0	.02	.04	.06	.06
	70	-.02	-.02	-.02	-.03	-.06	-.04	-.06	-.06	-.06	-.06	.02	.02	.02	.01	.01	.02	.02	.04	.05	.05
	80	.04	.03	.04	.03	0	-.02	-.01	.02	.01	-.02	.05	.04	.04	.04	.03	.04	.03	.04	.04	.04
0.60	0	.42	.46	.31	.01	-.47	-.99	-1.37	-1.69	-1.14	-1.03	-.17	.03	.14	.25	.29	.34	.39	.42	.44	.46
	1.25	.17	-.11	-.38	-.64	-.96	-1.30	-1.47	-1.21	-1.08	-.94	-.26	-.04	.16	.29	.36	.42	.45	.48	.48	.48
	2.5	.06	-.17	-.38	-.61	-.85	-1.01	-1.21	-1.06	-.87	-.83	-.26	-.04	.16	.29	.36	.42	.45	.48	.48	.48
	5	-.01	-.18	-.36	-.51	-.67	-.73	-.91	-.91	-.82	-.83	-.21	-.02	.08	.18	.25	.30	.34	.38	.40	.42
	10	-.05	-.16	-.28	-.35	-.44	-.53	-.63	-.73	-.74	-.79	-.20	-.06	0	.09	.15	.19	.23	.27	.30	.33
	20	-.07	-.16	-.24	-.27	-.34	-.39	-.46	-.73	-.77	-.82	-.19	-.11	-.05	.03	.06	.09	.12	.16	.19	.21
	30	-.11	-.17	-.23	-.25	-.30	-.34	-.38	-.68	-.78	-.81	-.18	-.12	-.08	-.02	.01	.03	.06	.09	.12	.14
	40	-.10	-.16	-.21	-.22	-.25	-.28	-.31	-.59	-.63	-.65	-.17	-.11	-.09	-.05	-.02	-.01	.01	.03	.05	.07
	50	-.08	-.14	-.18	-.18	-.20	-.23	-.24	-.42	-.41	-.41	-.14	-.11	-.09	-.05	-.02	-.01	.01	.03	.05	.07
	60	-.10	-.11	-.12	-.12	-.15	-.15	-.17	-.14	-.12	-.12	-.07	-.08	-.07	-.02	0	.01	.01	.03	.04	.06
	70	.02	0	-.02	-.02	-.03	-.03	-.04	-.08	-.12	-.17	-.02	-.03	-.04	.01	.01	.02	.02	.03	.04	.04
	80	.03	.02	.01	.03	.02	.01	.01	-.04	-.07	-.12	.03	.03	.03	.05	.05	.04	.04	.04	.03	.03
0.80	0	.34	.47	.37	.14	-.20	-.60	-1.02	-1.30	-1.31	-1.15	-.24	-.03	.11	.22	.30	.34	.39	.42	.43	.43
	4	.03	-.20	-.39	-.58	-.80	-.93	-1.03	-1.01	-.94	-.87	-.24	-.06	.03	.13	.20	.23	.28	.31	.33	.34
	8	-.02	-.18	-.29	-.39	-.48	-.60	-.72	-.77	-.82	-.82	-.20	-.09	-.01	.08	.13	.16	.21	.24	.27	.28
	12	-.09	-.17	-.23	-.26	-.34	-.40	-.45	-.55	-.55	-.53	-.18	-.12	-.06	.02	.06	.08	.13	.15	.18	.19
	20	-.10	-.16	-.20	-.22	-.25	-.28	-.30	-.35	-.48	-.53	-.17	-.13	-.08	-.03	.01	.03	.07	.08	.10	.11
	30	-.09	-.14	-.17	-.18	-.20	-.23	-.24	-.22	-.23	-.36	-.16	-.13	-.10	-.04	-.01	0	.03	.04	.06	.06
	40	-.08	-.11	-.11	-.11	-.13	-.16	-.15	-.14	-.12	-.26	-.13	-.12	-.09	-.05	-.02	-.01	.02	.03	.04	.04
	50	-.04	-.04	-.04	-.05	-.06	-.08	-.09	-.08	-.08	-.20	-.10	-.10	-.07	-.03	-.01	0	.02	.02	.03	.03
	60	.03	.01	0	.01	-.01	-.03	-.03	-.06	-.08	-.17	-.05	-.05	-.05	-.05	-.05	-.05	-.05	-.05	-.05	-.05
	70	.05	.05	.04	.04	.04	.03	.02	-.03	-.07	-.15	.05	.05	.06	.08	.07	.06	.06	.04	.02	-.01
	80	.05	.05	.05	.05	.05	.05	.05	.05	.05	.05	.05	.05	.05	.05	.05	.05	.05	.05	.05	.05
	90	.05	.05	.05	.05	.05	.05	.05	.05	.05	.05	.05	.05	.05	.05	.05	.05	.05	.05	.05	.05
0.99	0	.34	.47	.37	.14	-.20	-.60	-1.02	-1.30	-1.31	-1.15	-.24	-.03	.11	.22	.30	.34	.39	.42	.43	.43
	4	.03	-.20	-.39	-.58	-.80	-.93	-1.03	-1.01	-.94	-.87	-.24	-.06	.03	.13	.20	.23	.28	.31	.33	.34
	8	-.02	-.18	-.29	-.39	-.48	-.60	-.72	-.77	-.82	-.82	-.20	-.09	-.01	.08	.13	.16	.21	.24	.27	.28
	12	-.09	-.17	-.23	-.26	-.34	-.40	-.45	-.55	-.55	-.53	-.18	-.12	-.06	.02	.06	.08	.13	.15	.18	.19
	20	-.10	-.16	-.20	-.22	-.25	-.28	-.30	-.35	-.48	-.53	-.17	-.13	-.08	-.03	.01	.03	.07	.08	.10	.11
	30	-.09	-.14	-.17	-.18	-.20	-.23	-.24	-.22	-.23	-.36	-.16	-.13	-.10	-.04	-.01	0	.03	.04	.06	.06
	40	-.08	-.11	-.11	-.11	-.13	-.16	-.15	-.14	-.12	-.26	-.13	-.12	-.09	-.05	-.02	-.01	.02	.03	.04	.04
	50	-.04	-.04	-.04	-.05	-.06	-.08	-.09	-.08	-.08	-.20	-.10	-.10	-.07	-.03	-.01	0	.02	.02	.03	.03
	60	.03	.01	0	.01	-.01	-.														

TABLE II.- PRESSURE COEFFICIENTS AT SIX SPANWISE STATIONS; $M = 0.50$
 (b) $\alpha = 10.50^\circ$ to 19.82°

η	Per- cent chord	Upper surface										Lower surface									
		Angle of attack, deg										Angle of attack, deg									
		10.50	11.56	12.59	13.62	14.66	15.73	16.78	17.79	18.80	19.82	10.50	11.56	12.59	13.62	14.66	15.73	16.78	17.79	18.80	19.82
0	5.58	-0.09	-0.12	-0.13	-0.14	-0.15	-0.16	-0.17	-0.18	-0.19	-0.21	0.16	0.19	0.22	0.24	0.24	0.26	0.27	0.29	0.31	0.37
	26.6	-0.26	-0.31	-0.34	-0.36	-0.38	-0.40	-0.42	-0.44	-0.45	-0.48	0.20	0.23	0.25	0.26	0.28	0.31	0.32	0.36	0.38	0.42
	37.2	-0.27	-0.32	-0.33	-0.36	-0.37	-0.40	-0.42	-0.42	-0.43	-0.45	0.22	0.25	0.26	0.28	0.30	0.33	0.33	0.37	0.39	0.43
	47.7	-0.26	-0.31	-0.33	-0.36	-0.38	-0.39	-0.41	-0.42	-0.42	-0.43	0.21	0.24	0.24	0.27	0.28	0.31	0.32	0.37	0.38	0.42
	58.2	-0.26	-0.28	-0.31	-0.33	-0.35	-0.36	-0.37	-0.38	-0.39	-0.39	0.17	0.21	0.22	0.24	0.25	0.28	0.28	0.33	0.34	0.38
	68.8	-0.23	-0.26	-0.27	-0.30	-0.32	-0.33	-0.34	-0.36	-0.37	-0.36	0.16	0.18	0.19	0.22	0.23	0.25	0.26	0.31	0.31	0.34
	79.3	-0.17	-0.18	-0.19	-0.21	-0.23	-0.25	-0.26	-0.27	-0.29	-0.29	0.13	0.15	0.16	0.18	0.18	0.19	0.20	0.23	0.23	0.28
	89.3	-0.08	-0.09	-0.10	-0.13	-0.14	-0.15	-0.16	-0.18	-0.20	-0.21	0.10	0.12	0.12	0.13	0.13	0.14	0.15	0.17	0.18	0.20
	100.2	-0.04	-0.04	-0.05	-0.06	-0.07	-0.08	-0.08	-0.09	-0.11	-0.11	0.09	0.11	0.11	0.12	0.11	0.12	0.13	0.15	0.16	0.17
	110.9	0	-0.01	-0.02	-0.03	-0.04	-0.05	-0.06	-0.07	-0.08	-0.09	0.05	0.05	0.05	0.05	0.05	0.06	0.07	0.08	0.07	0.09
0.20	0	-1.06	-1.30	-1.46	-1.66	-1.78	-1.92	-1.97	-1.96	-1.86	-1.71	-	-	-	-	-	-	-	-	-	-
	1.25	-2.43	-2.12	-2.05	-2.31	-2.42	-2.36	-2.26	-2.05	-1.87	-1.65	-	-	-	-	-	-	-	-	-	-
	2.5	-1.48	-2.18	-2.16	-2.42	-2.51	-2.44	-2.31	-2.08	-1.88	-1.64	-	-	-	-	-	-	-	-	-	-
	5	-1.07	-1.84	-2.12	-2.19	-2.19	-2.18	-2.22	-2.06	-1.89	-1.64	-	-	-	-	-	-	-	-	-	-
	10	-0.95	-1.37	-1.80	-1.89	-2.00	-2.10	-2.04	-1.88	-1.62	-1.37	-	-	-	-	-	-	-	-	-	-
	20	-0.76	-1.08	-1.49	-1.69	-1.90	-2.17	-2.11	-1.96	-1.63	-1.37	-	-	-	-	-	-	-	-	-	-
	30	-0.52	-0.78	-1.23	-1.61	-1.98	-2.28	-2.18	-2.03	-1.68	-1.42	-	-	-	-	-	-	-	-	-	-
	40	-0.42	-0.62	-1.28	-1.68	-2.07	-2.38	-2.28	-2.13	-1.78	-1.52	-	-	-	-	-	-	-	-	-	-
	50	-0.32	-0.50	-1.22	-1.63	-2.02	-2.33	-2.23	-2.08	-1.73	-1.47	-	-	-	-	-	-	-	-	-	-
	60	-0.22	-0.41	-1.16	-1.58	-2.01	-2.32	-2.22	-2.07	-1.72	-1.46	-	-	-	-	-	-	-	-	-	-
0.40	0	-1.23	-1.21	-1.12	-1.06	-1.00	-0.95	-0.92	-0.93	-0.93	-0.87	-	-	-	-	-	-	-	-	-	-
	1.25	-1.26	-1.17	-1.07	-1.03	-0.97	-0.94	-0.93	-0.91	-0.87	-0.86	-	-	-	-	-	-	-	-	-	-
	2.5	-1.03	-1.13	-1.07	-1.02	-0.97	-0.94	-0.92	-0.91	-0.87	-0.87	-	-	-	-	-	-	-	-	-	-
	5	-0.99	-1.11	-1.08	-1.03	-0.98	-0.94	-0.93	-0.92	-0.87	-0.87	-	-	-	-	-	-	-	-	-	-
	10	-1.03	-1.14	-1.08	-1.03	-0.98	-0.94	-0.93	-0.93	-0.87	-0.87	-	-	-	-	-	-	-	-	-	-
	20	-1.18	-1.28	-1.22	-1.14	-1.07	-1.02	-0.99	-0.96	-0.91	-0.87	-	-	-	-	-	-	-	-	-	-
	30	-0.84	-0.83	-1.17	-1.18	-1.12	-1.13	-1.09	-1.05	-1.02	-0.96	-	-	-	-	-	-	-	-	-	-
	40	-0.14	-0.18	-0.66	-0.91	-0.99	-1.05	-1.03	-1.03	-1.01	-0.96	-	-	-	-	-	-	-	-	-	-
	50	-0.10	-0.09	-0.15	-0.38	-0.68	-0.97	-0.93	-0.96	-0.97	-0.94	-	-	-	-	-	-	-	-	-	-
	60	-0.08	-0.07	-0.04	-0.08	-0.27	-0.51	-0.66	-0.77	-0.84	-0.87	-	-	-	-	-	-	-	-	-	-
0.60	0	-0.93	-0.68	-0.61	-0.57	-0.55	-0.54	-0.53	-0.52	-0.51	-0.51	-	-	-	-	-	-	-	-	-	-
	1.25	-0.81	-0.61	-0.54	-0.53	-0.52	-0.51	-0.51	-0.49	-0.48	-0.48	-	-	-	-	-	-	-	-	-	-
	2.5	-0.77	-0.60	-0.54	-0.53	-0.52	-0.51	-0.51	-0.49	-0.48	-0.48	-	-	-	-	-	-	-	-	-	-
	5	-0.79	-0.60	-0.54	-0.52	-0.52	-0.51	-0.51	-0.49	-0.48	-0.48	-	-	-	-	-	-	-	-	-	-
	10	-0.77	-0.60	-0.56	-0.55	-0.53	-0.52	-0.52	-0.50	-0.50	-0.50	-	-	-	-	-	-	-	-	-	-
	20	-0.61	-0.62	-0.77	-0.55	-0.54	-0.53	-0.53	-0.52	-0.53	-0.53	-	-	-	-	-	-	-	-	-	-
	30	-0.82	-0.64	-0.79	-0.57	-0.56	-0.56	-0.56	-0.54	-0.53	-0.53	-	-	-	-	-	-	-	-	-	-
	40	-0.75	-0.69	-0.62	-0.59	-0.58	-0.59	-0.58	-0.57	-0.55	-0.54	-	-	-	-	-	-	-	-	-	-
	50	-0.60	-0.75	-0.66	-0.63	-0.62	-0.61	-0.61	-0.59	-0.57	-0.57	-	-	-	-	-	-	-	-	-	-
	60	-0.49	-0.78	-0.71	-0.68	-0.65	-0.65	-0.65	-0.63	-0.63	-0.60	-	-	-	-	-	-	-	-	-	-
0.80	0	-0.68	-0.36	-0.32	-0.32	-0.33	-0.37	-0.38	-0.38	-0.39	-0.41	-	-	-	-	-	-	-	-	-	-
	1.25	-0.65	-0.40	-0.35	-0.33	-0.33	-0.32	-0.33	-0.33	-0.35	-0.35	-	-	-	-	-	-	-	-	-	-
	2.5	-0.54	-0.34	-0.33	-0.32	-0.32	-0.33	-0.34	-0.34	-0.34	-0.34	-	-	-	-	-	-	-	-	-	-
	5	-0.45	-0.32	-0.34	-0.33	-0.33	-0.35	-0.35	-0.35	-0.35	-0.36	-	-	-	-	-	-	-	-	-	-
	10	-0.46	-0.34	-0.36	-0.36	-0.37	-0.38	-0.37	-0.36	-0.36	-0.37	-	-	-	-	-	-	-	-	-	-
	20	-0.42	-0.36	-0.37	-0.38	-0.38	-0.39	-0.39	-0.37	-0.37	-0.38	-	-	-	-	-	-	-	-	-	-
	30	-0.38	-0.37	-0.38	-0.39	-0.39	-0.38	-0.38	-0.37	-0.36	-0.37	-	-	-	-	-	-	-	-	-	-
	40	-0.35	-0.38	-0.38	-0.37	-0.37	-0.37	-0.37	-0.37	-0.36	-0.36	-	-	-	-	-	-	-	-	-	-
	50	-0.33	-0.38	-0.38	-0.37	-0.37	-0.37	-0.36	-0.36	-0.36	-0.36	-	-	-	-	-	-	-	-	-	-
	60	-0.30	-0.37	-0.37	-0.37	-0.38	-0.38	-0.38	-0.37	-0.37	-0.37	-	-	-	-	-	-	-	-	-	-
0.95	0	-0.45	-0.26	-0.14	-0.14	-0.19	-0.25	-0.27	-0.28	-0.32	-0.37	-	-	-	-	-	-	-	-	-	-
	1.25	-0.63	-0.43	-0.26	-0.23	-0.25	-0.27	-0.27	-0.27	-0.29	-0.31	-	-	-	-	-	-	-	-	-	-
	2.5	-0.61	-0.42	-0.26	-0.23	-0.26	-0.27	-0.27	-0.27	-0.28	-0.30	-	-	-	-	-	-	-	-	-	-
	5	-0.59	-0.43	-0.25	-0.23	-0.25	-0.26	-0.27	-0.28	-0.30	-0.33	-	-	-	-	-	-	-	-	-	-
	10	-0.48	-0.37	-0.24	-0.23	-0.25	-0.26	-0.27	-0.28	-0.30	-0.34	-	-	-	-	-	-	-	-	-	-
	20	-0.33	-0.28	-0.24	-0.23	-0.24	-0.25	-0.27	-0.28	-0.30	-0.34	-	-	-	-	-	-	-	-	-	-
	30	-0.23	-0.22	-0.22	-0.23	-0.24	-0.25	-0.27	-0.27	-0.27	-0.30	-	-	-	-	-	-	-	-	-	-
	40	-0.18	-0.21	-0.22	-0.22	-0.23	-0.24	-0.27	-0.27	-0.28	-0.30	-	-	-	-	-	-	-	-	-	-
	50	-0.15	-0.18	-0.19	-0.21	-0.23	-0.24	-0.26	-0.26	-0.27	-0.28	-	-	-	-	-	-	-	-	-	-
	60	-0.13	-0.17	-0.19	-0.20	-0.22	-0.23	-0.25	-0.25	-0.25	-0.27	-	-	-	-	-	-	-	-	-	-
70	-0.11	-0.16	-0.18	-0.19	-0.22	-0.22	-0.24	-0.24	-0.24	-0.26	-	-	-	-	-	-	-	-	-	-	

TABLE III.- PRESSURE COEFFICIENTS AT SIX SPANWISE STATIONS; $M = 0.70$
 (a) $\alpha = -1.22^\circ$ to 9.84°

η	Per- cent chord	Upper surface										Lower surface									
		Angle of attack, deg										Angle of attack, deg									
		-1.22	1.00	2.17	3.26	4.35	5.46	6.57	7.65	8.72	9.84	-1.22	1.00	2.17	3.26	4.35	5.46	6.57	7.65	8.72	9.84
0	5.98	0.01	0.02	0	-0.01	-0.02	-0.03	-0.04	-0.05	-0.07	-0.08	0.03	0.04	0.04	0.05	0.07	0.09	0.12	0.13	0.15	0.17
	26.6	0	-0.03	-0.07	-0.09	-0.13	-0.15	-0.19	-0.23	-0.27	-0.32	-0.03	0.01	0.03	0.05	0.07	0.10	0.15	0.17	0.19	0.20
	37.2	-0.02	-0.06	-0.09	-0.13	-0.15	-0.18	-0.22	-0.26	-0.30	-0.34	-0.06	0	0.02	0.04	0.07	0.11	0.13	0.16	0.19	0.22
	47.7	-0.05	-0.08	-0.13	-0.15	-0.18	-0.21	-0.25	-0.29	-0.33	-0.36	-0.08	-0.01	0	0.02	0.05	0.09	0.12	0.15	0.18	0.19
	58.8	-0.06	-0.08	-0.13	-0.15	-0.18	-0.21	-0.24	-0.27	-0.31	-0.35	-0.10	-0.04	-0.03	0	0.03	0.07	0.09	0.12	0.14	0.17
	68.3	-0.06	-0.08	-0.13	-0.15	-0.17	-0.19	-0.23	-0.26	-0.30	-0.33	-0.11	-0.05	-0.04	-0.02	0.02	0.06	0.07	0.10	0.12	0.15
	79.3	-0.06	-0.08	-0.13	-0.15	-0.17	-0.19	-0.23	-0.26	-0.30	-0.33	-0.10	-0.05	-0.04	-0.02	0.01	0.04	0.05	0.08	0.10	0.13
	89.3	-0.06	-0.07	-0.10	-0.12	-0.14	-0.14	-0.17	-0.19	-0.20	-0.23	-0.09	-0.05	-0.04	-0.03	0	0.04	0.05	0.07	0.09	0.11
	100.2	-0.06	-0.07	-0.10	-0.12	-0.14	-0.14	-0.17	-0.19	-0.20	-0.23	-0.08	-0.04	-0.04	-0.02	0	0.03	0.04	0.05	0.08	0.09
	110.9	-0.02	-0.02	-0.05	-0.06	-0.06	-0.06	-0.09	-0.09	-0.11	-0.12	-0.04	-0.01	-0.01	0	0.01	0.03	0.03	0.05	0.07	0.08
0.20	121.3	-0.01	-0.01	-0.03	-0.03	-0.04	-0.02	-0.09	-0.04	-0.05	-0.05	-0.04	-0.01	-0.01	0	0.01	0.04	0.05	0.07	0.07	0.07
	147.8	0	-0.01	-0.01	-0.01	-0.02	0	-0.02	-0.02	-0.03	-0.03	0	0.01	0.01	0.01	0.01	0.04	0.02	0.02	0.02	0.03
	0	.39	.46	.38	.29	.16	0	-.16	-.27	-.39	-.48	-.18	-.09	-.16	-.24	-.32	-.37	-.42	-.44	-.46	-.48
	1.25	.12	.13	.39	-.59	-.83	-1.08	-1.06	-1.02	-1.04	-1.07	-.18	-.09	-.16	-.24	-.32	-.37	-.42	-.44	-.46	-.48
	2.5	.07	.12	.36	-.51	-.79	-1.06	-1.06	-1.02	-1.04	-1.07	-.20	0	-.08	-.16	-.24	-.32	-.37	-.42	-.44	-.48
	5	.01	.13	.26	-.34	-.44	-.59	-.69	-1.00	-1.43	-1.66	-.20	0	-.08	-.16	-.24	-.32	-.37	-.42	-.44	-.48
	10	-.05	.14	.24	-.30	-.39	-.50	-.57	-.62	-1.02	-1.30	-.17	-.04	-.08	0.08	-.14	-.20	-.24	-.28	-.32	-.36
	20	-.06	.16	.23	-.33	-.39	-.41	-.47	-.54	-.62	-.61	-.20	-.09	-.04	0.08	-.05	-.10	-.15	-.18	-.22	-.25
	30	-.14	.19	.24	-.28	-.31	-.36	-.41	-.42	-.48	-.53	-.19	-.10	-.06	0.04	-.01	-.06	-.10	-.13	-.14	-.18
	40	-.15	.18	.23	-.26	-.29	-.33	-.36	-.38	-.43	-.46	-.19	-.13	-.11	-.08	0	-.02	-.04	-.06	-.08	-.10
0.40	50	-.12	.15	.19	-.22	-.23	-.26	-.28	-.30	-.34	-.36	-.17	-.12	-.09	-.07	-.05	-.02	-.01	-.02	-.03	-.04
	60	-.07	.09	.12	-.14	-.17	-.18	-.19	-.24	-.26	-.26	-.12	-.07	-.05	-.04	-.03	-.01	-.02	-.03	-.04	-.04
	70	-.02	.03	.05	-.07	-.07	-.09	-.11	-.10	-.14	-.16	-.05	0	-.01	-.01	-.01	-.02	-.03	-.04	-.04	-.06
	80	.04	.03	.02	-.01	-.01	-.02	-.02	-.01	-.05	-.06	0	.04	.03	.03	.04	.04	.04	.04	.04	.06
	90	.04	.03	.02	-.01	-.01	-.02	-.02	-.01	-.05	-.06	0	.04	.03	.03	.04	.04	.04	.04	.04	.06
	0	.42	.43	.28	-.06	-.24	-.54	-.64	-.82	-.93	-1.04	-.26	0	-.14	-.25	-.32	-.39	-.42	-.45	-.48	-.50
	1.25	.18	.10	.36	-.66	-1.01	-1.36	-1.22	-1.02	-1.05	-1.09	-.28	0	-.08	-.17	-.24	-.32	-.37	-.42	-.44	-.48
	2.5	.06	.19	.42	-.04	-.08	-1.30	-1.08	-1.08	-1.06	-1.06	-.22	-.03	-.08	-.17	-.24	-.32	-.37	-.42	-.44	-.48
	5	-.01	.17	.36	-.50	-.64	-.82	-.88	-1.04	-1.06	-1.06	-.22	-.06	-.08	-.17	-.24	-.32	-.37	-.42	-.44	-.48
	10	-.06	.16	.29	-.36	-.44	-.57	-.68	-1.04	-1.06	-1.06	-.20	-.10	-.08	0.01	-.04	-.11	-.14	-.18	-.22	-.24
0.60	20	-.14	.18	.24	-.28	-.32	-.38	-.43	-.42	-.48	-.53	-.20	-.18	-.08	0.01	-.04	-.11	-.14	-.18	-.22	-.24
	30	-.14	.18	.24	-.28	-.32	-.38	-.43	-.42	-.48	-.53	-.19	-.13	-.10	-.06	0	-.04	-.06	-.09	-.12	-.14
	40	-.12	.15	.19	-.20	-.22	-.26	-.29	-.34	-.41	-.46	-.19	-.13	-.10	-.06	0	-.04	-.06	-.09	-.12	-.14
	50	-.08	.11	.12	-.13	-.14	-.18	-.17	-.20	-.22	-.27	-.12	-.07	-.06	-.03	-.02	-.01	-.04	-.04	-.06	-.07
	60	-.04	.09	.05	-.08	-.08	-.09	-.11	-.13	-.12	-.10	-.06	-.01	-.03	-.01	-.01	-.02	-.04	-.04	-.06	-.06
	70	.02	.02	0	-.01	-.02	-.03	-.03	-.04	-.04	-.04	0	.03	.02	.02	.03	.04	.04	.04	.06	.06
	80	.06	.06	.04	.05	.04	.04	.04	.02	.03	.01	.04	.06	.06	.06	.06	.06	.06	.06	.06	.06
	90	.06	.06	.04	.05	.04	.04	.04	.02	.03	.01	.04	.06	.06	.06	.06	.06	.06	.06	.06	.06
	0	.40	.47	.34	.09	-.27	-.68	-.90	-1.02	-.96	-.76	-.27	-.05	-.20	-.23	-.37	-.44	-.46	-.46	-.47	-.52
	1.25	.19	-.09	-.38	-.66	-1.01	-1.51	-1.63	-1.35	-1.12	-.66	-.23	-.02	.11	.19	.26	.33	.37	.38	.40	.43
0.80	2.5	.06	.18	.43	-.05	-.04	-1.37	-1.06	-.93	-.93	-.65	-.27	-.05	.20	.23	.37	.44	.46	.46	.47	.52
	5	-.01	.19	.37	-.56	-.73	-.83	-.82	-.79	-.73	-.61	-.23	-.02	.11	.19	.26	.33	.37	.38	.40	.43
	10	-.04	.16	.29	-.36	-.47	-.57	-.69	-.64	-.60	-.61	-.22	-.07	.03	.10	.16	.22	.26	.28	.30	.33
	20	-.08	.16	.24	-.30	-.37	-.44	-.50	-.46	-.48	-.62	-.20	-.10	-.04	.02	.06	.12	.16	.18	.19	.24
	30	-.12	.17	.23	-.28	-.33	-.37	-.44	-.41	-.47	-.63	-.20	-.11	-.06	-.03	-.01	.06	.10	.12	.13	.17
	40	-.12	.16	.20	-.24	-.28	-.30	-.33	-.36	-.38	-.64	-.16	-.10	-.06	-.04	-.02	.02	.03	.04	.06	.08
	50	-.10	.13	.17	-.20	-.23	-.24	-.23	-.46	-.59	-.67	-.10	-.06	-.04	-.02	0	.02	.03	.04	.05	.06
	60	-.07	.10	.11	-.13	-.16	-.17	-.14	-.32	-.56	-.68	-.02	-.02	-.01	-.02	.02	.03	.04	.04	.05	.06
	70	-.01	.02	.01	-.02	-.02	-.03	-.03	-.10	-.32	-.54	-.02	-.02	-.01	-.02	.02	.03	.04	.04	.05	.06
	90	.04	.05	.04	.04	.04	.02	.02	-.02	-.12	-.34	.05	.08	.07	.06	.06	.06	.06	.06	.06	.06
0.95	0	.36	.49	.41	.23	-.01	-.21	-.27	-.36	-.41	-.38	-.26	0	.13	.23	.30	.36	.38	.41	.40	.41
	5	-.02	.21	.39	-.98	-.74	-.66	-.67	-.65	-.66	-.68	-.22	-.07	.02	.06	.13	.18	.21	.23	.24	.24
	10	-.02	.14	.27	-.35	-.44	-.66	-.67	-.65	-.66	-.68	-.20	-.12	-.07	-.03	.01	.04	.06	.08	.10	.10
	20	-.08	.14	.27	-.35	-.44	-.66	-.67	-.65	-.66	-.68	-.17	-.12	-.10	-.06	-.05	-.03	-.02	.01	.02	.02
	30	-.11	.13	.18	-.22	-.25	-.30	-.38	-.46	-.57	-.61	-.17	-.12	-.11	-.09	-.08	-.07	-.05	-.03	-.02	-.02
	40	-.12	.14	.16	-.18	-.20	-.24	-.28	-.38	-.44	-.46	-.12	-.11	-.11	-.09	-.08	-.07	-.05	-.03	-.02	-.02
	50	-.02	.10	.12	-.13	-.15	-.17	-.20	-.28	-.33	-.34	-.09	-.05	-.04	-.05	-.05	-.04	-.03	-.02	-.02	-.02
	60	-.05	.06	.06	-.07	-.08	-.11	-.14	-.19	-.24	-.24	-.09	-.05	-.04	-.05	-.05	-.04	-.03	-.02	-.02	-.02
	70	.01	.01	.01	-.01	-.01	-.01	-.01	-.09	-.13	-.17	.01	.02	.01	0	.01	.01	.01	.01	.01	.01
	90	.06	.09	.06	.06	.07	.02	-.01	-.03	-.08	-.12	.08	.09	.08	.08	.07	.04	.02	.02	.02	.02

~~CONFIDENTIAL~~

TABLE III.- PRESSURE COEFFICIENTS AT SIX SPANWISE STATIONS; $M = 0.70$
 (b) $\alpha = 10.91^\circ$ to 15.16°

η	Per- cent chord	Upper surface					Lower surface				
		Angle of attack, deg					Angle of attack, deg				
		10.91	11.96	13.02	14.08	15.16	10.91	11.96	13.02	14.08	15.16
0	5.58	-0.09	-0.10	-0.11	-0.11	-0.12	0.19	0.21	0.24	0.25	0.27
	26.6	-.09	-.10	-.11	-.11	-.12	.25	.28	.30	.30	.32
	37.2	-.36	-.39	-.42	-.43	-.46	.25	.27	.30	.32	.34
	47.7	-.37	-.42	-.44	-.45	-.47	.23	.25	.28	.30	.32
	58.2	-.40	-.43	-.44	-.45	-.48	.20	.23	.25	.27	.28
	68.8	-.37	-.39	-.41	-.42	-.45	.17	.19	.23	.24	.26
	79.3	-.34	-.35	-.38	-.38	-.42	.17	.18	.20	.21	.23
	89.3	-.23	-.24	-.27	-.27	-.30	.14	.15	.17	.18	.18
	100.2	-.23	-.24	-.27	-.28	-.30	.12	.13	.15	.16	.16
	110.9	-.12	-.13	-.15	-.15	-.18	.10	.11	.12	.13	.13
	121.3	-.05	-.07	-.08	-.07	-.10	.09	.10	.10	.11	.12
	147.8	-.03	-.03	-.03	-.03	-.05	.04	.04	.04	.04	.04
0.20	0	-.57	-.68	-.76	-.81	-.88	-.01	-.01	-.01	-.01	-.01
	1.25	-1.63	-1.67	-1.72	-1.75	-1.71	-.51	-.52	-.53	-.53	-.54
	2.5	-1.65	-1.70	-1.74	-1.77	-1.73	.48	.52	.54	.56	.58
	5	-1.66	-1.74	-1.76	-1.78	-1.76	.38	.42	.44	.46	.48
	10	-1.52	-1.74	-1.84	-1.88	-1.88	.28	.32	.36	.37	.40
	20	-1.30	-1.70	-1.86	-1.92	-1.89	.22	.24	.27	.29	.32
	30	-.63	-.50	-.51	-.79	-1.17	-.12	.14	.16	.17	.20
	40	-.42	-.33	-.32	-.55	-.83	.08	.12	.13	.14	.16
	50	-.32	-.28	-.32	-.44	-.62	.09	.10	.11	.12	.14
	60	-.22	-.21	-.28	-.31	-.43	.08	.08	.08	.09	.10
	70	-.12	-.12	-.18	-.19	-.28	.07	.07	.07	.06	.07
	80	-.02	-.02	-.06	-.07	-.15	.07	.07	.07	.06	.07
0.40	0	-1.06	-.99	-.91	-.92	-.91	-.01	-.01	-.01	-.01	-.01
	1.25	-1.00	-.92	-.87	-.89	-.88	.46	.49	.51	.51	.53
	2.5	-1.00	-.92	-.86	-.90	-.88	.38	.41	.43	.44	.46
	5	-.99	-.92	-.86	-.90	-.89	.27	.29	.32	.33	.36
	10	-1.01	-.93	-.88	-.91	-.90	.19	.21	.24	.24	.26
	20	-1.11	-1.01	-.95	-.94	-.92	.14	.14	.17	.17	.18
	30	-1.00	-1.05	-1.01	-1.02	-.98	.10	.09	.11	.10	.11
	40	-.53	-.85	-.93	-.97	-.96	.08	.08	.09	.08	.08
	50	-.10	-.36	-.71	-.83	-.87	.08	.08	.08	.06	.06
	60	-.03	-.09	-.33	-.52	-.67	.08	.07	.07	.04	.02
	70	-.02	-.02	-.08	-.18	-.37	.08	.07	.07	.04	.02
	80	-.02	-.02	-.08	-.18	-.37	.08	.07	.07	.04	.02
0.60	0	-.66	-.61	-.59	-.55	-.51	-.01	-.01	-.01	-.01	-.01
	1.25	-.54	-.52	-.53	-.49	-.46	.46	.46	.48	.48	.50
	2.5	-.52	-.52	-.52	-.50	-.47	.36	.38	.39	.40	.41
	5	-.53	-.52	-.53	-.48	-.48	.25	.26	.27	.28	.29
	10	-.54	-.52	-.52	-.49	-.49	.17	.18	.18	.19	.20
	20	-.53	-.53	-.54	-.51	-.49	.06	.06	.06	.06	.07
	30	-.56	-.53	-.55	-.52	-.50	.04	.02	.02	.02	.03
	40	-.57	-.54	-.56	-.54	-.53	.02	.01	.02	.02	.02
	50	-.61	-.56	-.58	-.57	-.56	.02	.01	.02	.02	.02
	60	-.63	-.58	-.60	-.60	-.58	.02	.01	.02	.02	.02
	70	-.62	-.62	-.62	-.62	-.61	.02	.01	.02	.02	.02
	80	-.62	-.62	-.62	-.62	-.60	.02	.01	.02	.02	.02
0.80	0	-.46	-.40	-.27	-.28	-.30	-.01	-.01	-.01	-.01	-.01
	1	-.64	-.56	-.32	-.31	-.31	.43	.43	.45	.45	.46
	2	-.22	-.30	-.29	-.30	-.31	.33	.34	.36	.37	.39
	4	-.23	-.26	-.30	-.32	-.33	.27	.27	.29	.31	.32
	6	-.23	-.26	-.30	-.32	-.33	.18	.18	.21	.22	.24
	8	-.23	-.26	-.30	-.32	-.33	.11	.11	.12	.14	.15
	10	-.26	-.30	-.32	-.34	-.35	.04	.04	.06	.06	.07
	12	-.29	-.32	-.33	-.34	-.35	0	0	.02	.01	.02
	14	-.31	-.32	-.34	-.34	-.36	-.03	-.03	-.02	-.02	-.02
	16	-.31	-.33	-.34	-.34	-.34	-.03	-.03	-.02	-.02	-.02
	18	-.31	-.33	-.34	-.35	-.35	-.03	-.03	-.02	-.02	-.02
	20	-.32	-.33	-.34	-.35	-.36	-.13	-.13	-.13	-.13	-.14
0.95	0	-.46	-.36	-.18	-.18	-.21	-.01	-.01	-.01	-.01	-.01
	1	-.74	-.56	-.30	-.29	-.28	.26	.27	.29	.29	.29
	2	-.74	-.56	-.30	-.30	-.29	.10	.12	.13	.14	.14
	4	-.61	-.59	-.29	-.29	-.29	0	.01	.03	.04	.03
	6	-.73	-.58	-.29	-.29	-.29	-.06	-.05	-.04	-.04	-.04
	8	-.42	-.46	-.28	-.28	-.29	-.09	-.08	-.08	-.08	-.09
	10	-.23	-.32	-.26	-.27	-.28	-.09	-.08	-.08	-.09	-.09
	12	-.18	-.24	-.24	-.25	-.27	-.07	-.08	-.09	-.09	-.10
	14	-.15	-.21	-.22	-.24	-.26	-.06	-.08	-.10	-.10	-.11
	16	-.14	-.20	-.21	-.23	-.25	-.06	-.08	-.10	-.10	-.11
	18	-.13	-.18	-.20	-.22	-.24	-.06	-.08	-.12	-.12	-.14
	20	-.13	-.18	-.20	-.22	-.24	-.06	-.08	-.12	-.12	-.14

~~CONFIDENTIAL~~

CONFIDENTIAL

TABLE IV.- PRESSURE COEFFICIENTS AT SIX SPANWISE STATIONS; $M = 0.75$
(a) $\alpha = -1.24^\circ$ to 8.81°

η	Percent chord	Upper surface										Lower surface									
		Angle of attack, deg										Angle of attack, deg									
		-1.24	1.00	2.20	3.31	4.38	5.50	6.60	7.69	8.81	-1.24	1.00	2.20	3.31	4.38	5.50	6.60	7.69	8.81		
0	5.58	0.02	0	-0.02	-0.03	-0.03	-0.03	-0.04	-0.04	-0.05	-0.01	0.01	0.02	0.04	0.05	0.08	0.10	0.13	0.15		
	26.6	-0.02	-0.06	-0.09	-0.12	-0.14	-0.17	-0.22	-0.23	-0.28	-0.06	-0.01	0.01	0.04	0.05	0.09	0.13	0.16	0.18		
	37.2	-0.03	-0.07	-0.12	-0.15	-0.17	-0.20	-0.24	-0.27	-0.32	-0.10	-0.05	-0.01	0.02	0.04	0.08	0.11	0.15	0.19		
	47.7	-0.07	-0.11	-0.15	-0.19	-0.21	-0.23	-0.28	-0.31	-0.36	-0.13	-0.07	-0.04	-0.02	0.01	0.05	0.08	0.12	0.15		
	58.2	-0.08	-0.12	-0.16	-0.19	-0.21	-0.23	-0.27	-0.30	-0.34	-0.14	-0.08	-0.06	-0.03	-0.01	0.04	0.07	0.10	0.12		
	68.8	-0.09	-0.13	-0.17	-0.19	-0.21	-0.22	-0.27	-0.28	-0.32	-0.13	-0.09	-0.07	-0.04	-0.02	0.03	0.05	0.08	0.11		
	79.3	-0.07	-0.11	-0.13	-0.15	-0.16	-0.17	-0.19	-0.20	-0.21	-0.12	-0.08	-0.07	-0.05	-0.03	0.02	0.04	0.07	0.10		
	89.3	-0.04	-0.05	-0.07	-0.08	-0.08	-0.09	-0.09	-0.11	-0.11	-0.08	-0.06	-0.05	-0.04	-0.02	0.01	0.04	0.06	0.08		
	100.2	-0.03	-0.04	-0.04	-0.05	-0.04	-0.03	-0.04	-0.04	-0.05	-0.06	-0.05	-0.03	-0.02	-0.01	0.02	0.03	0.05	0.07		
	110.9	-0.03	-0.03	-0.03	-0.04	-0.03	-0.02	-0.03	-0.03	-0.03	-0.03	-0.03	-0.03	-0.02	-0.01	0.02	0.03	0.05	0.07		
0.20	0	.38	.43	.36	.28	.19	.03	-.10	-.20	-.30	-.18	-.03	-.16	-.25	-.29	-.37	-.41	-.43	-.47		
	1.25	.13	.15	.41	.64	.80	-1.27	-1.56	-1.68	-1.62	-.18	-.03	-.16	-.25	-.29	-.37	-.41	-.43	-.47		
	2.5	.08	.15	.35	.55	.74	-1.10	-1.53	-1.68	-1.64	-.21	-.03	-.16	-.25	-.29	-.37	-.41	-.43	-.47		
	5	.02	.16	.30	.37	.44	-.63	-.98	-1.30	-1.51	-.21	-.03	-.16	-.25	-.29	-.37	-.41	-.43	-.47		
	10	-.04	-.16	.27	.34	.40	-.51	-.75	-.62	-1.13	-.19	-.07	-.01	.08	.12	.18	.23	.26	.32		
	20	-.09	-.19	.27	.32	.36	-.44	-.50	-.56	-.66	-.22	-.13	-.06	-.01	.03	.09	.13	.16	.21		
	30	-.16	-.22	.28	.31	.35	-.40	-.44	-.46	-.48	-.22	-.13	-.09	-.04	-.01	.04	.08	.10	.15		
	40	-.17	-.22	.27	.31	.33	-.36	-.38	-.41	-.43	-.22	-.18	-.13	-.08	-.07	-.03	-.01	.02	.06		
	50	-.14	-.18	.22	.25	.26	-.28	-.30	-.34	-.34	-.20	-.16	-.12	-.09	-.08	-.04	-.02	0	.03		
	60	-.09	-.11	.15	.17	.18	-.19	-.21	-.22	-.23	-.13	-.12	-.08	-.05	-.04	0	0	.01	.04		
0.40	0	.42	.42	.26	.02	-.16	-.44	-.56	-.65	-.81	-.31	-.03	-.14	-.24	-.30	-.38	-.41	-.43	-.47		
	1.25	.17	.21	.72	.75	-1.01	-1.48	-1.59	-1.27	-1.24	-.25	-.06	.07	.17	.21	.29	.33	.37	.40		
	2.5	.05	.23	.48	.73	.93	-1.41	-.95	-.89	-.96	-.25	-.06	.07	.17	.21	.29	.33	.37	.40		
	5	-.02	.21	.39	.60	.69	-.92	-.69	-.61	-.91	-.24	-.09	.01	.08	.13	.20	.24	.27	.31		
	10	-.07	.20	.33	.40	.49	-.63	-.66	-.69	-.91	-.24	-.14	-.06	0	.03	.10	.13	.17	.20		
	20	-.15	.22	.28	.33	.36	-.42	-.60	-.79	-.93	-.24	-.16	-.09	-.04	-.01	.04	.07	.10	.13		
	30	-.13	.19	.22	.24	.26	-.29	-.30	-.29	-.50	-.23	-.18	-.13	-.08	-.06	-.02	.01	.04	.07		
	40	-.09	.15	.15	.17	.19	-.21	-.22	-.21	-.26	-.15	-.12	-.07	-.05	-.04	-.02	.01	.02	.04		
	50	-.04	.05	.08	.10	.12	-.13	-.14	-.15	-.16	-.07	-.06	-.05	-.03	-.02	0	.01	.02	.04		
	60	0	0	.03	.05	.06	-.06	-.07	-.07	-.08	-.03	-.02	-.01	-.01	0	.01	.02	.03	.04		
0.60	0	.40	.45	.31	.04	-.19	-.58	-.80	-.94	-.96	-.31	-.01	.19	.30	.35	.41	.44	.45	.48		
	1.25	.18	.20	.72	.75	-1.02	-1.45	-1.57	-1.50	-1.17	-.27	-.05	.09	.19	.25	.31	.35	.37	.40		
	2.5	.05	.22	.50	.76	.95	-1.38	-1.27	-1.20	-1.04	-.27	-.05	.09	.19	.25	.31	.35	.37	.40		
	5	-.05	.20	.34	.40	.48	-.63	-.75	-.72	-.75	-.26	-.10	.01	.09	.14	.20	.24	.27	.30		
	10	-.09	.20	.28	.35	.39	-.51	-.76	-.76	-.79	-.24	-.14	-.06	.01	.04	.09	.13	.16	.19		
	20	-.13	.21	.27	.32	.35	-.42	-.67	-.78	-.82	-.23	-.15	-.09	-.04	-.01	.03	.07	.09	.12		
	30	-.14	.20	.24	.28	.30	-.34	-.41	-.54	-.68	-.23	-.15	-.09	-.04	-.01	.03	.07	.09	.12		
	40	-.11	.18	.20	.23	.25	-.26	-.24	-.22	-.39	-.19	-.14	-.09	-.06	-.04	0	.01	.01	.03		
	50	-.08	.13	.15	.16	.17	-.19	-.16	-.16	-.32	-.11	-.10	-.06	-.03	-.02	0	.01	.02	.02		
	60	.01	.02	.04	.04	.04	-.04	-.10	-.14	-.25	-.05	-.06	-.03	0	0	.01	.02	.02	.02		
0.80	0	.38	.48	.36	.16	-.01	-.28	-.46	-.55	-.57	-.30	-.03	.12	.23	.28	.35	.38	.40	.41		
	1.25	.03	.22	.48	.73	.93	-1.36	-1.46	-1.03	-.84	-.26	-.07	.04	.13	.17	.24	.28	.31	.31		
	2.5	-.03	.19	.36	.47	.57	-.82	-.88	-.99	-.85	-.24	-.10	-.01	.07	.11	.18	.21	.23	.24		
	5	-.09	.19	.27	.35	.39	-.46	-.55	-.55	-.50	-.22	-.13	-.06	0	.04	.09	.12	.15	.16		
	10	-.13	.19	.24	.27	.29	-.31	-.49	-.56	-.56	-.21	-.15	-.09	-.04	-.01	.04	.06	.08	.08		
	20	-.13	.19	.24	.27	.29	-.31	-.49	-.56	-.56	-.21	-.15	-.09	-.04	-.01	.04	.06	.08	.08		
	30	-.11	.16	.20	.22	.23	-.24	-.29	-.33	-.42	-.17	-.13	-.09	-.06	-.03	0	.01	.01	.03		
	40	-.09	.13	.13	.14	.15	-.17	-.15	-.14	-.30	-.11	-.10	-.07	-.04	-.02	0	0	0	-.01		
	50	-.04	.03	.06	.08	.08	-.09	-.07	-.08	-.23	-.04	.05	.05	.05	.05	.05	.05	.05	.05		
	60	.02	.01	.01	.02	.02	-.03	-.05	-.07	-.22	.04	.05	.05	.05	.05	.05	.05	.05	.05		
0.95	0	.33	.47	.38	.18	-.04	-.16	-.23	-.33	-.35	-.25	-.09	0	.07	.12	.18	.21	.24	.24		
	1.25	.03	.25	.46	.70	.83	-.82	-.71	-.71	-.67	-.25	-.09	0	.07	.12	.18	.21	.24	.24		
	2.5	-.04	.18	.33	.40	.46	-.68	-.64	-.64	-.64	-.24	-.15	-.10	-.04	-.02	.04	.06	.09	.10		
	5	-.11	.17	.27	.30	.34	-.48	-.50	-.57	-.61	-.20	-.16	-.14	-.10	-.08	-.04	-.02	0	.04		
	10	-.14	.17	.22	.25	.27	-.34	-.40	-.50	-.56	-.17	-.15	-.14	-.11	-.10	-.08	-.06	-.05	-.04		
	20	-.11	.13	.15	.16	.17	-.18	-.24	-.31	-.35	-.07	-.07	-.08	-.08	-.07	-.06	-.04	-.04	-.04		
	30	-.06	.07	.09	.10	.10	-.12	-.17	-.22	-.26	-.01	0	-.03	-.03	-.03	-.02	-.01	0	-.03		
	40	-.03	.03	.03	.03	.03	-.02	-.08	-.09	-.13	.05	.03	.03	.03	.03	.02	.01	0	-.02		
	50	.05	.06	.05	.05	.04	-.02	-.03	-.04	-.10	.07	.06	.05	.05	.05	.04	.02	.02	-.01		
	60	.05	.06	.05	.05	.04	-.02	-.03	-.04	-.10	.07	.06	.05	.05	.05	.04	.02	.02	-.01		

CONFIDENTIAL

TABLE IV.- PRESSURE COEFFICIENTS AT SIX SPANWISE STATIONS; $M = 0.75$
 (b) $\alpha = 9.92^\circ$ to 13.15°

η	Per- cent chord	Upper surface				Lower surface			
		Angle of attack, deg				Angle of attack, deg			
		9.92	10.99	12.07	13.15	9.92	10.99	12.07	13.15
0	5.58	-0.06	-0.06	-0.07	-0.07	0.17	0.20	0.22	0.23
	26.6	---	---	---	---	.21	.24	.27	.29
	37.2	-.32	-.34	-.39	-.43	.22	.25	.28	.30
	47.7	-.36	-.39	-.43	-.46	.20	.24	.27	.28
	58.2	-.39	-.42	-.46	-.48	.17	.20	.24	.25
	68.8	-.38	-.40	-.42	-.43	.16	.18	.21	.23
	79.3	-.34	-.36	-.37	-.39	.14	.16	.18	.20
	89.3	---	---	---	---	.12	.14	.16	.17
	100.2	-.23	-.23	-.25	-.30	.10	.12	.14	.15
	110.9	---	---	---	---	.09	.10	.12	.13
	121.3	-.11	-.11	-.13	-.17	.08	.09	.11	.10
	147.8	-.04	-.04	-.06	-.08	---	---	---	---
	178.0	-.02	-.02	-.02	-.04	.04	.04	.05	.03
0.20	0	-.39	-.44	-.54	-.61	---	---	---	---
	1.25	-1.60	-1.60	-1.62	-1.66	---	---	---	---
	2.5	-1.63	-1.63	-1.65	-1.67	.49	.51	.53	.54
	5	-1.63	-1.65	-1.69	-1.72	.45	.47	.51	.53
	10	-1.46	-1.52	-1.63	-1.75	.35	.38	.42	.44
	20	-1.00	-1.19	-1.54	-1.74	.23	.27	.31	.35
	30	---	---	---	---	.18	.20	.24	.27
	40	-.53	-.63	-.82	-.71	---	---	---	---
	50	-.46	-.49	-.38	-.40	.08	.11	.13	.16
	60	-.37	-.38	-.30	-.46	.06	.07	.10	.12
	70	-.26	-.26	-.21	-.40	.06	.07	.09	.10
	80	-.15	-.15	-.12	-.24	.05	.06	.07	.07
	90	-.04	-.04	-.03	-.10	.05	.05	.05	.04
0.40	0	-.99	-1.03	-1.05	-.94	---	---	---	---
	1.25	-1.05	-1.03	-.98	-.89	---	---	---	---
	2.5	-1.04	-1.03	-.98	-.89	.50	.51	.53	.54
	5	-1.04	-1.03	-.98	-.89	.44	.45	.48	.51
	10	-1.05	-1.04	-.99	-.91	.35	.37	.41	.43
	20	---	---	---	---	.24	.26	.29	.32
	30	-1.11	-1.13	-1.02	-.93	.17	.18	.21	.23
	40	---	---	---	---	.09	.11	.14	.16
	50	-.76	-.97	-1.05	-.98	---	---	---	---
	60	-.32	-.51	-.90	-.94	-.07	-.07	-.09	-.09
	70	-.23	-.11	-.48	-.79	-.06	-.06	-.07	-.07
	80	-.04	-.05	-.15	-.51	-.05	-.05	-.06	-.06
	90	0	-.01	-.05	-.20	-.05	-.05	-.06	.04
0.60	0	-.72	-.69	-.64	-.58	---	---	---	---
	1.25	-.64	-.59	-.55	-.51	---	---	---	---
	2.5	-.63	-.59	-.55	-.51	.50	.50	.51	.52
	5	-.62	-.58	-.55	-.51	.43	.44	.46	.47
	10	-.61	-.58	-.55	-.51	.33	.33	.37	.38
	20	-.62	-.59	-.55	-.53	.22	.22	.25	.26
	30	-.63	-.60	-.56	-.55	.16	.14	.16	.17
	40	-.64	-.61	-.57	-.57	---	---	---	---
	50	-.65	-.64	-.60	-.60	.05	.04	.04	.04
	60	-.66	-.66	-.63	-.64	.04	.02	.01	0
	70	---	---	---	---	.04	.01	-.03	-.04
	80	-.62	-.65	-.65	-.64	---	---	---	---
	90	-.46	-.59	-.64	-.62	0	-.09	-.17	-.17
0.80	0	-.39	-.41	-.28	-.26	---	---	---	---
	4	-.55	-.61	-.39	-.31	.39	.40	.43	.44
	8	-.24	-.28	-.34	-.31	.31	.31	.34	.36
	12	---	---	---	---	.24	.24	.27	.29
	20	-.24	-.25	-.31	-.32	.15	.15	.18	.20
	30	---	---	---	---	.08	.08	.10	.12
	40	-.27	-.29	-.34	-.34	.01	.02	.03	.04
	50	-.29	-.31	-.35	-.35	-.02	-.03	-.02	-.01
	60	-.32	-.33	-.36	-.36	-.05	-.06	-.05	-.04
	70	-.33	-.34	-.36	-.36	---	---	---	---
	80	-.34	-.35	-.36	-.36	---	---	---	---
	90	-.34	-.35	-.37	-.37	-.14	-.14	-.15	-.15
0.95	0	-.34	-.36	-.15	-.15	---	---	---	---
	5	-.62	-.62	-.32	-.28	---	---	---	---
	10	-.62	-.62	-.32	-.28	.25	.25	.26	.28
	20	-.69	-.67	-.31	-.28	.10	.09	.11	.12
	30	-.62	-.65	-.31	-.28	-.01	-.01	0	.02
	40	-.37	-.45	-.29	-.27	-.07	-.08	-.06	-.04
	50	-.24	-.30	-.26	-.27	---	---	---	---
	60	-.20	-.23	-.23	-.26	-.09	-.10	-.11	-.10
	70	-.17	-.20	-.21	-.24	-.08	-.09	-.10	-.10
	80	-.15	-.18	-.20	-.23	-.06	-.09	-.10	-.10
	90	-.12	-.16	-.19	-.22	-.06	-.08	-.10	-.12

CONFIDENTIAL

TABLE V.- PRESSURE COEFFICIENTS AT SIX SPANWISE STATIONS; $M = 0.80$

Y	Per- cent chord	Upper surface										Lower surface									
		Angle of attack, deg										Angle of attack, deg									
		-1.13	1.04	2.17	3.36	4.47	5.59	6.68	7.81	8.91	9.96	-1.13	1.04	2.17	3.36	4.47	5.59	6.68	7.81	8.91	9.96
0	5.58	0.05	0	-0.01	-0.03	-0.03	-0.04	-0.03	-0.03	-0.04	-0.04	0.02	0.02	0.03	0.04	0.05	0.07	0.10	0.13	0.16	0.18
	26.6	-0.02	-0.02	-0.02	-0.03	-0.03	-0.04	-0.04	-0.04	-0.04	-0.04	0.02	0.02	0.03	0.04	0.05	0.07	0.10	0.13	0.16	0.18
	37.2	-0.02	-0.02	-0.02	-0.03	-0.03	-0.04	-0.04	-0.04	-0.04	-0.04	0.02	0.02	0.03	0.04	0.05	0.07	0.10	0.13	0.16	0.18
	47.7	-0.01	-0.01	-0.01	-0.02	-0.02	-0.03	-0.03	-0.03	-0.03	-0.03	0.02	0.02	0.03	0.04	0.05	0.07	0.10	0.13	0.16	0.18
	58.2	-0.04	-0.13	-0.16	-0.21	-0.24	-0.28	-0.30	-0.36	-0.40	-0.45	-0.10	-0.07	-0.04	-0.02	-0.02	-0.02	-0.02	-0.02	-0.02	-0.02
	68.8	-0.05	-0.14	-0.17	-0.22	-0.25	-0.30	-0.32	-0.37	-0.42	-0.47	-0.12	-0.09	-0.06	-0.03	-0.01	-0.02	-0.02	-0.02	-0.02	-0.02
	79.3	-0.06	-0.15	-0.17	-0.22	-0.25	-0.29	-0.32	-0.36	-0.41	-0.47	-0.12	-0.10	-0.07	-0.05	-0.02	-0.01	-0.02	-0.02	-0.02	-0.02
	89.3	-0.06	-0.12	-0.14	-0.17	-0.19	-0.22	-0.21	-0.23	-0.26	-0.27	-0.11	-0.09	-0.06	-0.05	-0.02	0	0.04	0.06	0.09	0.11
	100.2	-0.06	-0.12	-0.14	-0.17	-0.19	-0.22	-0.21	-0.23	-0.26	-0.27	-0.09	-0.09	-0.06	-0.05	-0.03	-0.01	0.03	0.05	0.08	0.09
	110.9	-0.01	-0.06	-0.07	-0.10	-0.10	-0.11	-0.10	-0.11	-0.12	-0.13	-0.07	-0.07	-0.05	-0.04	-0.02	-0.01	0.03	0.04	0.06	0.06
0.20	121.3	0	-0.04	-0.04	-0.06	-0.05	-0.06	-0.03	-0.03	-0.06	-0.06	-0.04	-0.04	-0.03	-0.03	-0.01	0	0.04	0.04	0.06	0.07
	147.8	0	-0.03	-0.03	-0.04	-0.04	-0.04	-0.03	-0.03	-0.06	-0.06	-0.01	-0.01	-0.01	-0.02	0	-0.02	-0.02	-0.02	-0.02	-0.02
	178.0	0	-0.03	-0.03	-0.04	-0.04	-0.04	-0.03	-0.03	-0.06	-0.06	-0.01	-0.01	-0.01	-0.02	0	-0.02	-0.02	-0.02	-0.02	-0.02
	0	.40	.45	.38	.29	.20	.09	-.01	-.10	-.18	-.25	-.28	-.28	-.28	-.28	-.28	-.28	-.28	-.28	-.28	-.28
	1.25	.13	.17	.41	.65	.87	1.21	1.38	1.56	1.74	1.96	-.14	.06	.16	.24	.30	.37	.41	.44	.47	.49
	2.5	.08	.16	.35	.57	.83	1.18	1.35	1.54	1.74	1.96	-.14	.06	.16	.24	.30	.37	.41	.44	.47	.49
	5	.01	.17	.30	.49	.78	1.01	1.35	1.48	1.75	1.97	-.17	.02	.07	.15	.21	.28	.33	.37	.42	.45
	10	-.05	.18	.28	.37	.44	.51	.58	.68	1.16	1.36	-.15	.05	.01	.08	.12	.18	.23	.27	.32	.35
	20	-.08	.21	.28	.35	.41	.48	.53	.62	.80	1.07	-.19	.11	.07	.01	.03	.09	.13	.17	.22	.25
	30	-.14	.25	.30	.36	.41	.45	.50	.58	.62	.66	-.18	.13	.09	.04	0	.04	.08	.12	.16	.18
0.40	40	-.16	.25	.30	.35	.38	.42	.44	.50	.53	.58	-.20	.18	.15	.11	.08	.03	0	.03	.07	.08
	50	-.13	.21	.25	.29	.31	.33	.34	.38	.40	.41	-.17	.16	.13	.10	.08	.05	0	.01	.04	.06
	60	-.08	.14	.17	.20	.21	.22	.23	.27	.28	.28	-.11	.12	.09	.07	.05	.02	0	.02	.05	.06
	70	-.02	.07	.09	.11	.12	.12	.12	.16	.16	.16	-.05	.04	.03	.03	.02	.01	0	.02	.04	.05
	80	-.03	.01	.01	.03	.03	.03	.03	.06	.06	.06	-.02	.01	.01	.01	.01	.01	0	.03	.04	.05
	90	.03	.07	.09	.11	.12	.12	.12	.16	.16	.16	-.02	.01	.01	.01	.01	.01	0	.03	.04	.05
	0	.42	.40	.25	.03	-.17	-.37	-.53	-.69	-.82	-.90	-.28	-.02	.12	.23	.30	.37	.41	.44	.47	.49
	1.25	.16	.17	.47	.81	1.18	1.44	1.63	1.77	1.90	2.05	-.23	.03	.06	.15	.22	.28	.33	.37	.42	.45
	2.5	.05	.25	.53	.80	1.11	1.38	1.55	1.70	1.85	1.96	-.22	.09	.01	.07	.12	.19	.23	.27	.31	.35
	5	-.04	.24	.44	.68	.95	1.19	1.44	1.60	1.70	1.80	-.22	.14	.08	.02	.03	.08	.12	.16	.20	.23
0.60	10	-.09	.23	.38	.44	.53	.64	1.01	1.10	1.10	1.06	-.22	.16	.12	.06	.02	.03	.06	.10	.13	.15
	20	-.16	.25	.32	.37	.41	.46	.63	.96	1.12	1.19	-.21	.18	.14	.10	.06	.03	0	.03	.07	.09
	30	-.14	.20	.25	.27	.30	.31	.32	.30	.47	.76	-.14	.12	.09	.07	.04	.02	0	.02	.04	.06
	40	-.08	.17	.18	.20	.21	.22	.22	.20	.22	.29	-.14	.12	.09	.07	.04	.02	0	.02	.04	.06
	50	-.03	.10	.12	.13	.13	.13	.13	.14	.15	.13	-.05	.05	.06	.05	.03	.02	0	.01	.03	.05
	60	.01	.02	.05	.06	.06	.07	.08	.06	.05	.05	-.02	.02	.02	.02	.02	.01	0	.02	.04	.05
	70	.06	.02	.01	0	0	0	0	0	0	0	.03	.03	.02	.02	.02	.02	0	.03	.04	.05
	80	.01	.02	.05	.06	.06	.07	.08	.06	.05	.05	-.02	.02	.02	.02	.02	.01	0	.02	.04	.05
	90	.06	.02	.01	0	0	0	0	0	0	0	.03	.03	.02	.02	.02	.02	0	.03	.04	.05
	0	.41	.45	.30	.05	-.20	-.47	-.60	-.73	-.70	-.66	-.27	.03	.18	.30	.36	.42	.44	.45	.48	.49
0.80	1.25	.19	.19	.47	.83	1.20	1.39	1.54	1.70	1.84	1.93	-.23	.03	.09	.18	.25	.31	.34	.37	.40	.43
	2.5	.06	.24	.53	.85	1.14	1.32	1.44	1.68	1.75	1.82	-.27	.03	.09	.18	.25	.31	.34	.37	.40	.43
	5	-.05	.25	.47	.75	1.04	1.20	.95	.79	.65	.60	-.23	.03	.09	.18	.25	.31	.34	.37	.40	.43
	10	-.09	.22	.37	.42	.54	.64	.76	.61	.60	.59	-.23	.08	.06	.06	.14	.20	.24	.27	.30	.33
	20	-.09	.21	.30	.39	.43	.47	.68	.77	.79	.79	-.21	.13	.07	0	.05	.10	.12	.16	.19	.21
	30	-.12	.22	.29	.36	.39	.45	.66	.76	.76	.76	-.21	.14	.10	.05	0	.04	.07	.10	.12	.13
	40	-.12	.21	.27	.31	.33	.36	.53	.63	.62	.62	-.16	.13	.10	.07	.05	.02	0	.02	.04	.06
	50	-.11	.18	.23	.26	.27	.28	.39	.49	.48	.48	-.07	.09	.06	.05	.03	.01	0	.03	.05	.06
	60	-.08	.15	.16	.18	.19	.20	.28	.37	.36	.36	-.03	.02	.03	.02	.02	.01	0	.03	.05	.06
	70	-.01	.04	.05	.05	.05	.05	.08	.08	.08	.08	.05	.05	.03	.03	.03	.04	.03	.03	.04	.05
0.95	0	.39	.50	.36	.16	-.03	-.21	-.34	-.45	-.57	-.55	-.26	-.01	.12	.22	.29	.35	.37	.39	.39	.39
	1.25	.04	.25	.52	.84	1.12	1.34	1.38	.99	.58	.56	-.22	-.06	.04	.12	.19	.24	.27	.29	.30	.30
	2.5	-.01	.22	.38	.53	.74	.91	.96	1.04	.92	.92	-.20	.08	.01	.07	.12	.17	.20	.22	.23	.24
	5	-.07	.21	.30	.38	.42	.49	.54	.54	.39	.27	-.19	.12	.06	0	.05	.09	.11	.13	.14	.14
	10	-.10	.20	.26	.30	.32	.36	.45	.60	.43	.30	-.18	.14	.12	.07	.04	.01	0	.01	.01	.01
	20	-.11	.17	.22	.24	.25	.26	.29	.16	.30	.31	-.14	.12	.10	.06	.04	.02	0	.02	.02	.03
	30	-.06	.13	.14	.16	.16	.17	.14	.12	.27	.32	-.08	.08	.07	.05	.03	.01	0	.03	.04	.06
	40	-.01	.01	.07	.08	.08	.09	.08	.13	.29	.33	-.07	.07	.07	.07	.07	.07	.07	.07	.07	.07
	50	.05	.02	.02	.02	.02	.02	.07	.15	.30	.34	-.07	.07	.07	.07	.07	.07	.07	.07	.07	.07
	60	.06	.07	.03	.03	.03	.03	.06	.16	.30	.35	-.07	.07	.07	.07	.07	.07	.07	.07	.07	.07

TABLE VI.- PRESSURE COEFFICIENTS AT SIX SPANWISE STATIONS; $M = 0.85$

η	Percent chord	Upper surface										Lower surface									
		Angle of attack, deg.										Angle of attack, deg.									
		1.25	1.14	2.29	3.41	4.60	5.69	6.84	7.96	9.01	10.09	1.25	1.14	2.29	3.41	4.60	5.69	6.84	7.96	9.01	10.09
0	5.58	0.01	0.01	-0.01	-0.02	-0.02	-0.02	-0.02	-0.03	-0.03	-0.02	0	0.02	0.04	0.04	0.06	0.08	0.11	0.13	0.15	0.17
	26.6	-	-	-	-	-	-	-	-	-	-	-0.04	0	0.04	0.05	0.07	0.11	0.14	0.17	0.19	0.22
	37.2	-0.01	-0.06	-0.09	-0.13	-0.15	-0.18	-0.22	-0.25	-0.28	-0.31	-0.07	-0.02	0.03	0.04	0.07	0.11	0.15	0.17	0.20	0.23
	47.7	-0.04	-0.09	-0.13	-0.17	-0.20	-0.23	-0.27	-0.30	-0.32	-0.35	-0.11	-0.04	0.01	0.02	0.06	0.09	0.12	0.15	0.18	0.22
	58.2	-0.06	-0.14	-0.18	-0.23	-0.26	-0.29	-0.34	-0.37	-0.40	-0.42	-0.15	-0.08	-0.03	-0.02	0.02	0.06	0.09	0.12	0.15	0.18
	68.8	-0.10	-0.16	-0.20	-0.25	-0.29	-0.34	-0.38	-0.41	-0.44	-0.48	-0.18	-0.10	-0.05	-0.04	-0.01	0.03	0.07	0.09	0.12	0.16
	79.3	-0.11	-0.17	-0.22	-0.27	-0.31	-0.36	-0.41	-0.44	-0.46	-0.50	-0.19	-0.12	-0.07	-0.05	-0.02	0.02	0.05	0.07	0.10	0.13
	89.3	-	-	-	-	-	-	-	-	-	-	-0.18	-0.11	-0.06	-0.05	-0.02	0.01	0.04	0.06	0.08	0.11
	100.2	-0.11	-0.14	-0.18	-0.21	-0.23	-0.27	-0.37	-0.43	-0.49	-0.54	-0.16	-0.10	-0.07	-0.06	-0.03	0	0.02	0.04	0.07	0.09
	110.9	-	-	-	-	-	-	-	-	-	-	-0.13	-0.08	-0.05	-0.05	-0.03	0	0.02	0.04	0.06	0.07
	121.3	-0.05	-0.07	-0.08	-0.10	-0.10	-0.11	-0.11	-0.11	-0.11	-0.09	-0.09	-0.05	-0.03	-0.03	-0.01	0.01	0.02	0.04	0.05	0.07
147.8	-0.04	-0.04	-0.04	-0.06	-0.05	-0.05	-0.05	-0.05	-0.05	-0.05	-	-	-	-	-	-	-	-	-	-	
178.0	-0.03	-0.03	-0.03	-0.04	-0.04	-0.03	-0.04	-0.03	-0.04	-0.04	-0.03	-0.02	-0.01	-0.02	-0.01	0	0.01	0.01	0.01	0.02	
0.20	0	0.41	0.45	0.39	0.32	0.23	0.15	0.05	-0.01	-0.06	-0.15	-	-	-	-	-	-	-	-	-	-
	1.25	0.10	0.18	0.24	0.23	0.16	0.11	0.07	0.01	0.01	0.01	-0.16	0.06	0.18	0.24	0.32	0.38	0.43	0.45	0.48	0.51
	2.5	0.05	0.17	0.26	0.36	0.45	0.51	0.55	0.58	0.61	0.64	-0.11	0.04	0.12	0.19	0.26	0.32	0.36	0.38	0.42	0.46
	5	-0.01	0.18	0.31	0.40	0.50	0.76	1.17	1.39	1.45	1.47	-0.20	-0.01	0.09	0.15	0.22	0.29	0.35	0.38	0.42	0.46
	10	-0.07	0.20	0.29	0.36	0.45	0.51	0.64	0.88	1.04	1.24	-0.19	-0.05	0.03	0.07	0.14	0.20	0.25	0.28	0.32	0.36
	20	-0.12	0.22	0.29	0.36	0.43	0.54	0.74	0.98	1.20	1.48	-0.24	-0.12	0.05	0.02	0.04	0.10	0.14	0.18	0.21	0.25
	30	-	-	-	-	-	-	-	-	-	-	-0.25	-0.14	0.06	0.05	0	0.06	0.09	0.12	0.16	0.19
	40	-0.20	0.28	0.34	0.41	0.46	0.52	0.60	0.64	0.67	0.69	-	-	-	-	-	-	-	-	-	-
	50	-0.23	0.29	0.35	0.41	0.48	0.54	0.61	0.66	0.70	0.72	-0.29	-0.20	0.14	0.12	0.08	-0.03	0	0.03	0.05	0.09
	60	-0.19	0.24	0.28	0.33	0.36	0.45	0.59	0.65	0.69	0.74	-0.26	-0.18	0.13	0.12	0.08	-0.04	-0.01	0.01	0.03	0.06
	70	-0.14	0.16	0.18	0.21	0.22	0.24	0.30	0.36	0.41	0.42	-0.18	-0.13	0.09	0.08	0.05	0.02	0	0.02	0.04	0.06
80	-0.07	0.08	0.09	0.11	0.12	0.12	0.15	0.17	0.17	0.20	-0.11	-0.05	0.04	0.05	0.03	0	0.01	0.02	0.03	0.05	
90	-0.02	0	0	-0.02	-0.02	-0.03	-0.05	-0.06	-0.06	-0.06	-0.02	0	0.01	0.01	0.02	0.03	0.03	0.03	0.03	0.04	
0.40	0	0.42	0.40	0.24	0.05	-0.12	-0.27	-0.46	-0.60	-0.68	-0.78	-	-	-	-	-	-	-	-	-	-
	1.25	0.13	0.19	0.22	0.12	-0.03	-0.12	-0.29	-0.43	-0.50	-0.54	-	-	-	-	-	-	-	-	-	-
	2.5	0.01	0.29	0.39	0.27	-0.11	-0.31	-0.45	-0.72	-0.81	-0.83	-0.33	0	0.17	0.23	0.31	0.37	0.42	0.44	0.47	0.49
	5	-0.07	0.27	0.30	0.27	-0.15	-0.31	-0.45	-0.72	-0.81	-0.83	-0.29	-0.04	0.08	0.15	0.23	0.28	0.33	0.36	0.40	0.44
	10	-0.12	0.26	0.31	0.27	-0.19	-0.39	-0.59	-0.88	-1.04	-1.20	-0.28	-0.09	0.01	0.06	0.13	0.19	0.24	0.27	0.31	0.35
	20	-	-	-	-	-	-	-	-	-	-	-0.29	-0.14	0.07	0.03	0.04	0.09	0.13	0.16	0.20	0.24
	30	-0.21	0.27	0.34	0.40	0.45	0.51	0.61	0.68	0.71	0.73	-0.29	-0.17	0.11	0.06	0.02	0.03	0.07	0.09	0.13	0.17
	40	-	-	-	-	-	-	-	-	-	-	-0.29	-0.19	0.13	0.10	0.06	-0.03	0.01	0.03	0.06	0.10
	50	-0.19	0.22	0.25	0.29	0.29	0.28	0.31	0.44	0.62	0.86	-	-	-	-	-	-	-	-	-	-
	60	-0.13	0.18	0.17	0.21	0.21	0.20	0.22	0.30	0.39	0.44	-0.21	-0.12	0.06	0.07	0.04	-0.02	0	0.01	0.04	0.06
	70	-0.07	0.06	0.10	0.13	0.12	0.12	0.15	0.18	0.22	0.26	-0.10	-0.05	0.05	0.05	0.03	0	0.01	0.01	0.03	0.06
80	-0.03	0.02	0.04	0.06	0.06	0.06	0.09	0.07	0.06	0.04	-0.02	-0.02	0.02	0.02	0.01	0.01	0.02	0.02	0.03	0.05	
90	0.02	0.03	0.02	0.01	0.01	0.01	0	0	0	0.01	0	0.03	0.03	0.02	0.03	0.03	0.04	0.03	0.04	0.06	
0.60	0	0.42	0.44	0.29	0.09	-0.15	-0.37	-0.59	-0.72	-0.66	-0.60	-	-	-	-	-	-	-	-	-	-
	1.25	0.16	0.27	0.30	0.14	-0.13	-0.27	-0.43	-0.68	-0.82	-0.96	-	-	-	-	-	-	-	-	-	-
	2.5	0.02	0.27	0.30	0.14	-0.14	-0.31	-0.45	-0.72	-0.83	-0.97	-0.32	0.04	0.21	0.30	0.37	0.42	0.46	0.47	0.49	0.51
	5	-0.05	0.27	0.33	0.27	-0.16	-0.31	-0.45	-0.72	-0.81	-0.96	-0.29	-0.03	0.12	0.18	0.26	0.32	0.36	0.39	0.40	0.43
	10	-0.10	0.24	0.30	0.21	-0.20	-0.37	-0.57	-0.77	-0.96	-1.07	-0.26	-0.08	0.03	0.08	0.16	0.21	0.26	0.28	0.31	0.34
	20	-0.14	0.24	0.31	0.39	0.46	0.54	0.64	0.77	0.98	1.08	-0.28	-0.13	0.04	0	0.06	0.10	0.15	0.17	0.19	0.22
	30	-0.18	0.24	0.30	0.37	0.47	0.54	0.69	0.74	0.89	0.97	-0.27	-0.15	0.08	0.05	0.01	0.05	0.08	0.10	0.12	0.15
	40	-0.17	0.23	0.27	0.33	0.44	0.53	0.63	0.73	0.85	0.93	-0.26	-0.16	0.09	0.07	0.03	0	0.02	0.03	0.04	0.06
	50	-0.15	0.20	0.22	0.26	0.27	0.25	0.23	0.42	0.66	0.88	-0.22	-0.14	0.08	0.08	0.04	-0.01	0.01	0.02	0.03	0.04
	60	-0.11	0.15	0.16	0.19	0.18	0.17	0.16	0.16	0.36	0.67	-0.13	-0.09	0.06	0.05	0.02	0	0.02	0.02	0.02	0.02
	70	-	-	-	-	-	-	-	-	-	-	-0.07	-0.02	0.02	0.02	0.02	0	0.02	0.02	0.02	0.01
80	-0.02	0.02	0.03	0.05	0.04	0.03	0.04	0.08	0.35	0.60	-	-	-	-	-	-	-	-	-	-	
90	0.02	0.02	0.02	0	0.01	0.01	0.01	0.05	0.25	0.53	0.02	0.04	0.04	0.03	0.04	0.04	0.03	0.01	-0.01	-0.07	
0.80	0	0.40	0.49	0.35	0.18	0	-0.13	-0.27	-0.35	-0.28	-0.26	-	-	-	-	-	-	-	-	-	-
	1.25	0.01	0.29	0.39	0.21	-0.15	-0.27	-0.43	-0.61	-0.61	-0.50	-0.32	0	0.16	0.23	0.30	0.36	0.39	0.40	0.41	0.40
	2.5	-0.06	0.27	0.30	0.24	-0.14	-0.31	-0.45	-0.72	-0.87	-0.97	-0.28	-0.05	0.07	0.13	0.20	0.26	0.28	0.31	0.31	0.30
	5	-	-	-	-	-	-	-	-	-	-	-0.27	-0.08	0.02	0.07	0.13	0.19	0.23	0.23	0.23	0.23
	10	-0.13	0.23	0.32	0.40	0.43	0.54	0.55	0.48	0.35	0.28	-0.27	-0.12	0.04	0	0.06	0.11	0.14	0.15	0.15	0.15
	20	-	-	-	-	-	-	-	-	-	-	-0.26	-0.14	0.08	0.04	0.01	0.04	0.07	0.08	0.07	0.07
	30	-0.16	0.22	0.26	0.31	0.32	0.44	0.53	0.48	0.36	0.33	-0.25	-0.15	0.09	0.07	0.03	0	0.02	0.03	0.01	0
	40	-0.16	0.19	0.21	0.24	0.24	0.30	0.30	0.50	0.39	0.35	-0.20	-0.13	0.08	0.06	0.04	-0.01	0.01	0.01	0.02	0.04
	50	-0.12	0.13	0.13	0.16	0.16	0.17	0.43	0.48	0.40	0.36	-0.11	-0.09	0.05	0.05	0.03	-0.01	0	0	0.05	0.07
	60	0.05	0.03	0.06	0.08	0.09	0.07	0.30	0.45	0.39	0.37	-	-	-	-	-	-	-	-	-	-
	70	0.01	0.01	0	0.02	0	0	0.18	0.38	0.37	0.37	-	-	-	-	-	-	-	-	-	-
80	0.04	0.06	0.05	0.03	0.03	0.03	0.06	0.30	0.36	0.38	0.04	0.07	0.06	0.05	0.05	0.05	0.04	0	-0.12		

TABLE VII.- PRESSURE COEFFICIENTS AT SIX SPANWISE STATIONS; $M = 0.90$

η	Percent chord	Upper surface									Lower surface								
		Angle of attack, deg									Angle of attack, deg								
		1.30	1.16	2.34	3.48	4.64	5.81	6.98	8.09	9.15	1.30	1.16	2.34	3.48	4.64	5.81	6.98	8.09	9.15
0	5.58	0.04	0.03	0.02	0.01	0	0.01	0.01	0.01	0	0.02	0.01	0.06	0.06	0.08	0.11	0.12	0.14	0.16
	26.6	-.02	-.03	-.06	-.09	-.13	-.15	-.19	-.22	-.25	-.02	-.04	-.06	-.08	-.10	-.14	-.16	-.19	-.22
	37.2	-.02	-.07	-.10	-.14	-.17	-.19	-.24	-.26	-.30	-.05	-.08	-.10	-.12	-.14	-.18	-.20	-.23	-.26
	47.7	-.07	-.13	-.16	-.20	-.24	-.26	-.30	-.33	-.36	-.14	-.06	-.03	0	0.04	0.08	0.11	0.14	0.16
	58.2	-.10	-.16	-.20	-.24	-.29	-.30	-.36	-.38	-.42	-.18	-.09	-.06	-.03	0.01	0.05	0.07	0.11	0.13
	79.3	-.13	-.19	-.23	-.28	-.32	-.34	-.38	-.41	-.44	-.20	-.11	-.07	-.04	-.01	0.03	0.05	0.08	0.10
	89.3	-.12	-.19	-.26	-.31	-.36	-.37	-.43	-.45	-.49	-.21	-.11	-.07	-.05	-.02	0.02	0.04	0.06	0.09
	100.2	-.04	-.05	-.07	-.08	-.15	-.24	-.41	-.47	-.53	-.16	-.08	-.06	-.05	-.03	0	0.02	0.03	0.05
	110.9	-.02	-.03	-.04	-.04	-.02	-.03	-.03	-.04	-.04	-.07	-.03	-.02	-.02	-.01	0.01	0.01	0.01	0.02
	121.3	-.02	-.01	-.02	-.02	0	0	-.01	-.01	-.02	-.02	0	0	0	0	0.02	0.02	0.02	0.02
0.20	0	.42	.46	.42	.34	.25	.20	.12	.06	-.01	-.15	-.08	-.19	-.26	-.33	-.40	-.44	-.47	-.49
	1.25	.13	.16	.38	.59	.88	1.11	1.28	1.36	1.40	-.36	-.01	.14	.23	.31	.36	.40	.44	.45
	2.5	.08	.15	.32	.51	.82	1.02	1.20	1.29	1.33	-.32	-.04	.07	.15	.23	.28	.32	.36	.39
	5	.02	.15	.28	.35	.48	.57	1.16	1.25	1.30	-.32	-.09	0	.07	.13	.18	.23	.27	.29
	10	-.04	.17	.26	.33	.42	.46	.68	.88	.98	-.34	-.14	-.07	-.02	.04	.08	.13	.16	.18
	20	-.10	.21	.27	.33	.41	.42	.49	.53	.62	-.34	-.17	-.10	-.06	-.01	.03	.06	.09	.11
	30	-.19	.32	.45	.54	.61	.65	.69	.78	.90	-.34	-.19	-.13	-.10	-.06	-.03	.01	.03	.04
	40	-.20	.29	.34	.40	.47	.50	.56	.59	.64	-.13	-.09	-.07	-.06	-.04	-.02	-.01	.01	.01
	50	-.24	.34	.38	.44	.50	.53	.60	.63	.67	-.07	-.05	-.04	-.04	-.03	-.01	0	.01	.01
	60	-.22	.33	.41	.46	.52	.55	.61	.64	.69	-.03	-.01	0	0	0	.01	.01	.01	.01
0.40	0	.42	.39	.26	.11	-.05	-.18	-.34	-.45	-.55	-.36	-.01	.14	.23	.31	.36	.40	.44	.45
	1.25	.13	.21	.49	.76	1.01	1.13	1.25	1.32	1.37	-.32	-.04	.07	.15	.23	.28	.32	.36	.39
	2.5	.01	.32	.59	.85	1.06	1.16	1.27	1.34	1.38	-.32	-.09	0	.07	.13	.18	.23	.27	.29
	5	-.05	.31	.51	.76	.97	1.11	1.24	1.31	1.35	-.34	-.14	-.07	-.02	.04	.08	.13	.16	.18
	10	-.11	.31	.44	.62	.86	1.04	1.17	1.24	1.29	-.34	-.17	-.10	-.06	-.01	.03	.06	.09	.11
	20	-.19	.32	.45	.54	.61	.65	.69	.78	.90	-.34	-.19	-.13	-.10	-.06	-.03	.01	.03	.04
	30	-.20	.29	.34	.40	.47	.50	.56	.59	.64	-.13	-.09	-.07	-.06	-.04	-.02	-.01	.01	.01
	40	-.24	.34	.38	.44	.50	.53	.60	.63	.67	-.07	-.05	-.04	-.04	-.03	-.01	0	.01	.01
	50	-.22	.33	.41	.46	.52	.55	.61	.64	.69	-.03	-.01	0	0	0	.01	.01	.01	.01
	60	-.22	.33	.41	.46	.52	.55	.61	.64	.69	-.03	-.01	0	0	0	.01	.01	.01	.01
0.60	0	.42	.43	.29	.11	-.10	-.26	-.46	-.58	-.66	-.36	-.08	.23	.31	.37	.42	.44	.47	.47
	1.25	.19	.22	.54	.85	1.06	1.12	1.26	1.33	1.28	-.32	0	.13	.20	.27	.32	.35	.38	.40
	2.5	.07	.33	.66	.91	1.10	1.17	1.28	1.34	1.29	-.32	-.04	.07	.15	.23	.28	.32	.36	.39
	5	-.01	.32	.62	.96	1.12	1.19	1.30	1.35	1.27	-.31	-.07	.04	.10	.16	.21	.25	.28	.30
	10	-.06	.28	.43	.82	1.03	1.12	1.24	1.29	1.23	-.28	-.11	-.03	.02	.06	.11	.14	.17	.19
	20	-.11	.25	.30	.41	.91	1.03	1.16	1.23	1.17	-.28	-.14	-.07	-.03	.02	.06	.11	.14	.16
	30	-.15	.26	.32	.33	.55	.91	1.09	1.09	1.03	-.28	-.14	-.07	-.03	.02	.06	.11	.14	.16
	40	-.15	.24	.29	.30	.27	.41	.76	.71	.82	-.20	-.13	-.08	-.06	-.03	0	.01	.03	.03
	50	-.13	.20	.23	.25	.20	.16	.42	.74	.82	-.12	-.07	-.04	-.03	-.01	.01	.02	.04	.03
	60	-.09	.14	.15	.17	.14	.10	.34	.71	.72	-.07	-.02	-.01	-.01	.01	.02	.03	.05	.03
0.80	0	.42	.49	.35	.19	-.03	-.09	-.24	-.25	-.22	-.35	-.03	.17	.26	.33	.37	.40	.43	.43
	4	.04	.34	.68	1.01	1.16	1.23	1.12	1.59	.45	-.29	-.03	.09	.15	.22	.27	.31	.34	.33
	8	-.02	.29	.48	.89	1.10	1.18	.97	.60	.46	-.28	-.06	.04	.10	.16	.20	.23	.27	.27
	12	-.02	.29	.48	.89	1.10	1.18	.97	.60	.46	-.28	-.06	.04	.10	.16	.20	.23	.27	.27
	20	-.10	.25	.33	.40	.75	.93	.61	.55	.47	-.28	-.11	-.03	.03	.08	.12	.15	.18	.18
	30	-.11	.23	.28	.31	.31	.41	.57	.61	.52	-.25	-.14	-.09	-.05	.02	.04	.07	.10	.11
	40	-.13	.20	.22	.24	.24	.33	.62	.57	.47	-.19	-.12	-.07	-.05	.02	.04	.07	.10	.11
	50	-.08	.12	.13	.15	.14	.16	.44	.60	.58	-.11	-.08	-.04	-.03	-.01	.02	.04	.07	.08
	60	-.02	.02	.05	.07	.06	.04	.29	.54	.53	-.05	-.02	-.01	-.01	.01	.02	.03	.04	.04
	70	-.02	.02	.05	.07	.06	.04	.29	.54	.53	-.05	-.02	-.01	-.01	.01	.02	.03	.04	.04
0.95	0	.39	.48	.35	.22	.06	-.07	-.20	-.06	-.04	-.35	-.06	.04	.10	.15	.21	.23	.24	.24
	5	-.04	.34	.66	1.00	1.20	1.07	.74	.39	.31	-.32	-.06	.04	.10	.15	.21	.23	.24	.24
	10	-.15	.26	.45	.86	1.10	.93	.70	.38	.30	-.34	-.15	-.09	-.05	.01	.05	.06	.07	.07
	20	-.18	.29	.38	.36	.74	.68	.67	.35	.29	-.24	-.17	-.15	-.13	-.11	-.06	-.06	-.05	-.05
	30	-.17	.21	.28	.20	.25	.56	.62	.33	.29	-.18	-.15	-.14	-.13	-.11	-.12	-.12	-.12	-.12
	40	-.12	.18	.20	.19	.15	.44	.55	.31	.29	-.18	-.15	-.14	-.13	-.11	-.12	-.12	-.12	-.12
	50	-.06	.11	.14	.14	.11	.34	.45	.29	.29	-.06	-.07	-.07	-.06	-.07	-.06	-.11	-.15	-.17
	60	.01	-.05	-.07	-.07	-.23	.34	.27	.28	.28	-.01	-.03	0	-.01	-.01	-.02	-.07	-.14	-.16
	70	.05	.02	.02	0	-.02	.14	.23	.25	.26	.01	.03	0	-.01	-.01	-.02	-.07	-.14	-.16
	80	.08	.07	.06	.05	.02	.17	.24	.26	.26	.05	.06	.05	.03	.02	.02	-.05	-.14	-.16
	90	.11	.10	.10	.08	.05	.12	.23	.25	.25	.09	.10	.06	.06	.05	.04	-.04	-.15	-.17

CONFIDENTIAL

TABLE VIII.- PRESSURE COEFFICIENTS AT SIX SPANWISE STATIONS; $M = 0.95$

q	Per- cent chord	Upper surface										Lower surface									
		Angle of attack, deg										Angle of attack, deg									
		1.27	1.16	2.39	3.55	4.70	5.84	6.99	8.08	9.19		1.27	1.16	2.39	3.55	4.70	5.84	6.99	8.08	9.19	
0	5.58	0.06	0.05	0.04	0.04	0.04	0.05	0.06	0.05	0.05		0.05	0.06	0.07	0.09	0.10	0.13	0.15	0.17	0.19	
	26.6	-.01	-.01	-.01	-.01	-.01	-.01	-.01	-.01	-.01		-.01	-.01	-.01	-.01	-.01	-.01	-.01	-.01	-.01	
	37.2	-.04	-.04	-.04	-.06	-.06	-.11	-.13	-.16	-.20		-.01	-.04	-.07	-.10	-.12	-.16	-.20	-.23	-.25	
	47.7	-.01	-.04	-.07	-.10	-.14	-.15	-.18	-.21	-.25		-.04	-.01	-.04	-.07	-.10	-.14	-.18	-.20	-.23	
	58.2	-.05	-.10	-.14	-.16	-.19	-.21	-.24	-.27	-.30		-.10	-.05	-.01	-.02	-.06	-.10	-.14	-.16	-.19	
	68.8	-.09	-.15	-.18	-.22	-.24	-.26	-.29	-.32	-.36		-.15	-.09	-.05	-.01	-.02	-.06	-.10	-.13	-.15	
	79.3	-.12	-.17	-.22	-.25	-.28	-.29	-.32	-.35	-.39		-.17	-.12	-.08	-.04	-.01	-.03	-.07	-.10	-.12	
	89.3	-.16	-.21	-.27	-.30	-.34	-.34	-.37	-.40	-.44		-.19	-.14	-.09	-.06	-.02	-.01	-.05	-.07	-.10	
	100.2	-.16	-.21	-.27	-.30	-.34	-.34	-.37	-.40	-.44		-.22	-.16	-.12	-.09	-.06	-.01	-.02	-.04	-.06	
	110.9	-.17	-.24	-.30	-.33	-.36	-.38	-.41	-.44	-.49		-.25	-.20	-.16	-.11	-.07	-.04	-.01	-.02	-.03	
0.20	121.3	-.17	-.24	-.30	-.33	-.36	-.38	-.41	-.44	-.49		-.22	-.17	-.12	-.08	-.06	-.04	-.01	-.01	-.01	
	147.8	-.07	-.01	-.04	-.06	-.11	-.14	-.16	-.20	-.25		-.02	-.02	-.01	-.01	-.01	-.01	-.01	0	-.02	
	178.0	0	.02	0	0	0	0	-.02	-.02	-.04		.02	.02	.01	.01	.01	.01	.01	0	-.02	
	0	.47	.49	.44	.38	.32	.26	.21	.15	.09		-.17	-.12	-.07	-.02	-.01	-.01	-.01	-.01	-.01	
	1.25	.14	.12	.36	.57	.79	.95	1.09	1.17	1.24		-.06	.11	.21	.28	.34	.41	.45	.47	.52	
	2.5	.09	.12	.30	.48	.72	.88	1.05	1.12	1.19		-.13	.03	.13	.19	.25	.32	.37	.41	.46	
	5	.03	.12	.25	.32	.45	.79	.98	1.06	1.15		-.12	.01	.06	.12	.17	.22	.26	.31	.36	
	10	-.02	.14	.23	.30	.37	.40	.61	.80	.96		-.19	-.09	.03	.02	.06	.12	.17	.20	.25	
	20	-.09	.18	.25	.29	.34	.37	.42	.48	.55		-.21	.13	.07	.02	.02	.07	.12	.15	.19	
	30	-.19	.28	.33	.38	.42	.44	.49	.52	.57		-.23	.18	.13	.09	.04	0	.02	.07	.10	
0.40	40	-.24	.31	.38	.42	.46	.48	.53	.56	.60		-.26	.19	.15	.11	.07	-.03	-.01	.03	.03	
	50	-.27	.35	.41	.45	.49	.51	.54	.57	.62		-.31	.25	.18	.15	.11	.07	-.03	-.02	.02	
	60	-.24	.32	.38	.42	.46	.48	.52	.56	.60		-.28	.24	.18	.15	.10	-.08	-.05	-.05	-.06	
	70	-.21	.29	.34	.37	.41	.44	.48	.52	.57		-.25	.21	.15	.12	.08	-.05	-.05	-.05	-.06	
	80	-.07	.08	.12	.14	.18	.20	.25	.29	.34		-.12	.07	.06	.03	.01	-.06	-.06	-.07	-.07	
	90	-.07	.08	.12	.14	.18	.20	.25	.29	.34		-.12	.07	.06	.03	.01	-.06	-.06	-.07	-.07	
	0	.43	.39	.29	.16	.06	-.06	-.18	-.30	-.42		-.29	-.04	.12	.20	.27	.34	.39	.42	.46	
	1.25	.10	.17	.43	.63	.79	.92	1.03	1.11	1.18		-.27	.09	.04	.12	.19	.26	.32	.35	.38	
	2.5	.03	.30	.54	.73	.86	.97	1.06	1.13	1.20		-.28	.13	.02	.04	.10	.16	.22	.25	.29	
	5	-.09	.29	.48	.68	.82	.94	1.04	1.11	1.18		-.32	.21	.11	.06	0	.06	.11	.14	.18	
0.60	10	-.15	.30	.43	.58	.74	.87	.98	1.05	1.12		-.36	.26	.17	.11	-.06	0	.04	.07	.11	
	20	-.27	.37	.46	.51	.55	.56	.60	.73	.93		-.40	.33	.23	.15	.12	-.07	-.02	0	.04	
	30	-.31	.42	.49	.55	.59	.62	.66	.69	.72		-.34	.27	.17	.12	.10	-.07	-.05	-.03	-.01	
	40	-.27	.37	.45	.53	.57	.61	.63	.67	.69		-.31	.27	.17	.12	.10	-.07	-.05	-.03	-.01	
	50	-.14	.32	.42	.38	.39	.45	.51	.55	.58		-.17	.09	.09	.09	.09	-.05	-.05	-.05	-.05	
	60	-.01	.07	.14	.17	.20	.24	.29	.34	.38		-.17	.03	.03	.06	.06	.05	.05	.05	.05	
	70	.06	.04	0	-.06	-.09	.13	.16	-.20	-.24		.04	.05	.02	-.03	-.04	-.04	-.06	-.06	-.06	
	80	.44	.42	.32	.20	.08	-.06	-.22	-.35	-.48		-.32	0	.18	.27	.33	.37	.42	.44	.47	
	1.25	.11	.20	.48	.66	.82	.92	1.02	1.09	1.16		-.31	.07	.09	.16	.22	.27	.32	.35	.38	
	2.5	-.02	.33	.61	.76	.87	.96	1.06	1.12	1.17		-.31	.07	.09	.16	.22	.27	.32	.35	.38	
0.80	5	-.08	.35	.66	.84	.93	.99	1.08	1.14	1.18		-.35	.12	0	.07	.12	.17	.21	.25	.28	
	10	-.12	.34	.54	.75	.87	.95	1.03	1.09	1.14		-.36	.12	0	.07	.12	.17	.21	.25	.28	
	20	-.13	.35	.47	.53	.53	.53	.53	.53	.53		-.36	.16	-.06	.02	.07	.11	.14	.17	.21	
	30	-.13	.36	.53	.58	.61	.60	.59	1.02	1.06		-.38	.15	-.10	-.06	-.03	.01	.05	.07	.10	
	40	-.12	.30	.56	.64	.68	.73	.92	.99	1.00		-.38	.15	-.10	-.06	-.03	.01	.05	.07	.10	
	50	-.12	.30	.56	.64	.68	.73	.92	.99	1.00		-.38	.15	-.10	-.06	-.03	.01	.05	.07	.10	
	60	-.08	.17	.42	.52	.58	.66	.80	.92	.87		-.14	.11	-.09	-.08	-.07	-.05	-.03	-.01	0	
	70	-.01	.02	.03	-.04	-.07	-.16	-.19	-.18	-.28		-.01	.01	-.01	-.01	-.02	-.01	-.01	0	0	
	80	.01	.02	.03	-.04	-.07	-.16	-.19	-.18	-.28		-.01	.01	-.01	-.01	-.02	-.01	-.01	0	0	
	90	.05	.06	.06	.03	-.03	-.10	-.14	-.14	-.09		.07	.06	.07	.06	.03	.02	.01	0	0	
0.95	0	.46	.50	.34	.23	.13	.03	-.08	-.17	-.22		-.29	.04	.18	.25	.29	.33	.37	.40	.42	
	4	.03	.31	.75	.90	.96	1.04	1.07	.88	.56		-.24	.03	.10	.15	.20	.23	.27	.30	.33	
	8	-.03	.26	.72	.87	.96	1.02	1.04	.87	.57		-.23	.06	.06	.09	.14	.17	.21	.24	.26	
	12	-.09	.22	.44	.74	.87	.94	.92	.81	.57		-.23	.11	.02	.02	.06	.09	.13	.15	.17	
	20	-.14	.25	.19	.26	.48	.56	.56	.54	.54		-.25	.14	.06	-.02	.01	.04	.07	.09	.10	
	30	-.13	.19	.18	.12	.28	.46	.53	.54	.54		-.24	.15	.08	-.05	-.03	.01	.02	.03	.04	
	40	-.08	.12	.11	.07	.06	.29	.47	.54	.54		-.10	.08	.04	-.03	-.02	.01	.01	.01	-.02	
	50	0	.03	.04	.01	.01	.22	.39	.49	.51		-.07	.07	.07	.07	.07	.07	.07	.07	.07	
	60	.04	.02	.02	.02	.04	0	.34	.46	.55		-.07	.07	.07	.07	.07	.07	.07	.07	.07	
	70	.06	.07	.06	.05	.04	.10	.22	.39	.46		.07	.07	.07	.07	.07	.07	.07	.07	.07	

CONFIDENTIAL

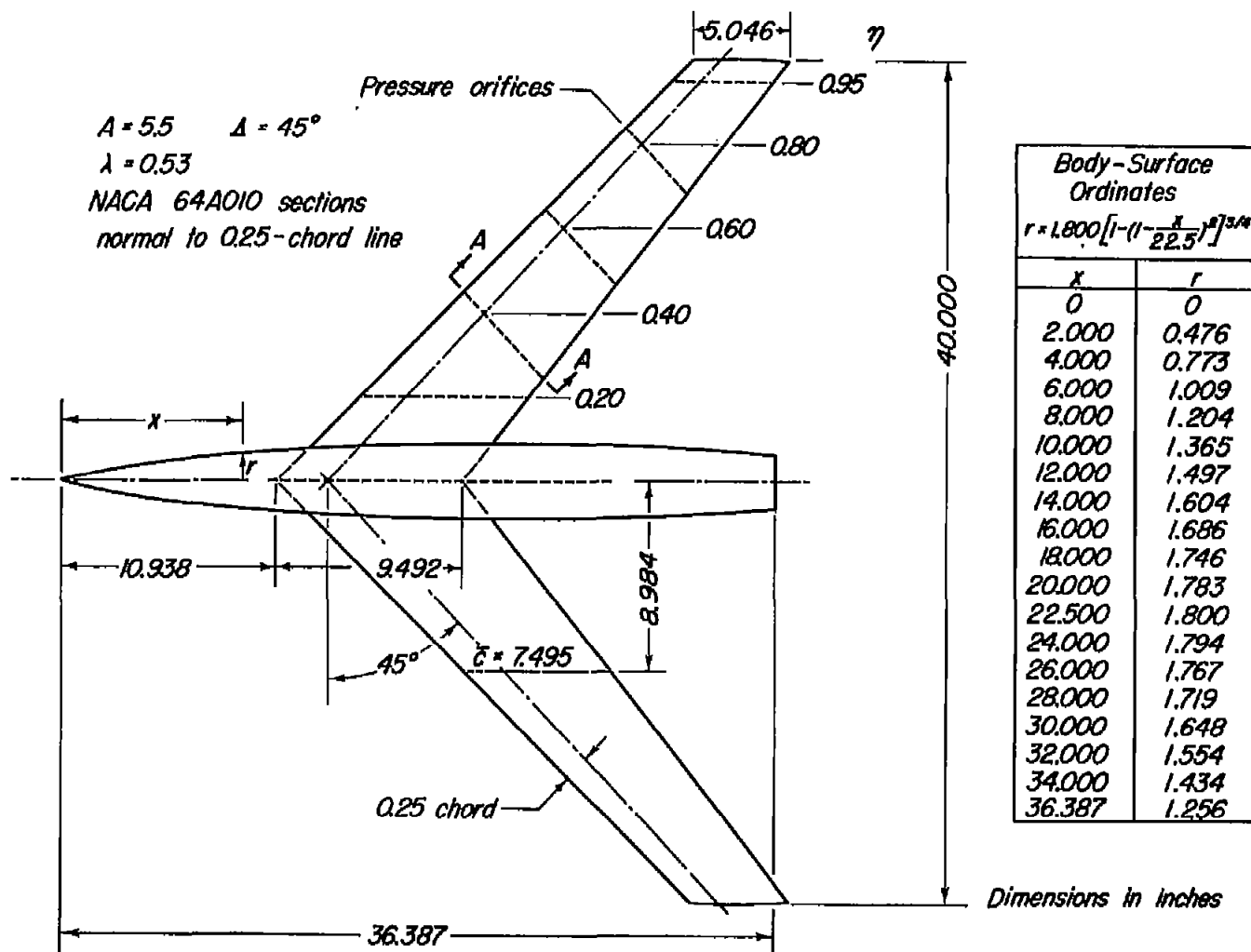


Figure 1.- Dimensions of the model and locations of the pressure orifices.

~~CONFIDENTIAL~~

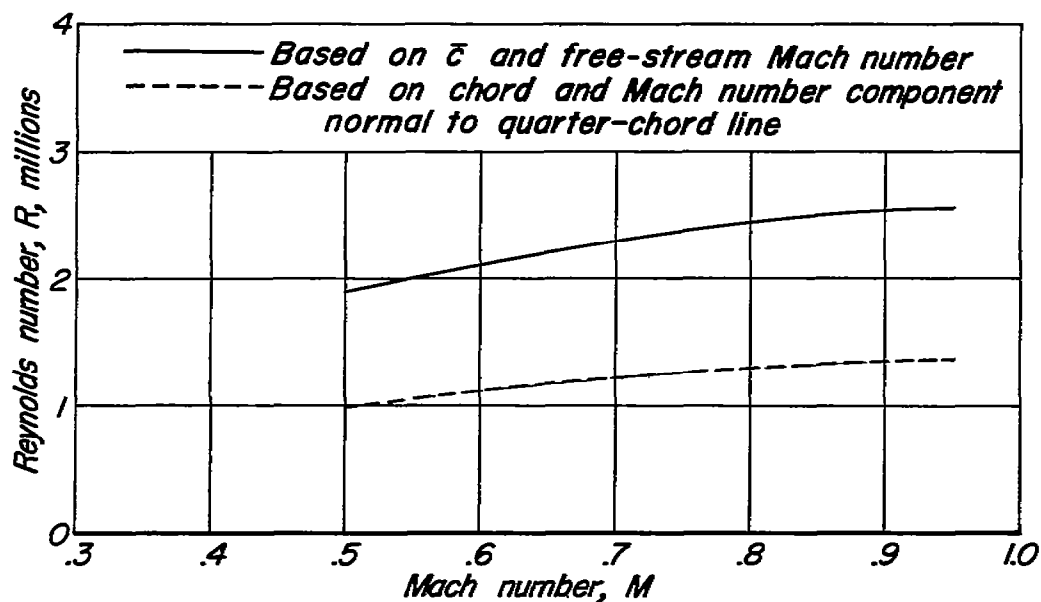
NACA RM A55C08



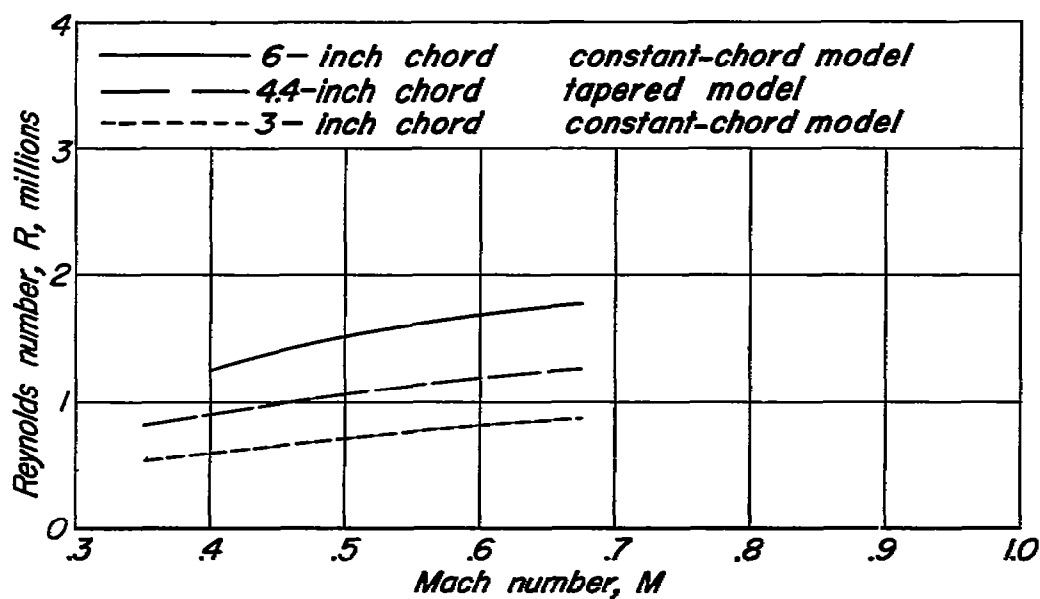
A-16440

Figure 2.- Model mounted in the Ames 16-foot high-speed wind tunnel.

~~CONFIDENTIAL~~



(a) Sweptback-wing model.



(b) Two-dimensional-flow models.

Figure 3. - Variation of Reynolds number with Mach number.

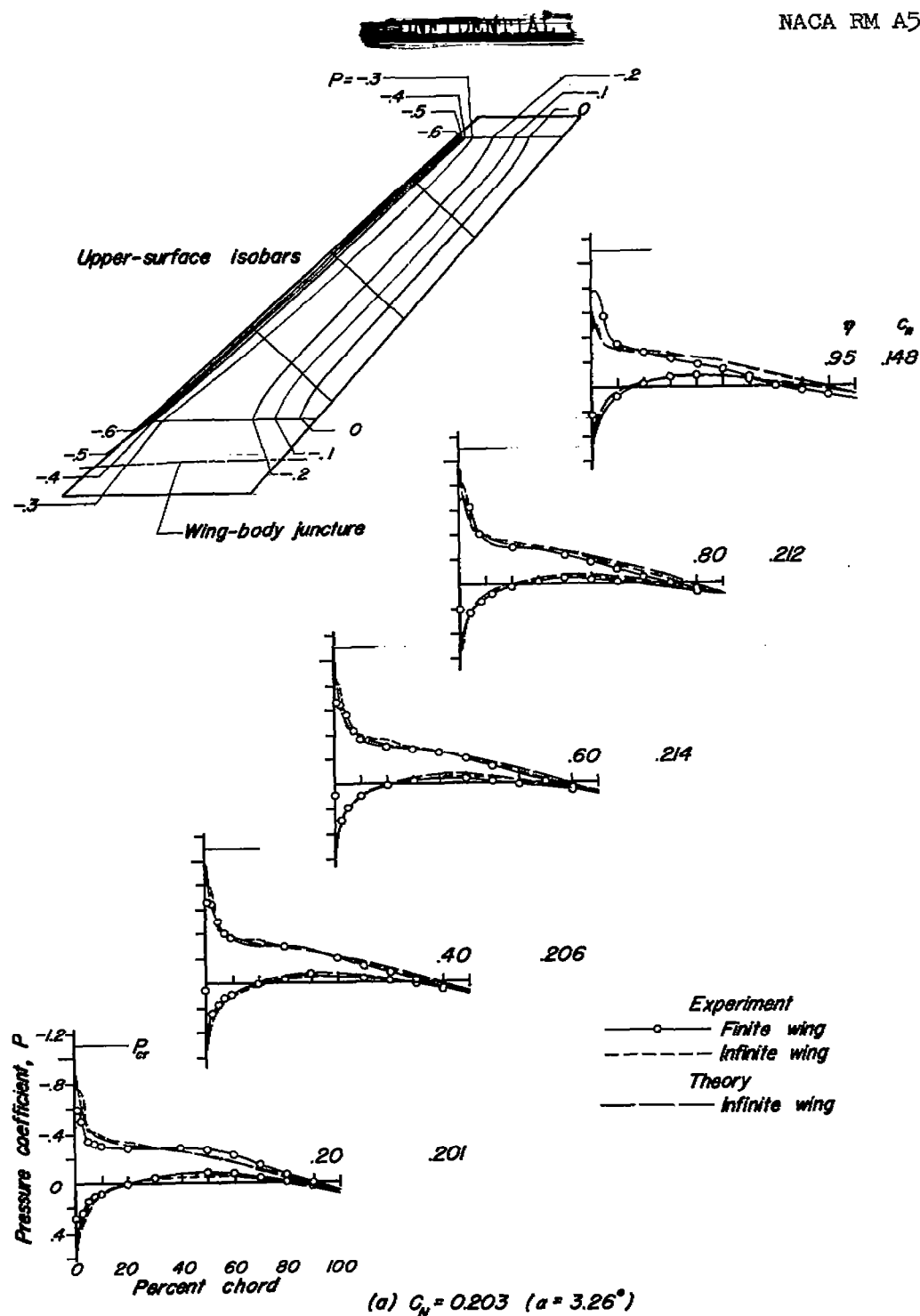
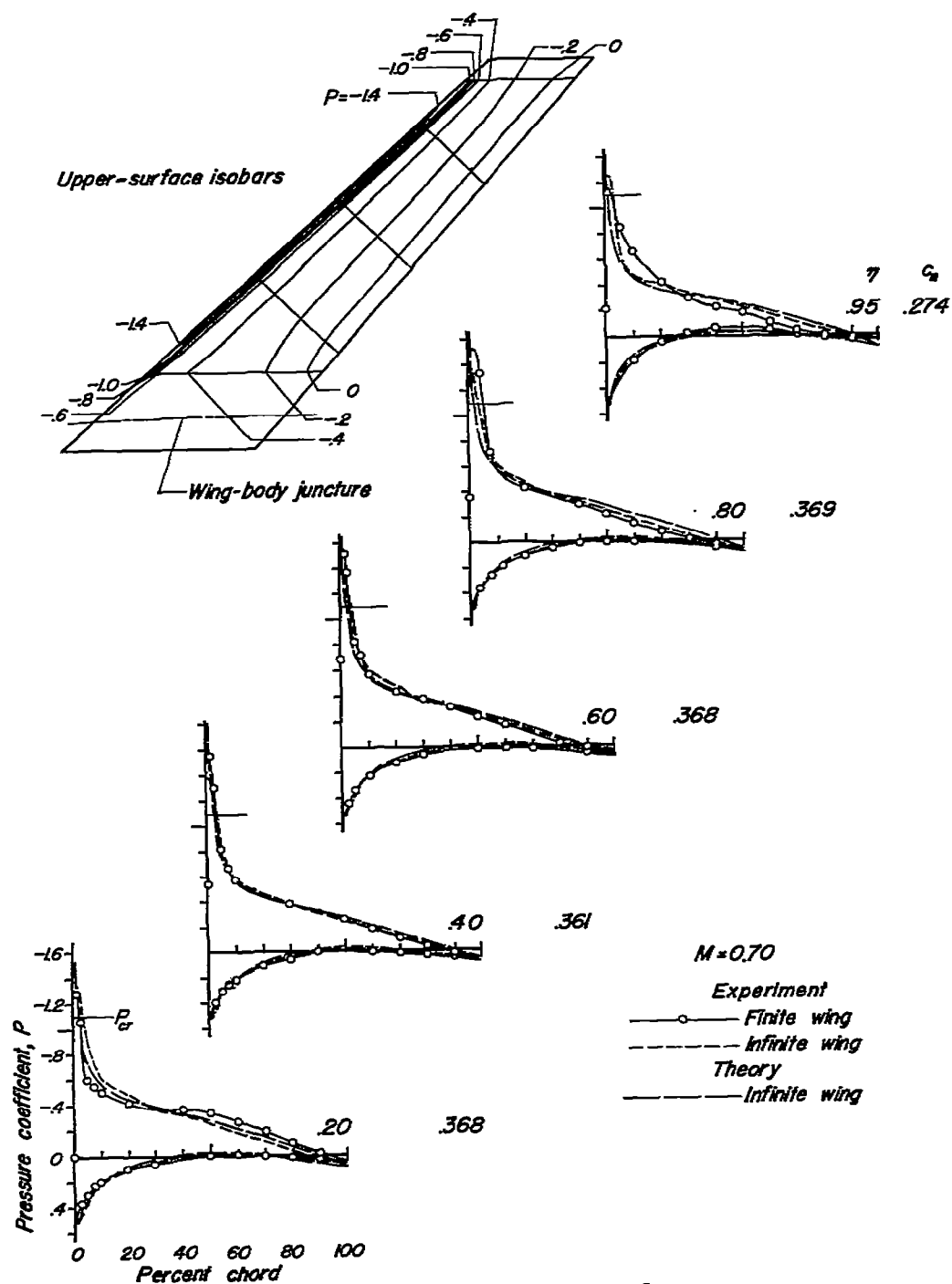


Figure 4.—Comparisons of experimental pressure distributions for five semispan stations with those for the NACA 64A010 section yawed 45° as derived from two-dimensional data and theory, plus experimental upper-surface isobars; $M = 0.70$.

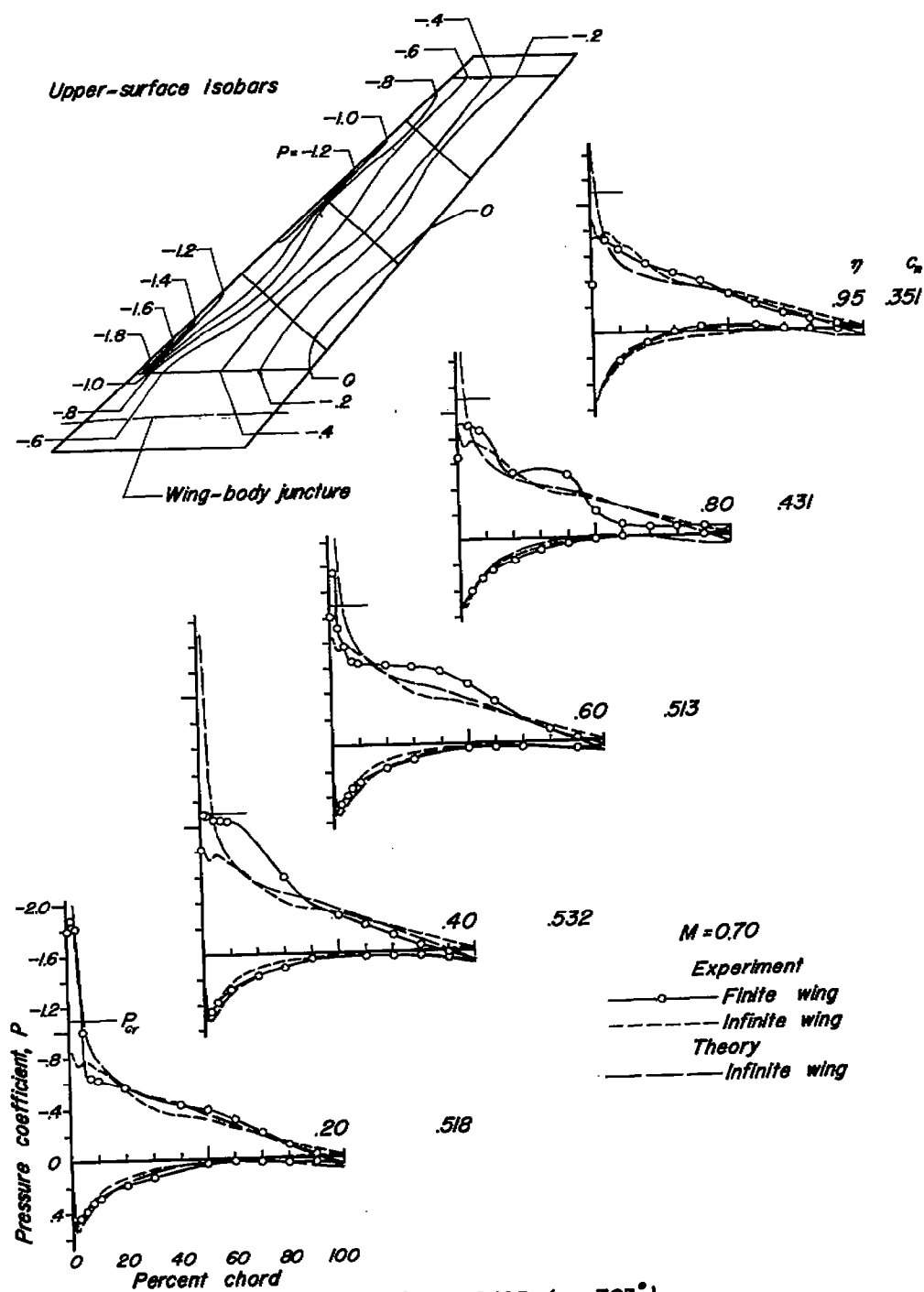
CONFIDENTIAL



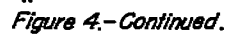
(b) $C_H = 0.363$ ($\alpha = 5.46^\circ$)

Figure 4.-Continued.

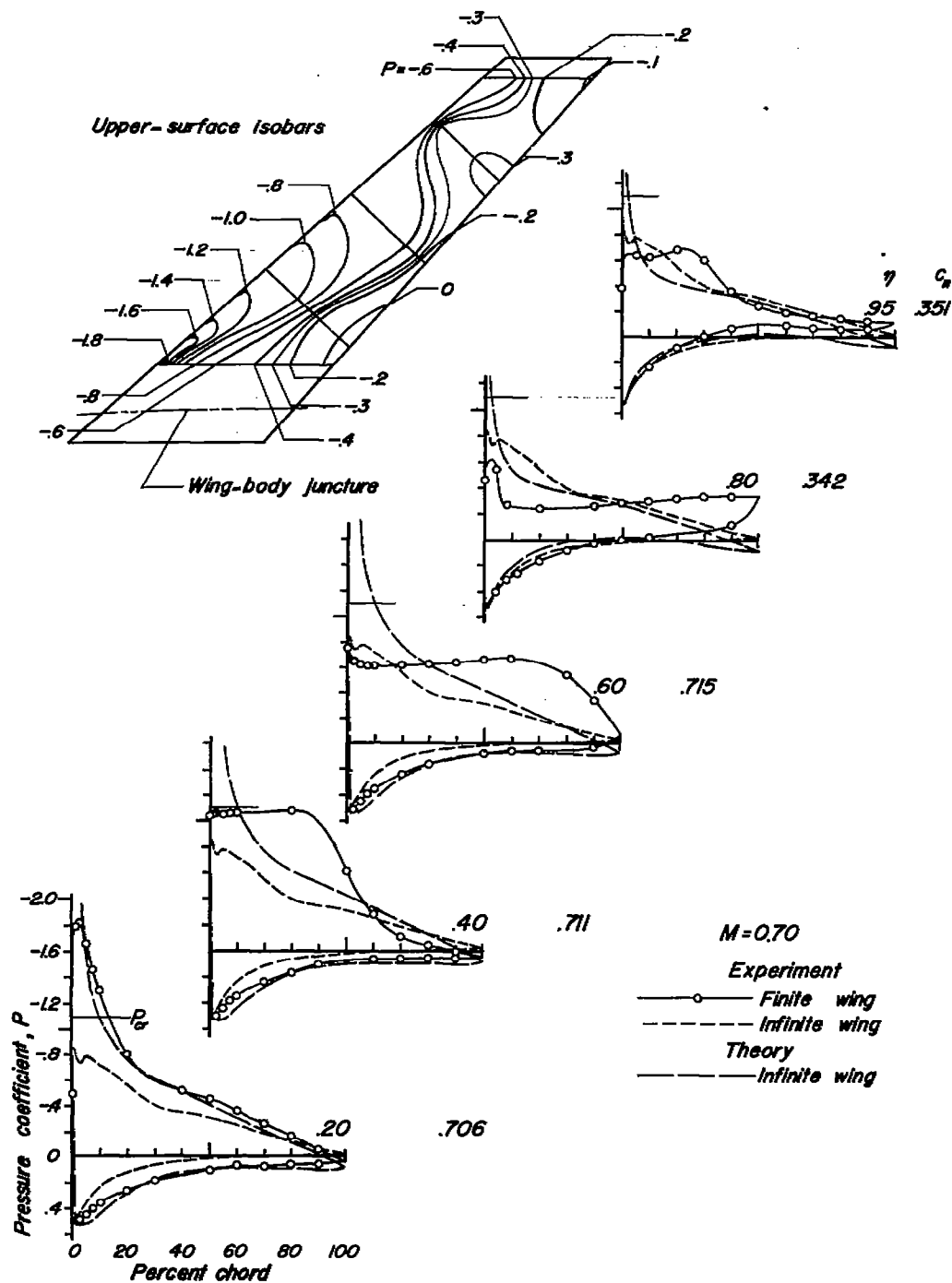
CONFIDENTIAL



CONFIDENTIAL



CONFIDENTIAL



CONFIDENTIAL

CONFIDENTIAL

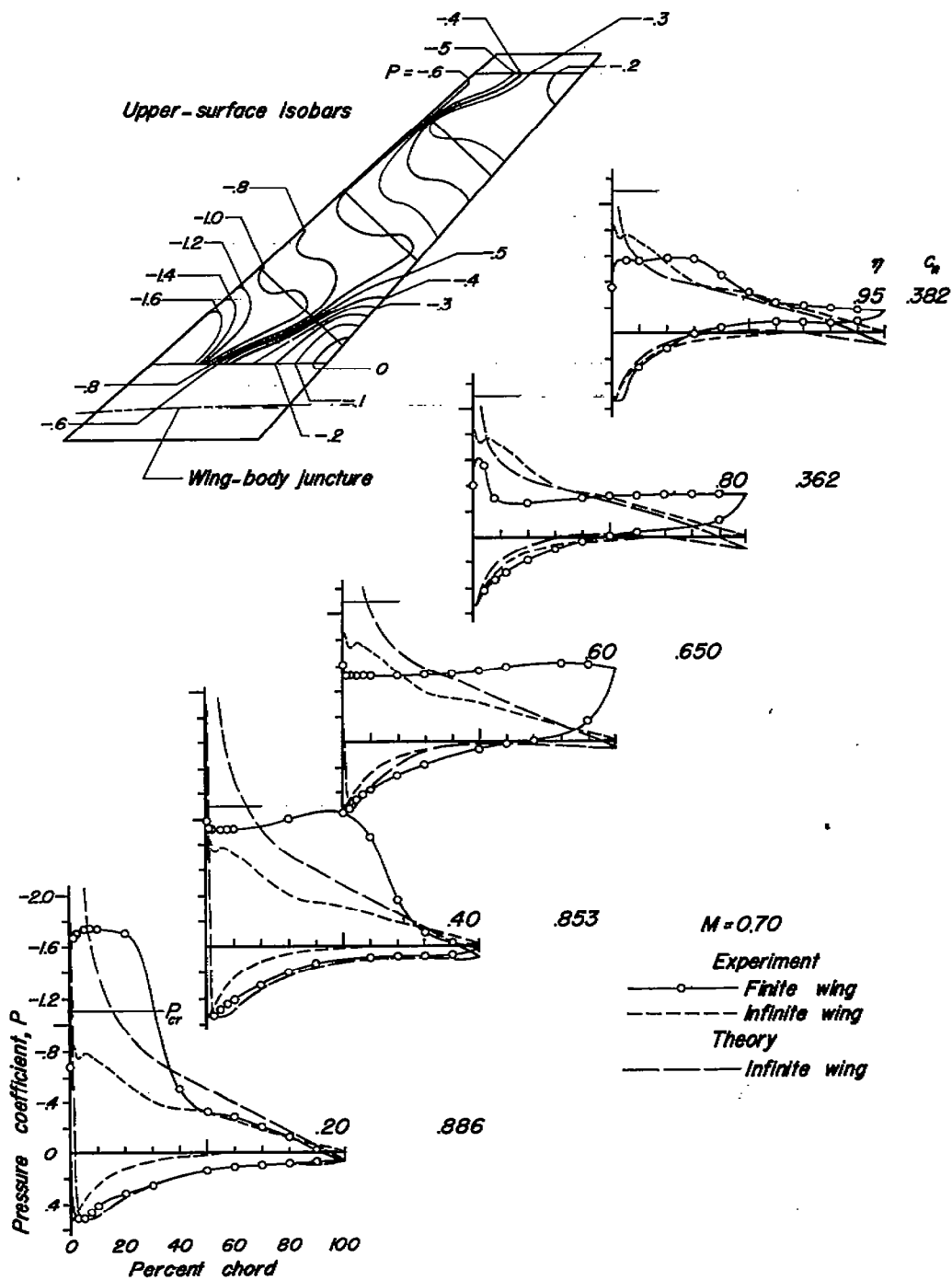
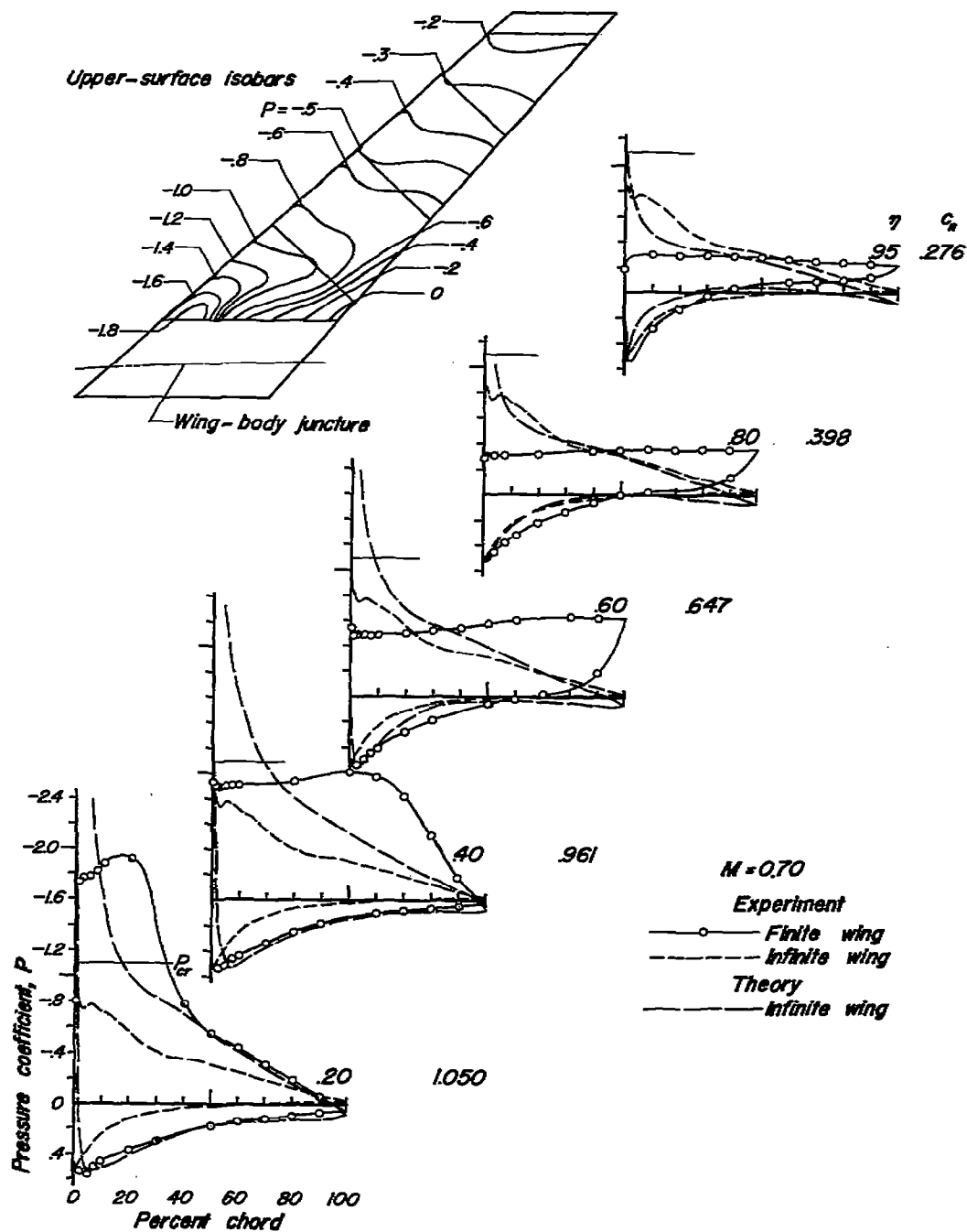
(g) $C_N = 0.714$ ($\alpha = 11.96^\circ$)

Figure 4.-Continued.

CONFIDENTIAL



(h) $C_N = 0.791$ ($\alpha = 14.08^\circ$)

Figure 4. - Concluded.

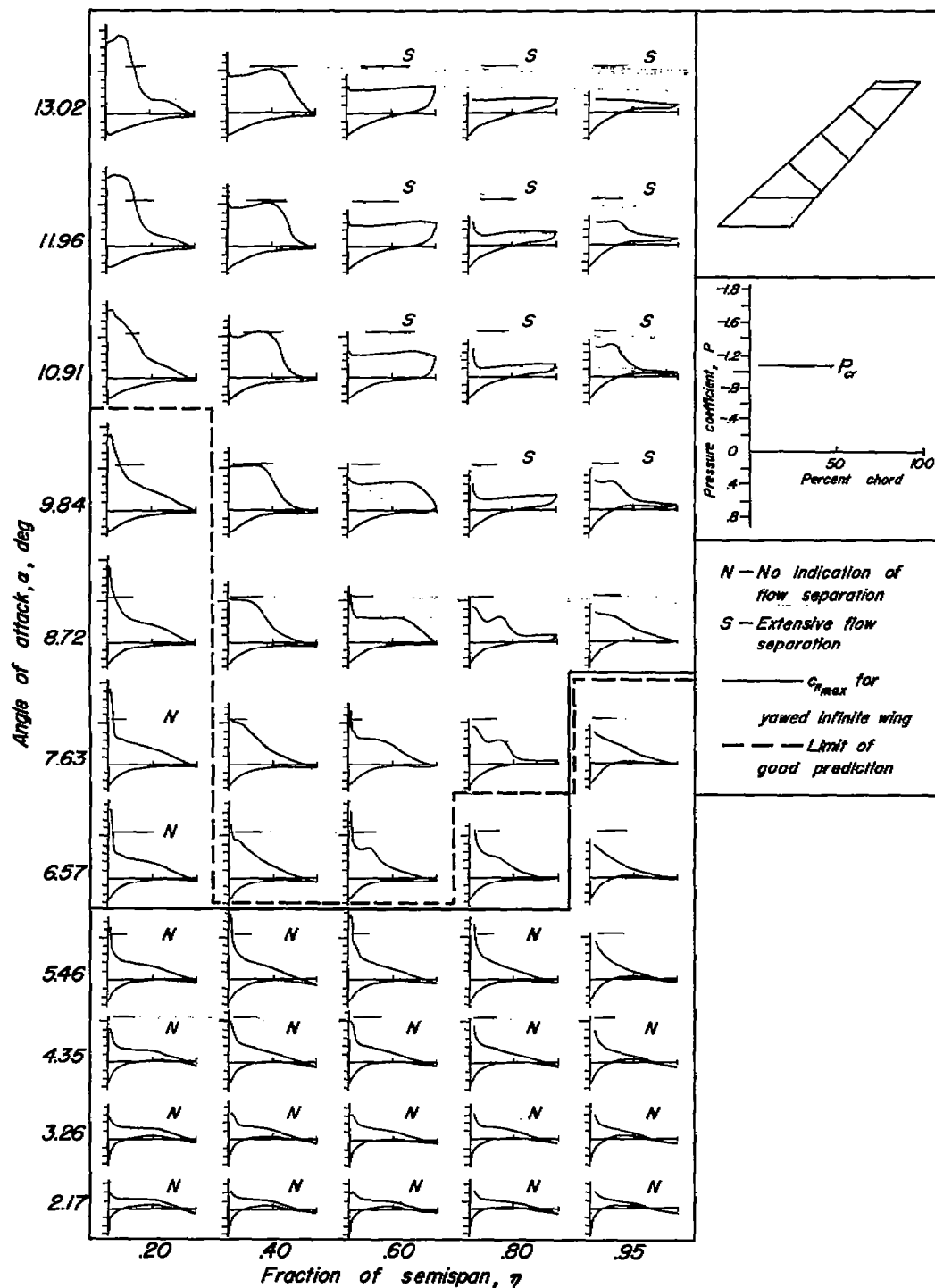


Figure 5.—Variation with angle of attack of pressure distributions at five semispan stations; $M=0.70$.

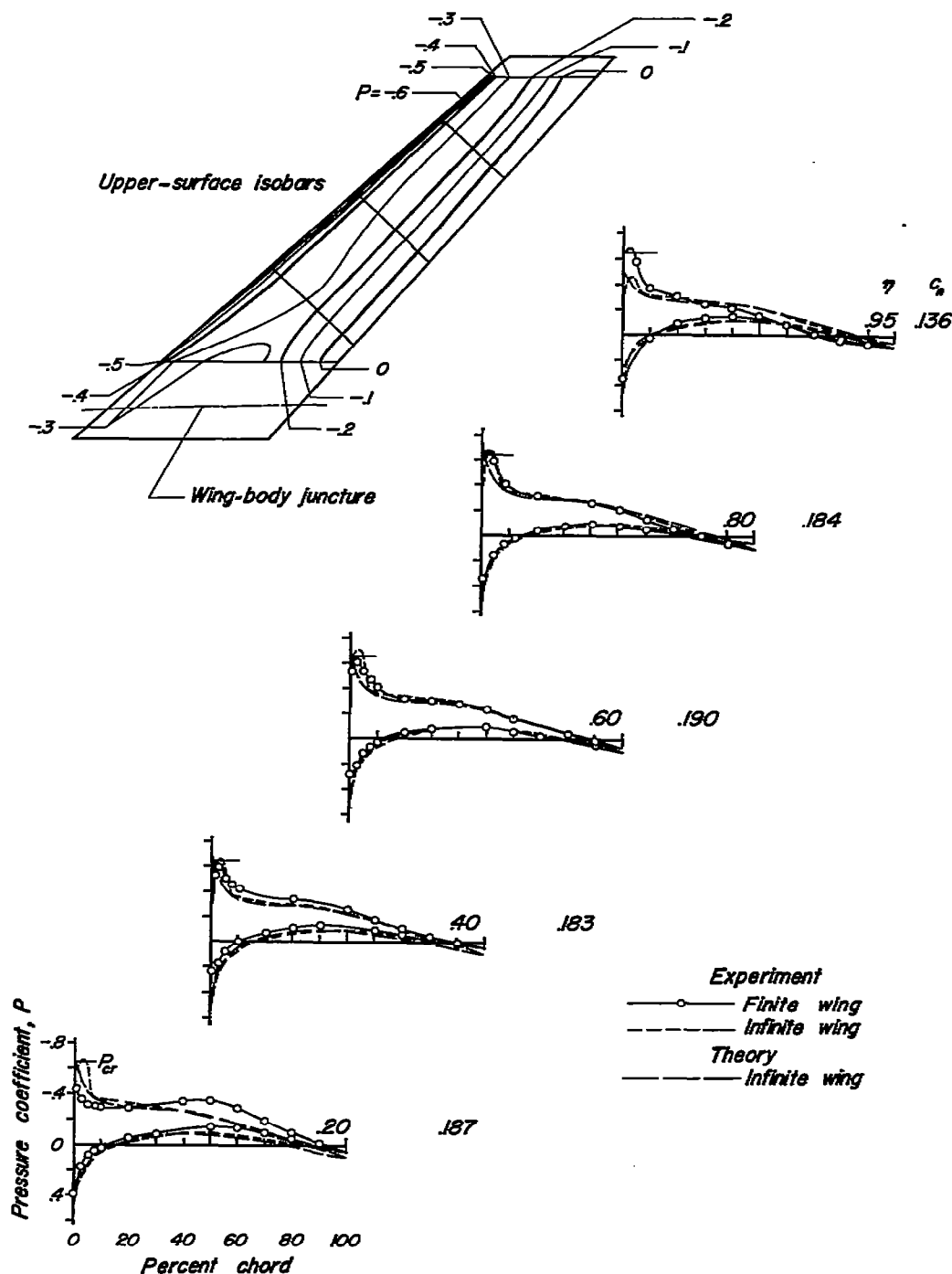


Figure 6.—Comparisons of experimental pressure distributions for five semispan stations with those for the NACA 64A010 section yawed 45° as derived from two-dimensional data and theory, plus experimental upper-surface isobars; $M = 0.85$.

CONFIDENTIAL

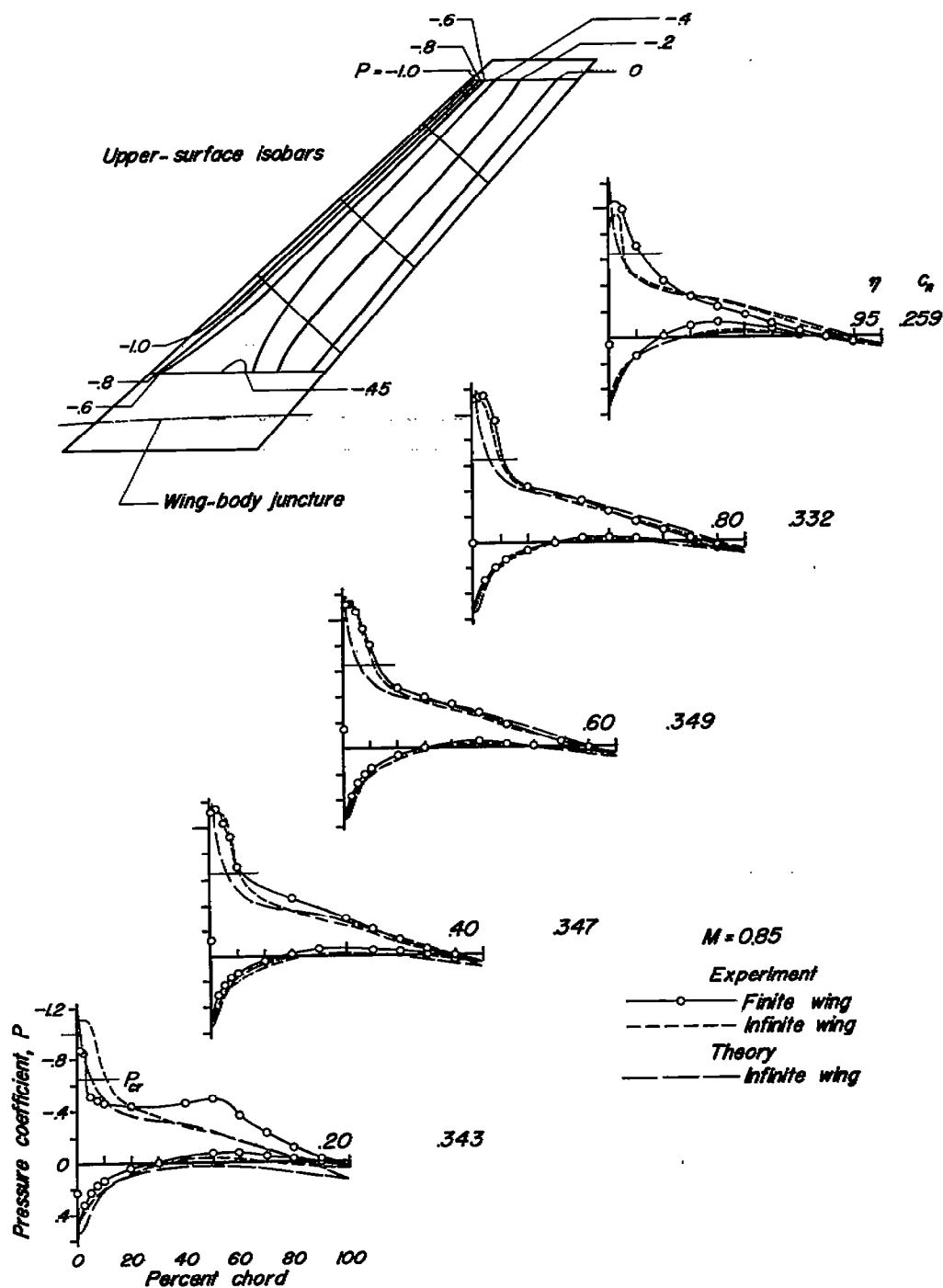
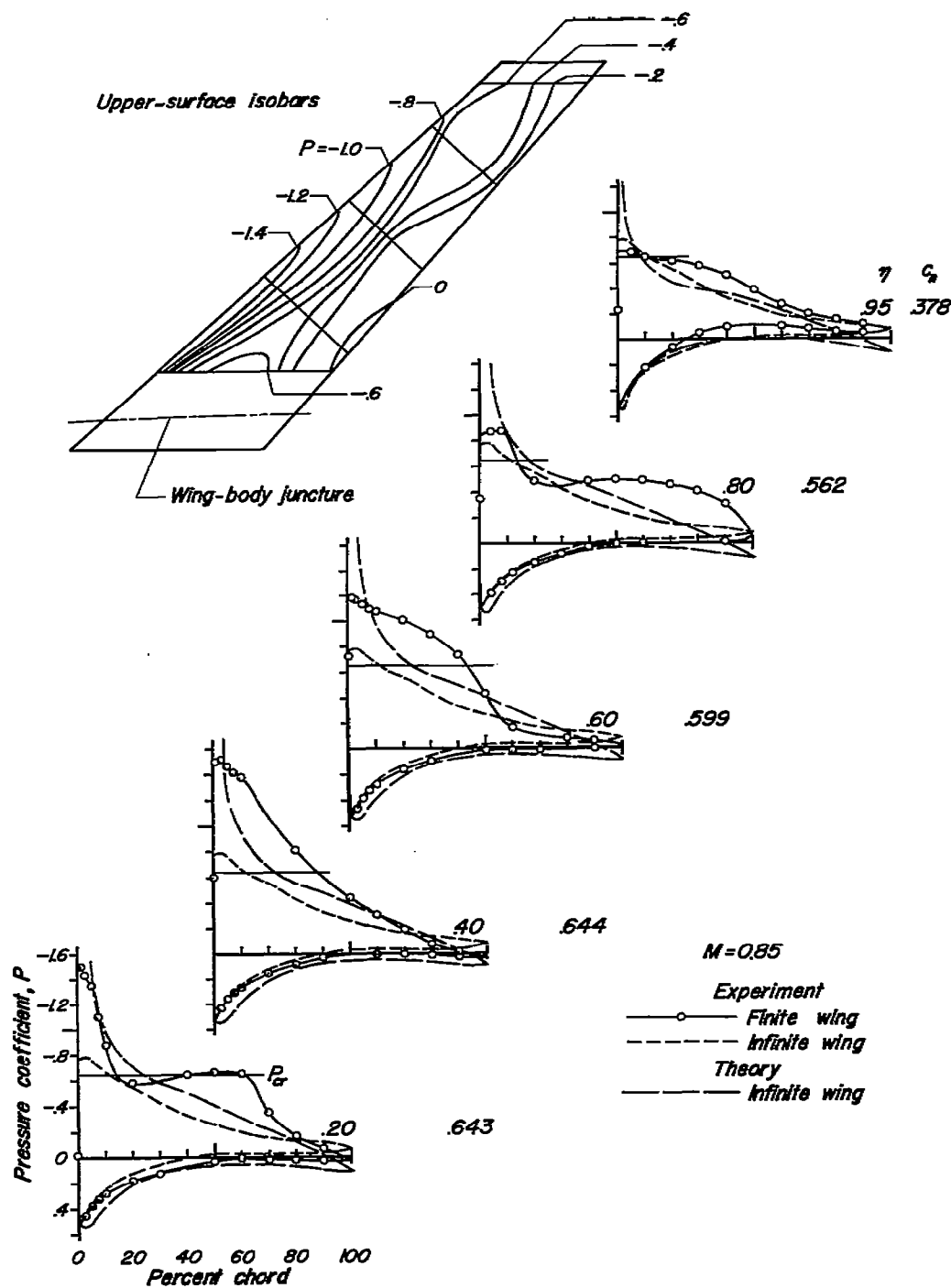
(b) $C_N = 0.339$ ($\alpha = 4.60^\circ$)

Figure 6.-Continued.

CONFIDENTIAL



CONFIDENTIAL

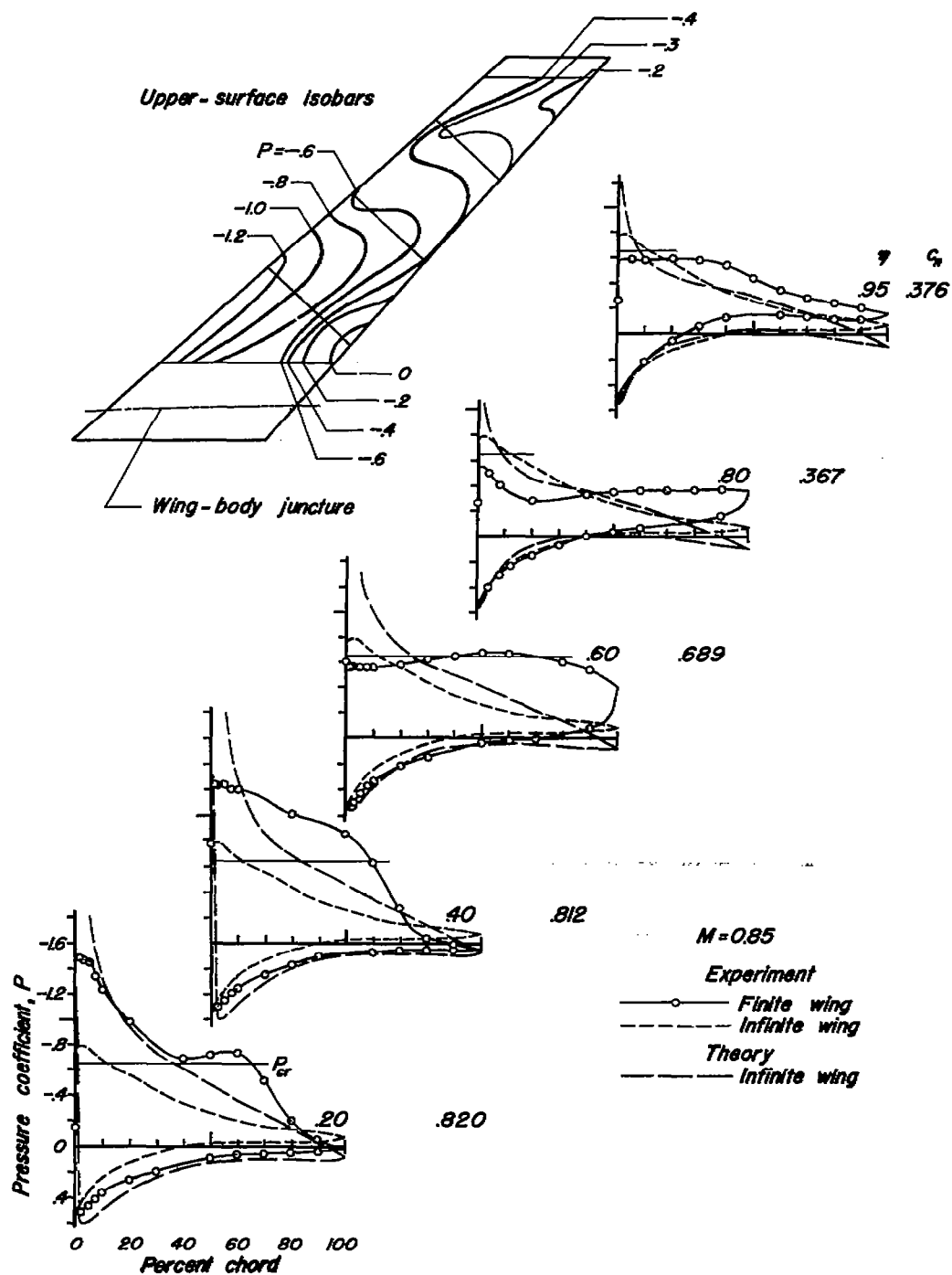
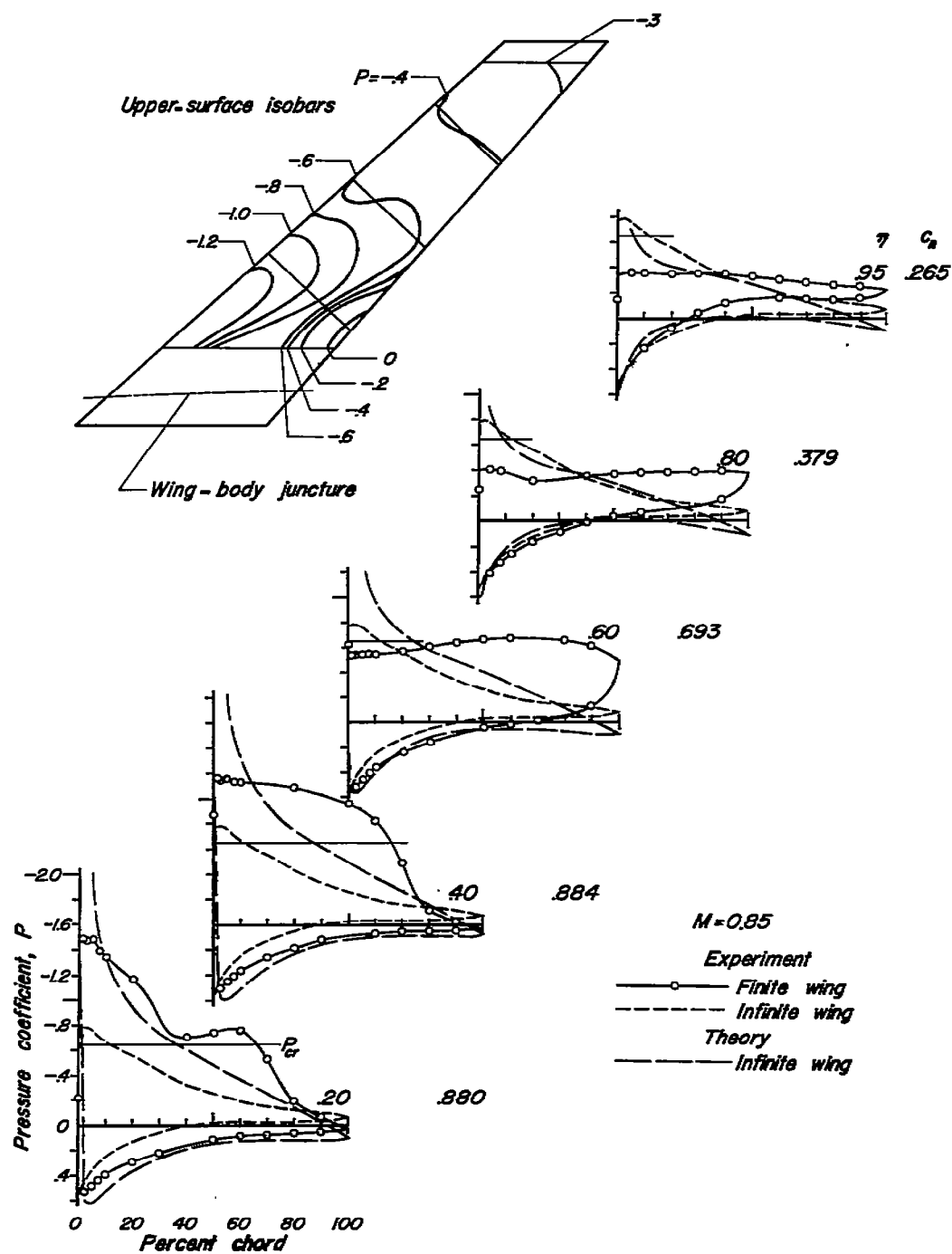
(d) $C_N = 0.691$ ($\alpha = 10.09^\circ$)

Figure 6.-Continued.

CONFIDENTIAL



(e) $C_N = 0.724$ ($\alpha = 11.15^\circ$)

Figure 6.- Concluded.

CONFIDENTIAL

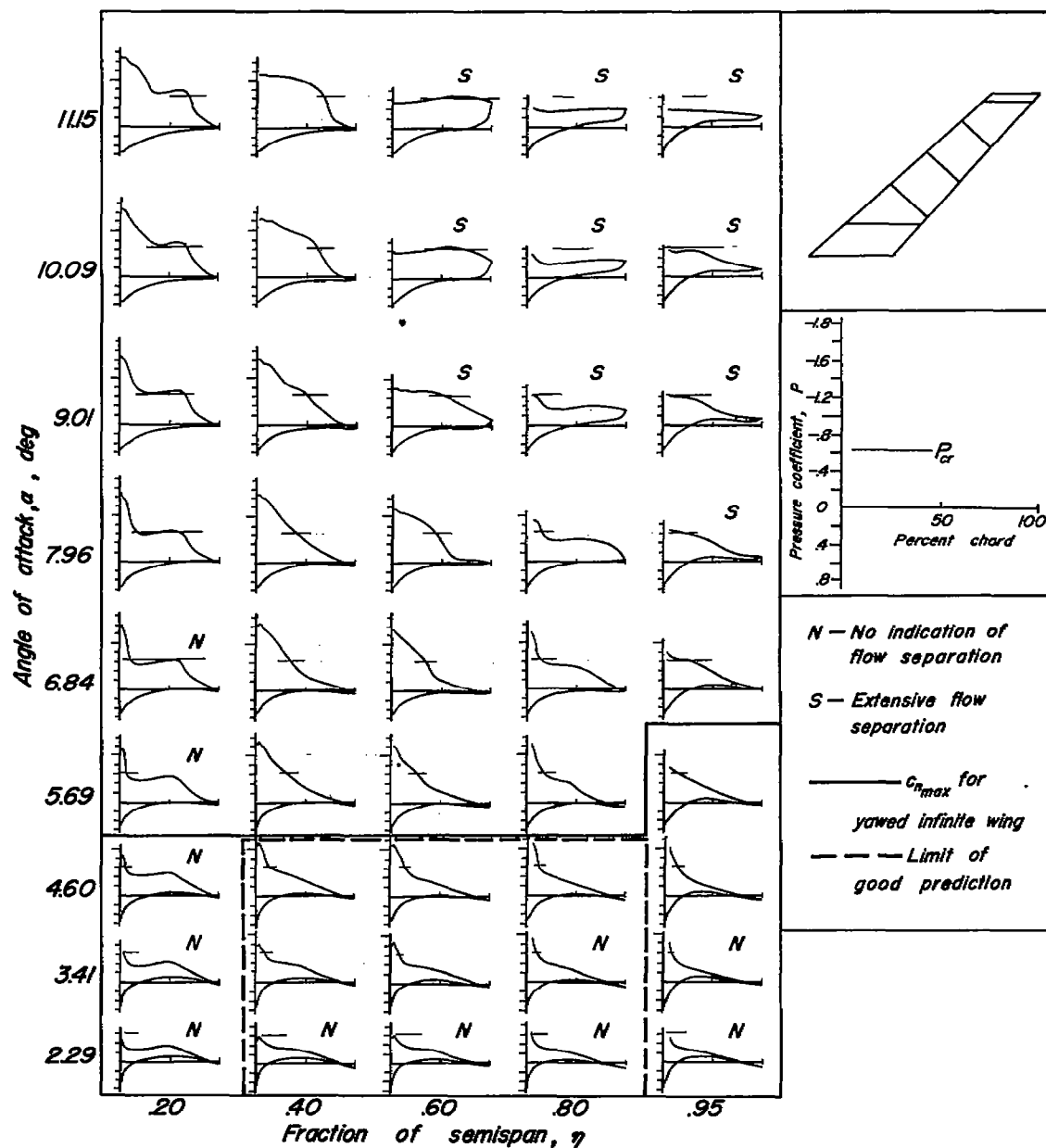


Figure 7.—Variation with angle of attack of pressure distributions at five semispan stations; $M=0.85$.

CONFIDENTIAL

CONFIDENTIAL

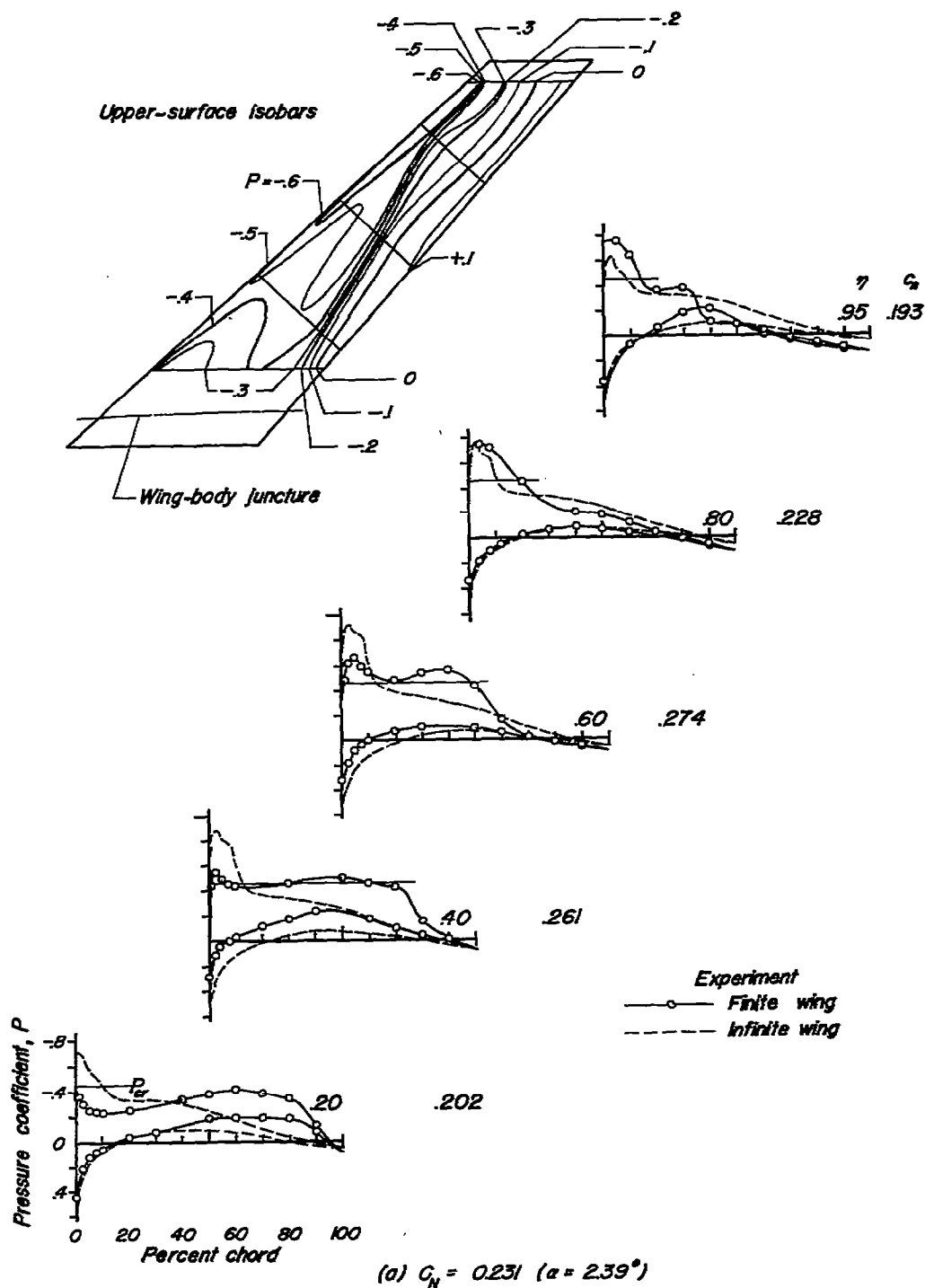


Figure 8.—Comparisons of experimental pressure distributions for five semispan stations with those for the NACA 64A010 section yawed 45° as derived from two-dimensional data, plus experimental upper-surface isobars; $M = 0.95$.

CONFIDENTIAL

CONFIDENTIAL

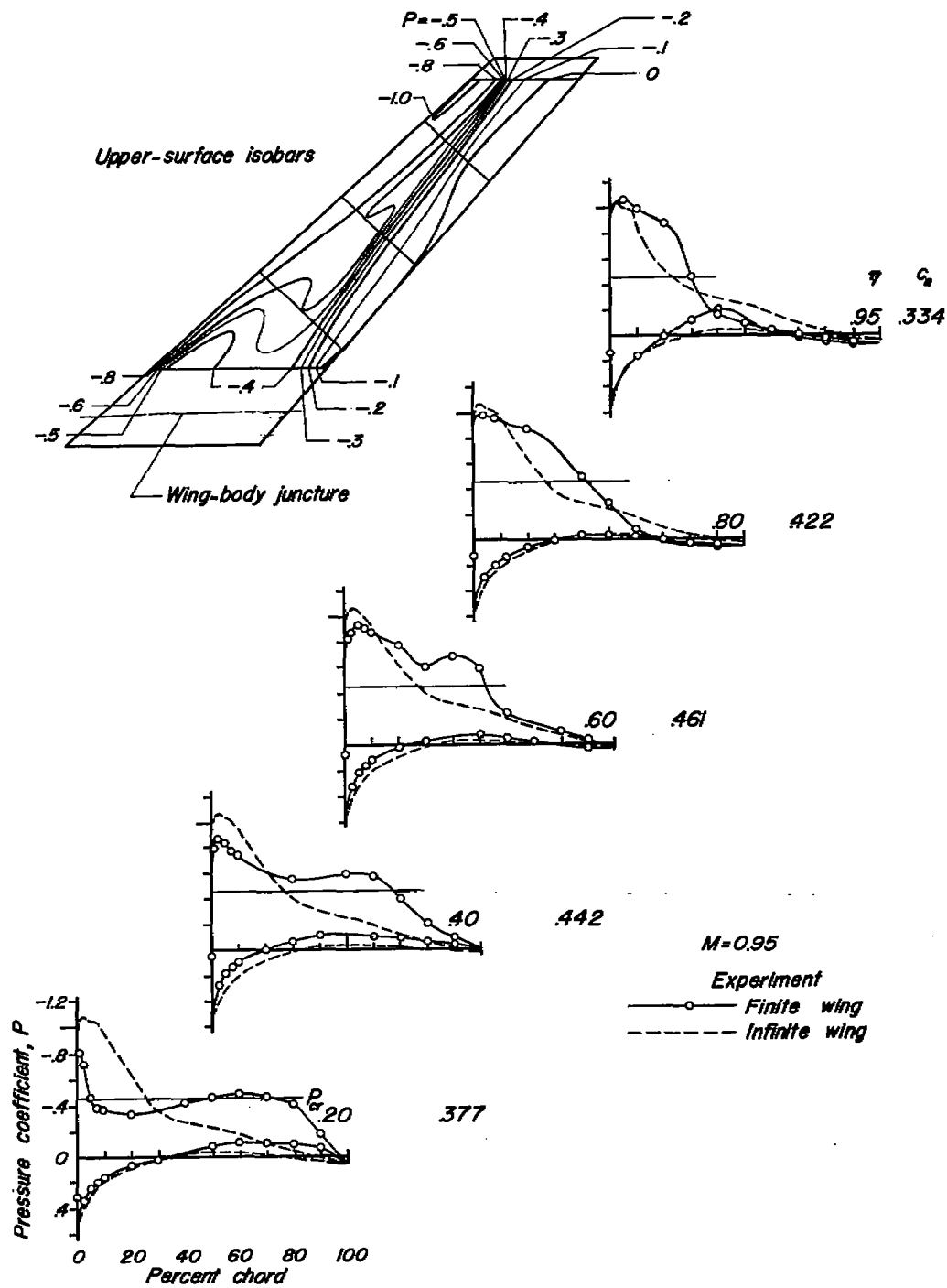
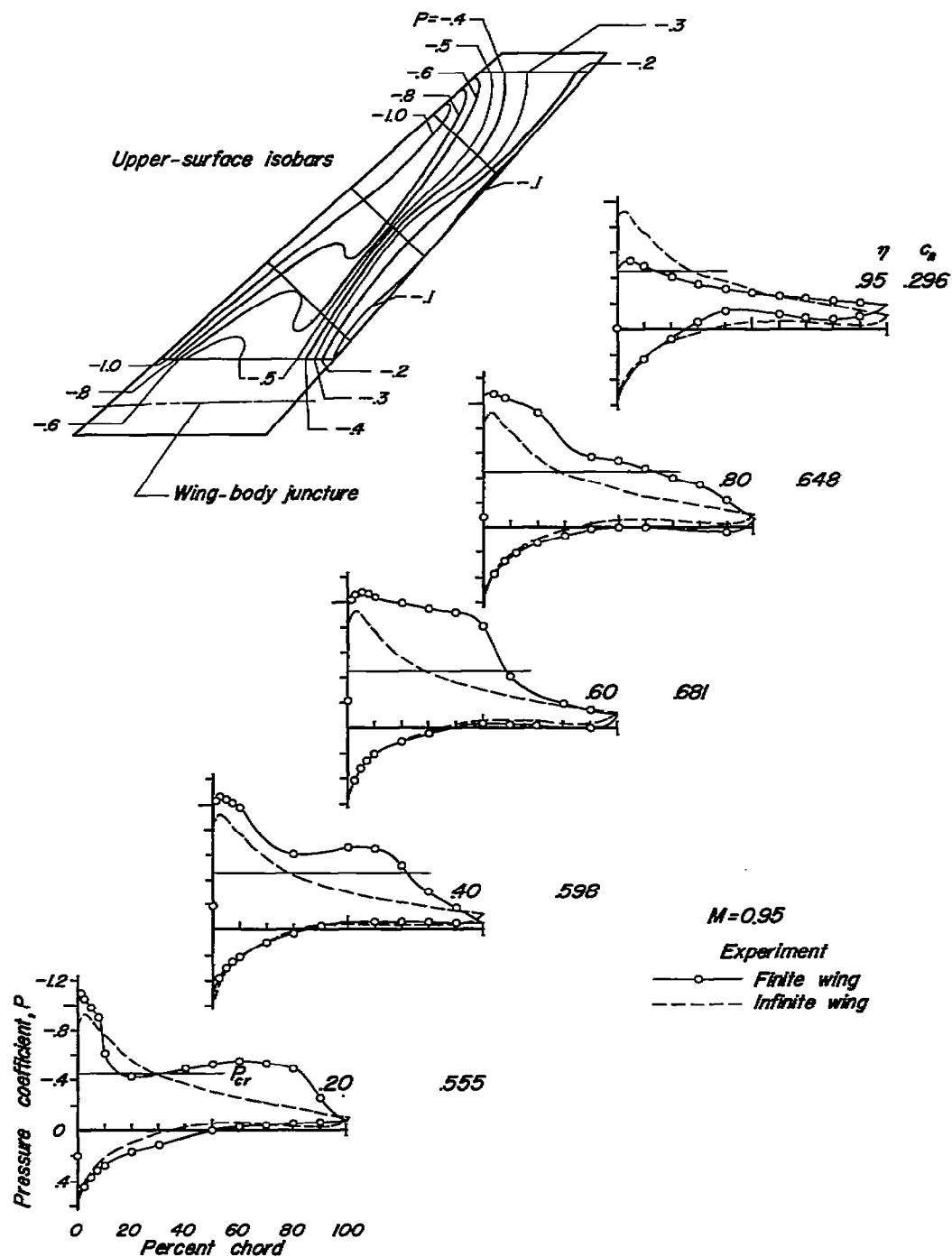
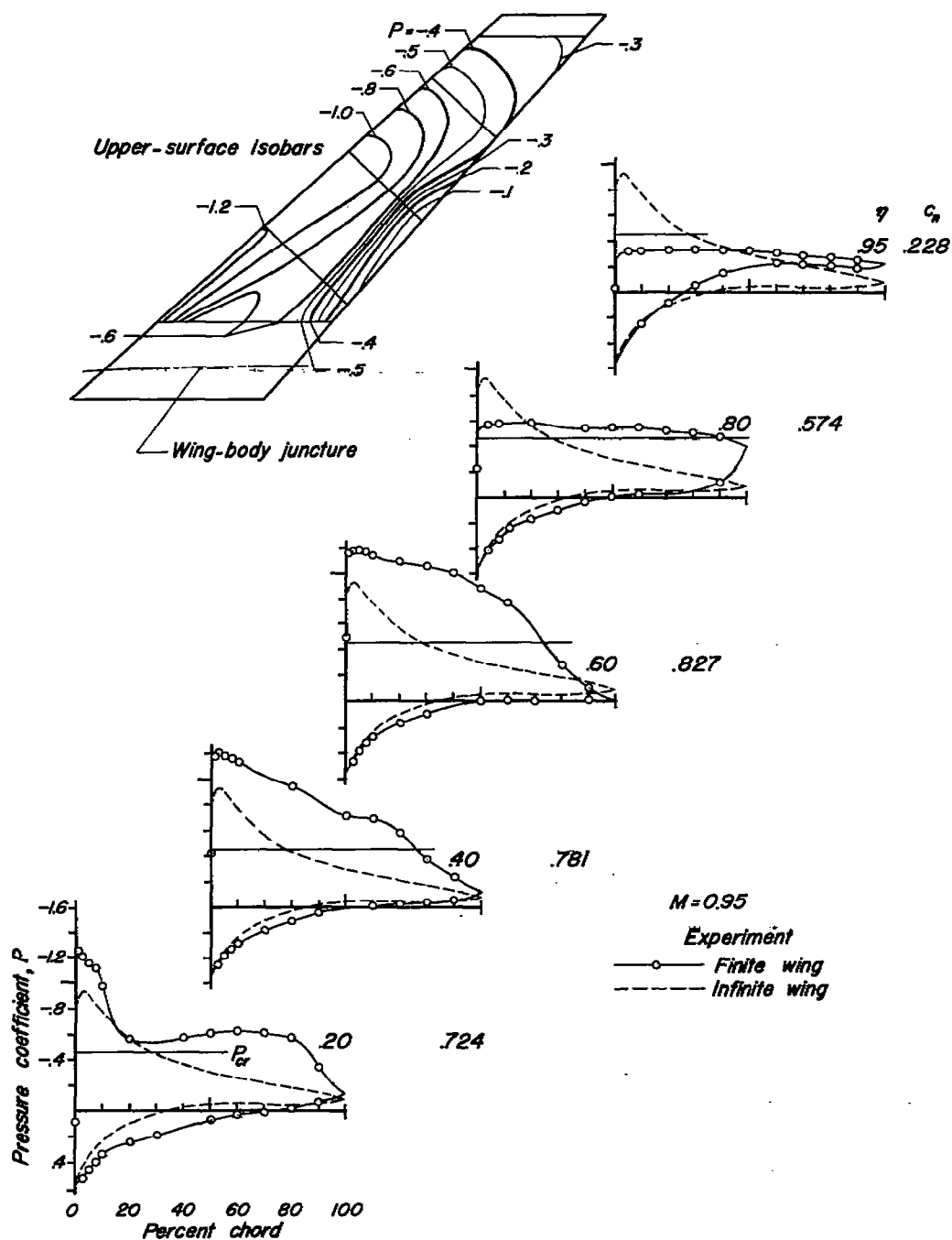
(b) $C_N = 0.411$ ($\alpha = 4.70^\circ$)

Figure 8.-Continued.

CONFIDENTIAL





(d) $C_N = 0.700$ ($\alpha = 9.19^\circ$)

Figure 8.- Concluded.

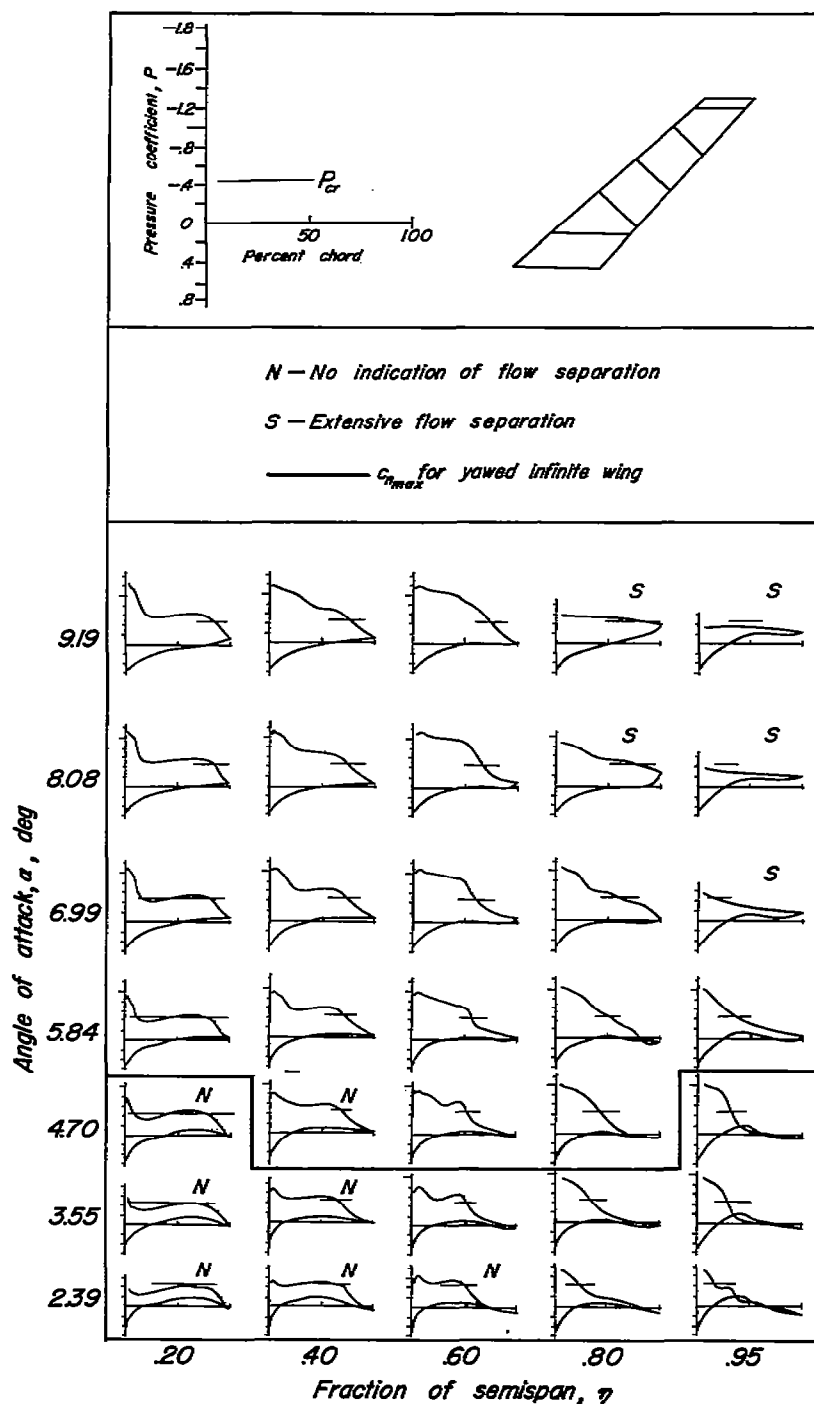


Figure 9.—Variation with angle of attack of pressure distributions at five semispan stations; $M=0.95$.

CONFIDENTIAL

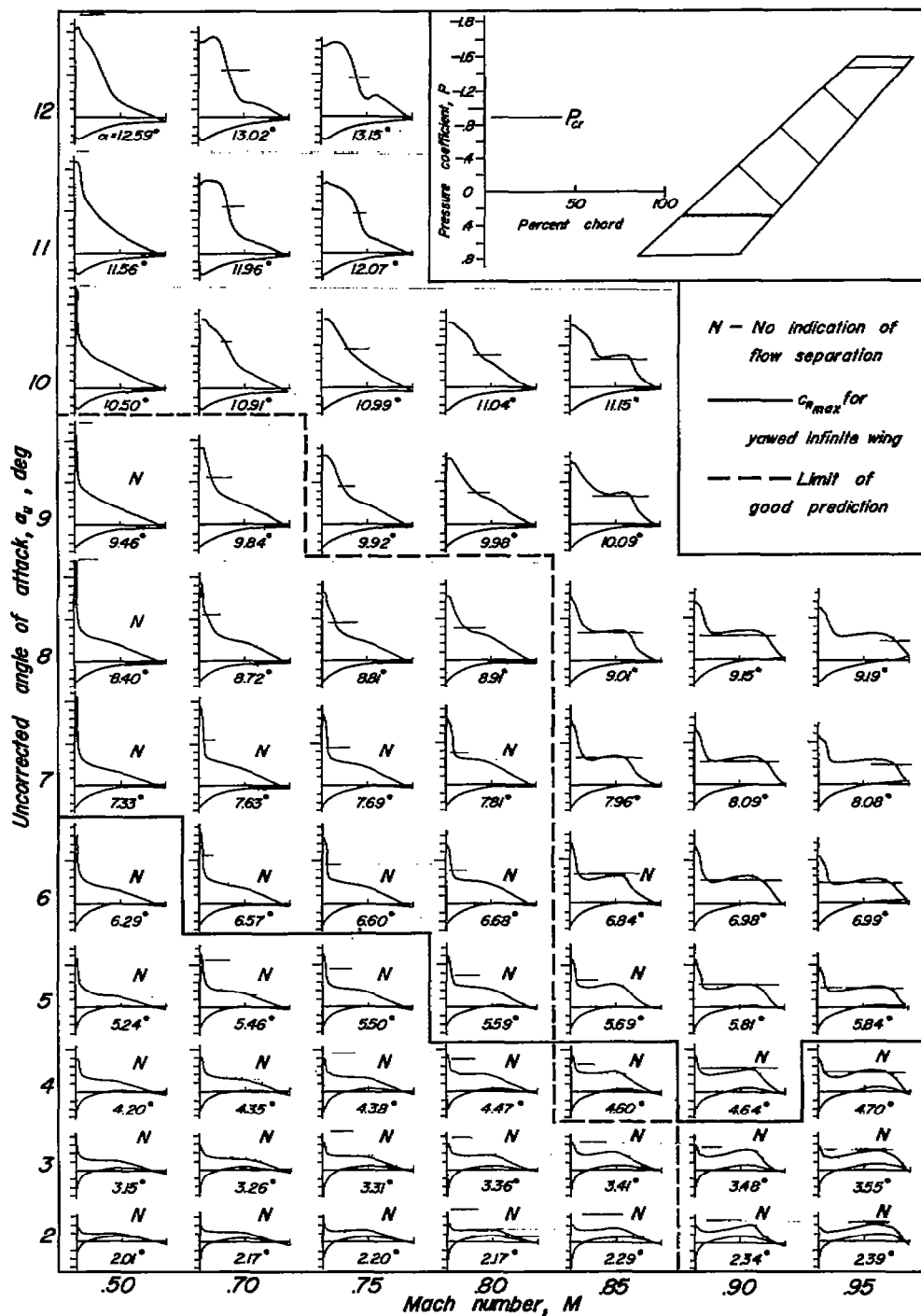


Figure 10.— Variation of pressure distributions with angle of attack and Mach number.

CONFIDENTIAL

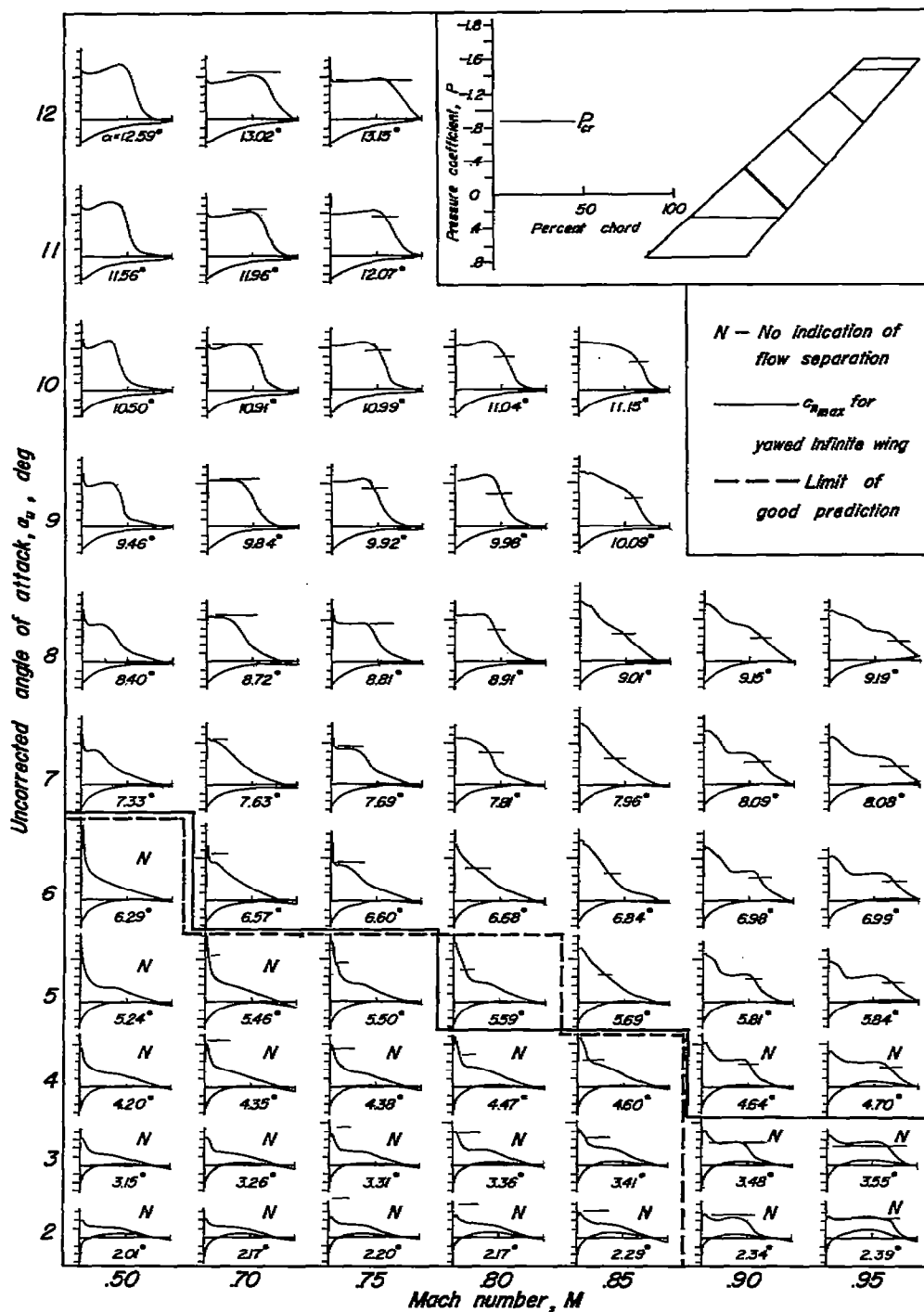


Figure 10.—Continued.

CONFIDENTIAL

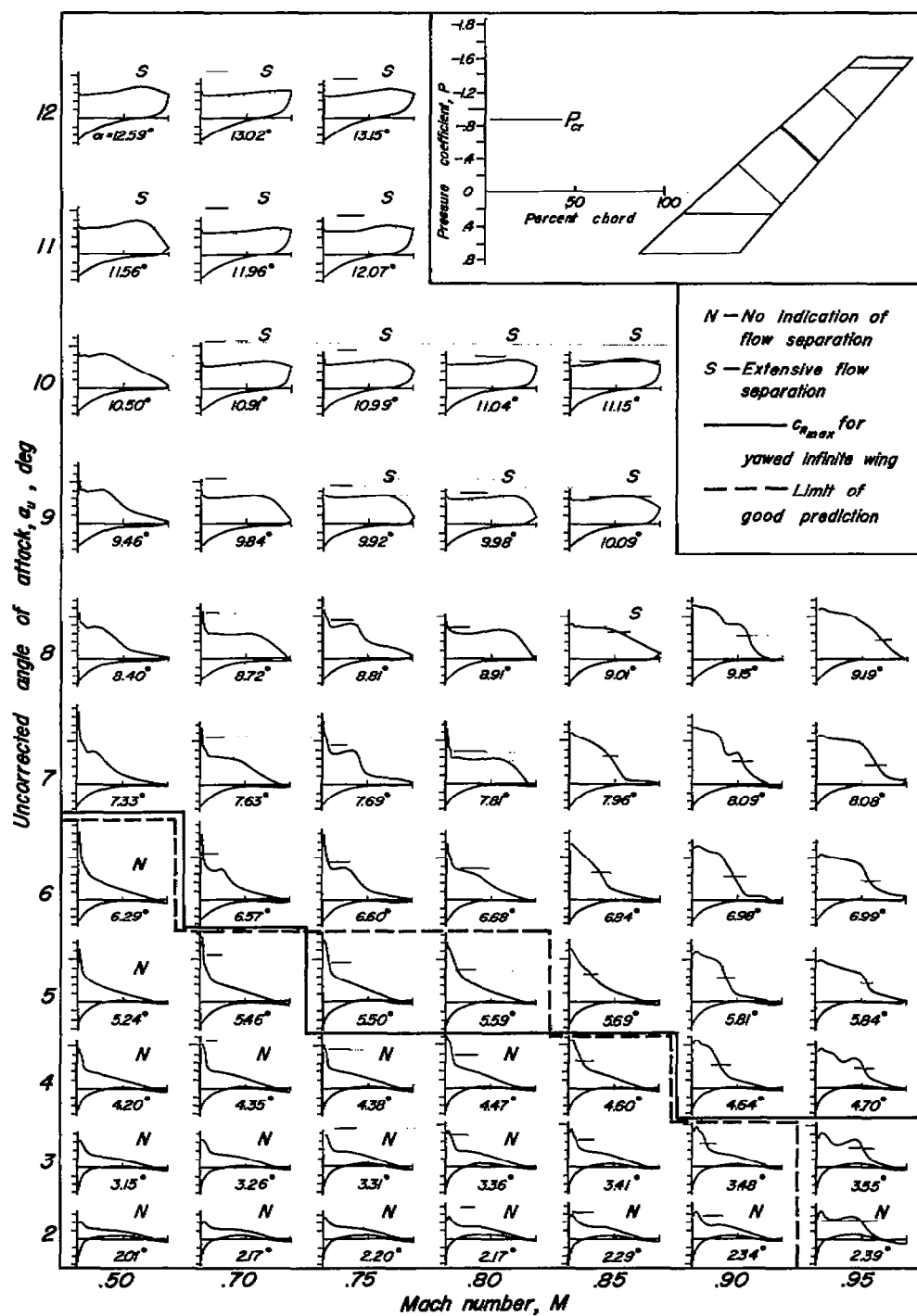
(c) $\gamma = 0.60$

Figure 10.— Continued.

CONFIDENTIAL

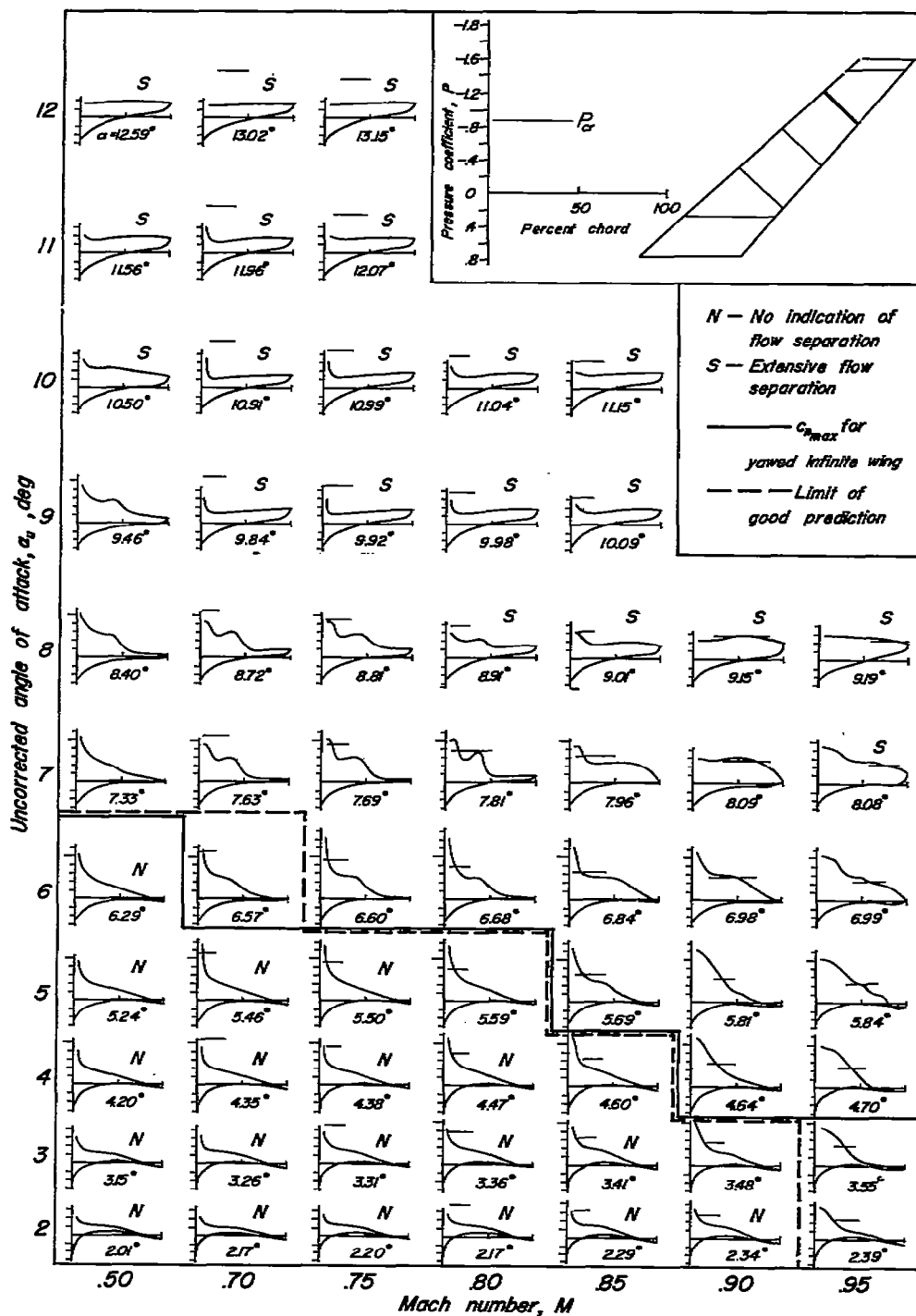
(d) $\eta = 0.80$

Figure 10.—Continued.

CONFIDENTIAL

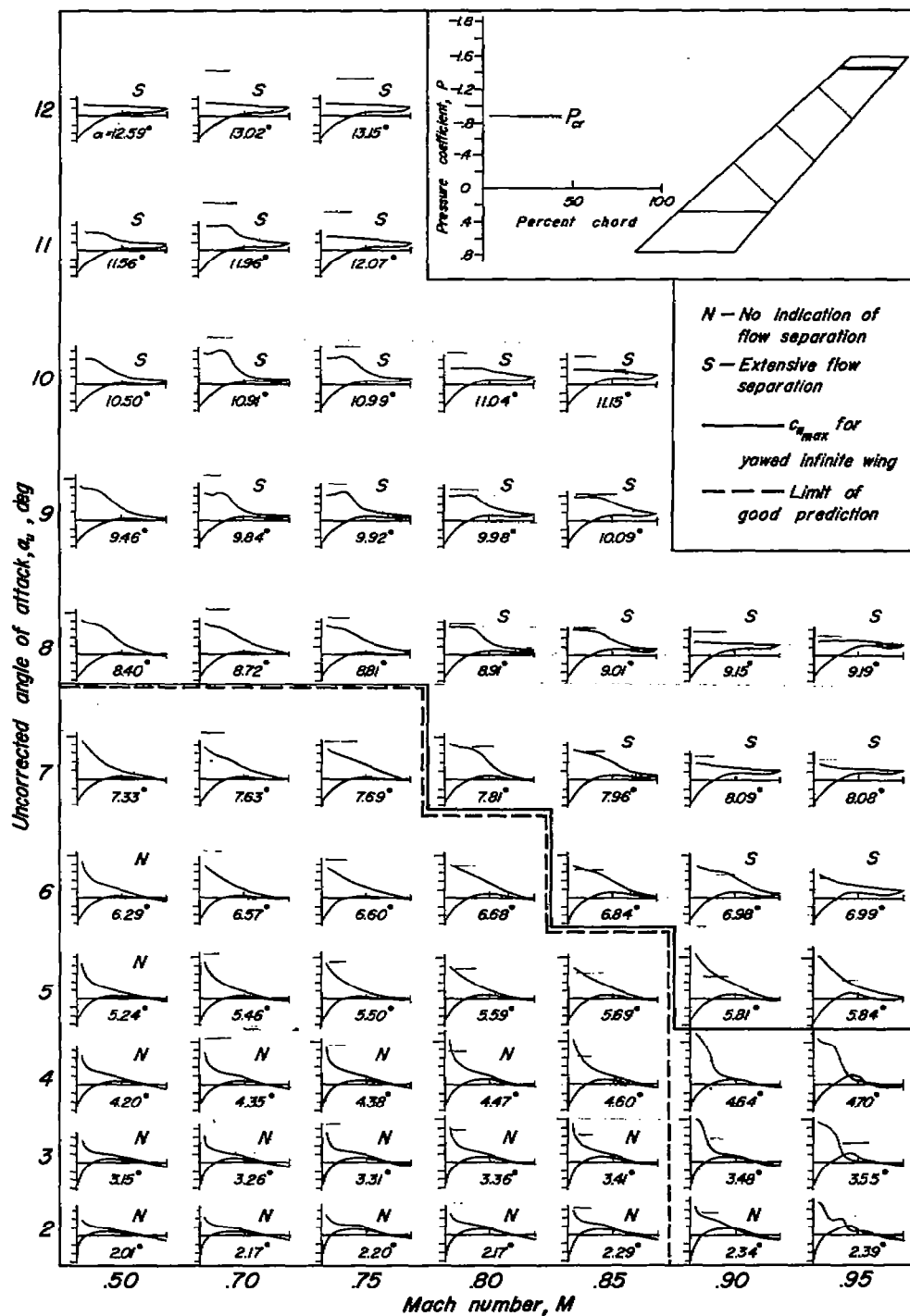
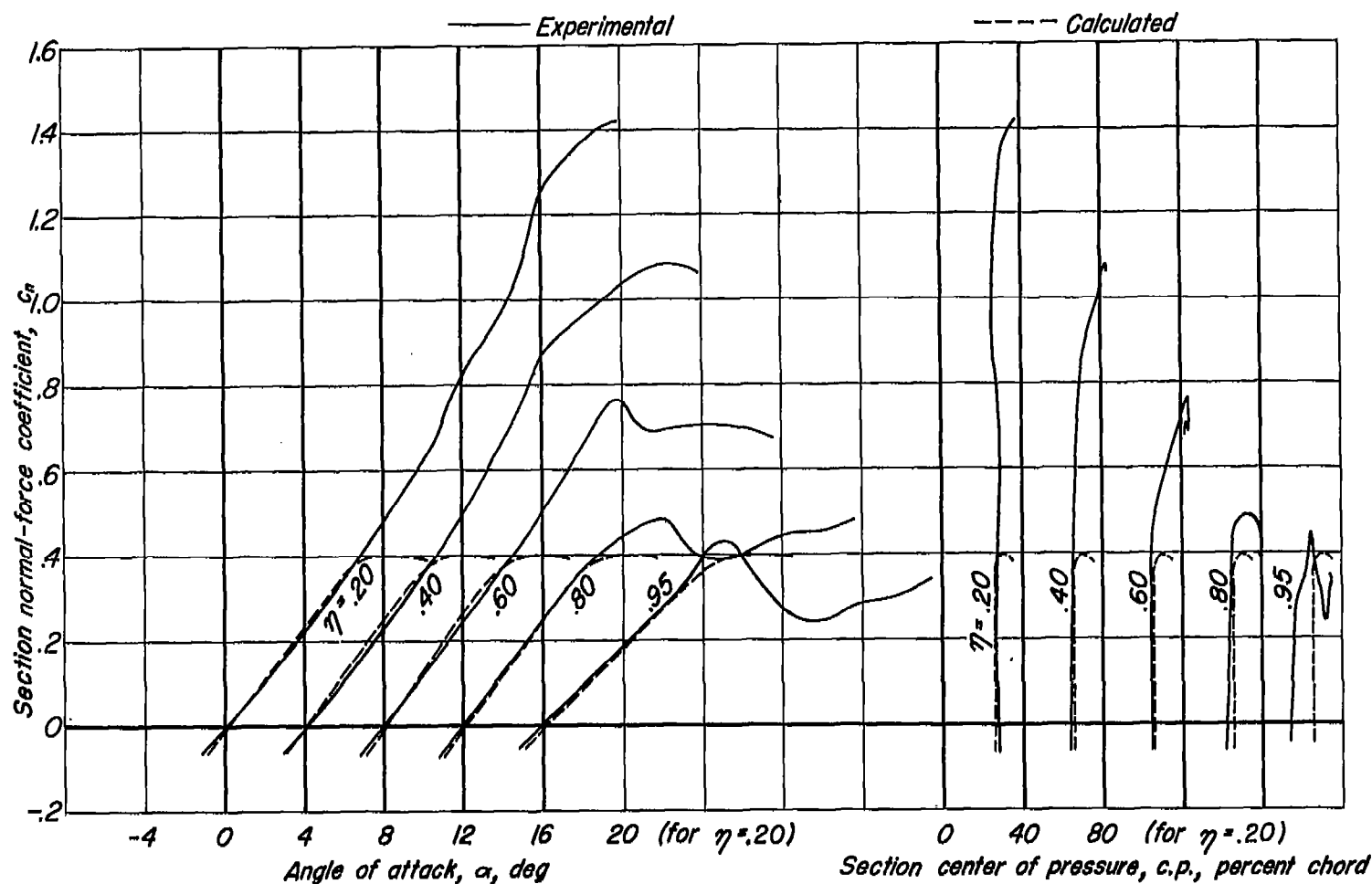
(e) $\eta = 0.95$

Figure 10 - Concluded.

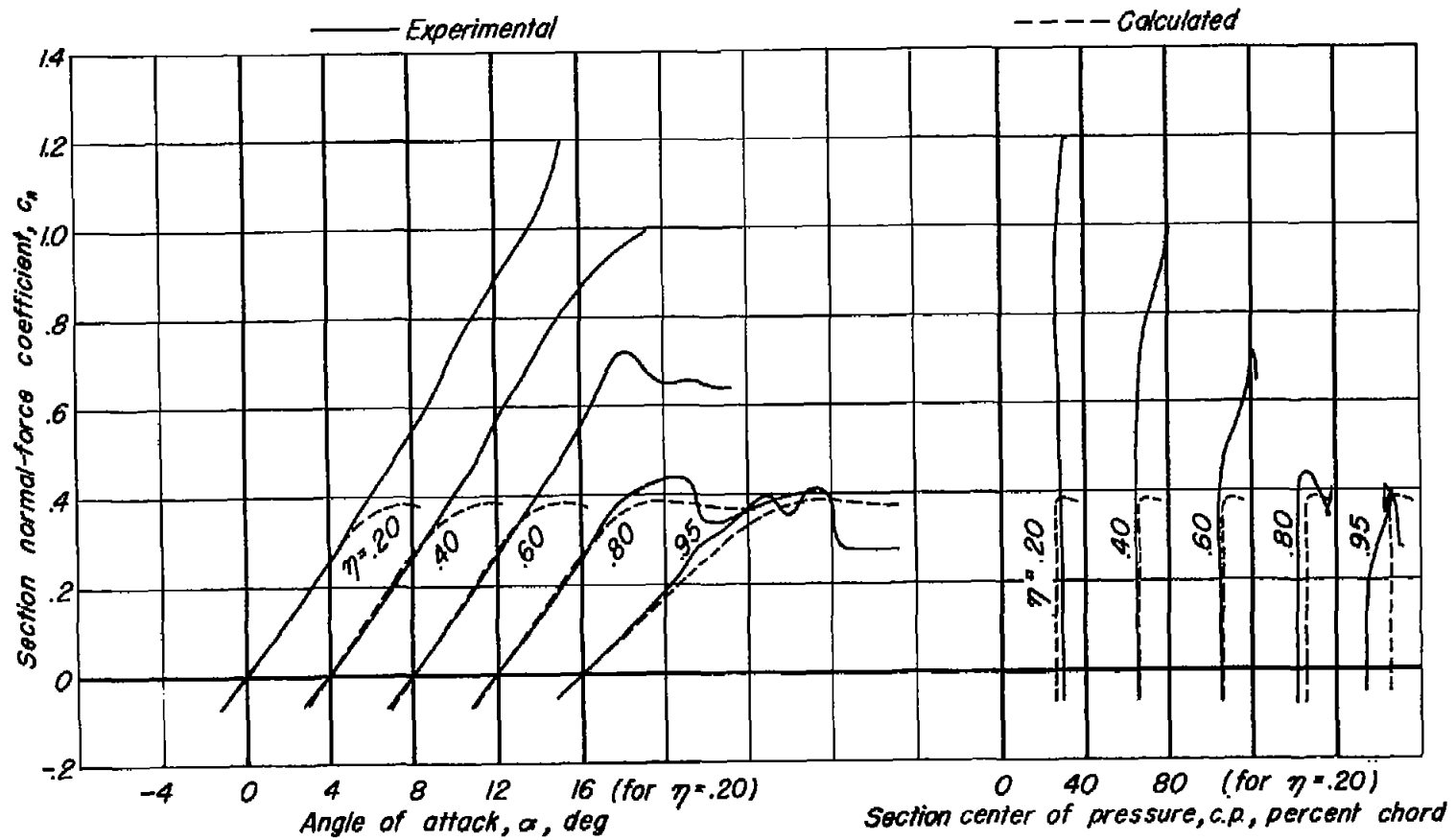
CONFIDENTIAL

CONFIDENTIAL



(a) $M = 0.50$

Figure 11.- Comparisons of the experimental section normal-force and center-of-pressure characteristics at several Mach numbers with those calculated from two-dimensional data.



(b) $M = 0.70$

Figure 11.-Continued.

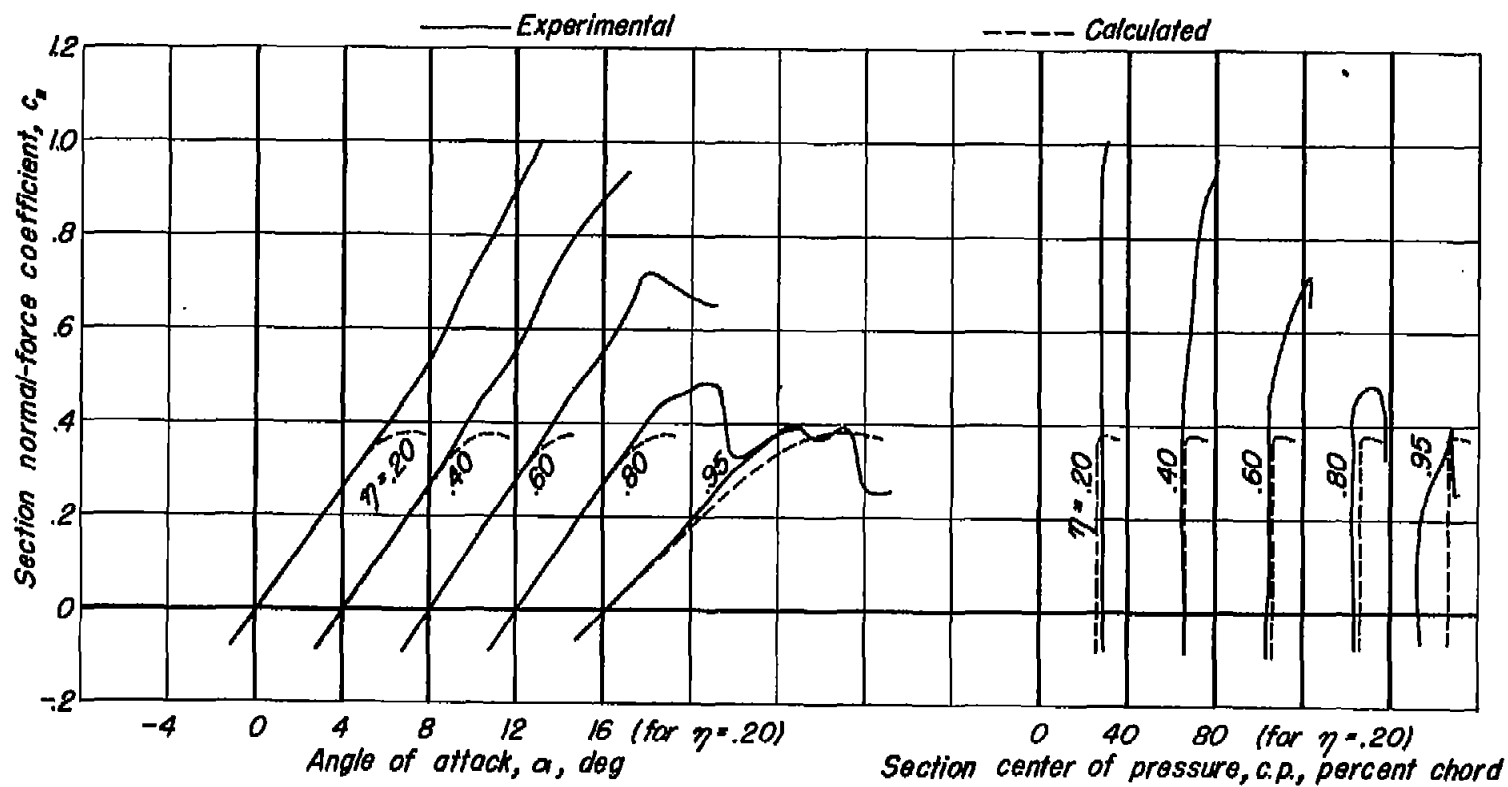


Figure 11.-Continued

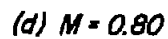


Figure 11.-Continued.

CONFIDENTIAL

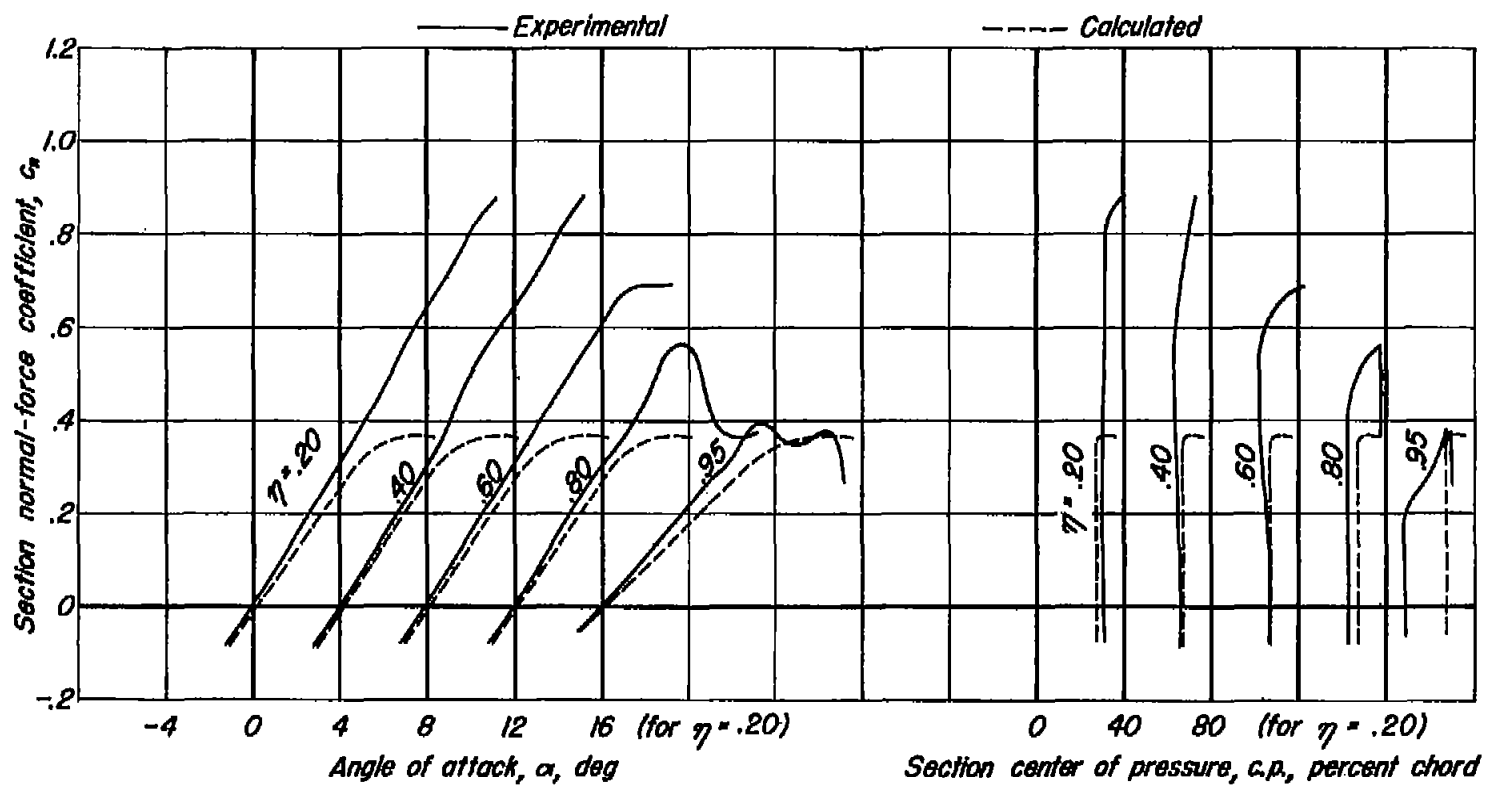
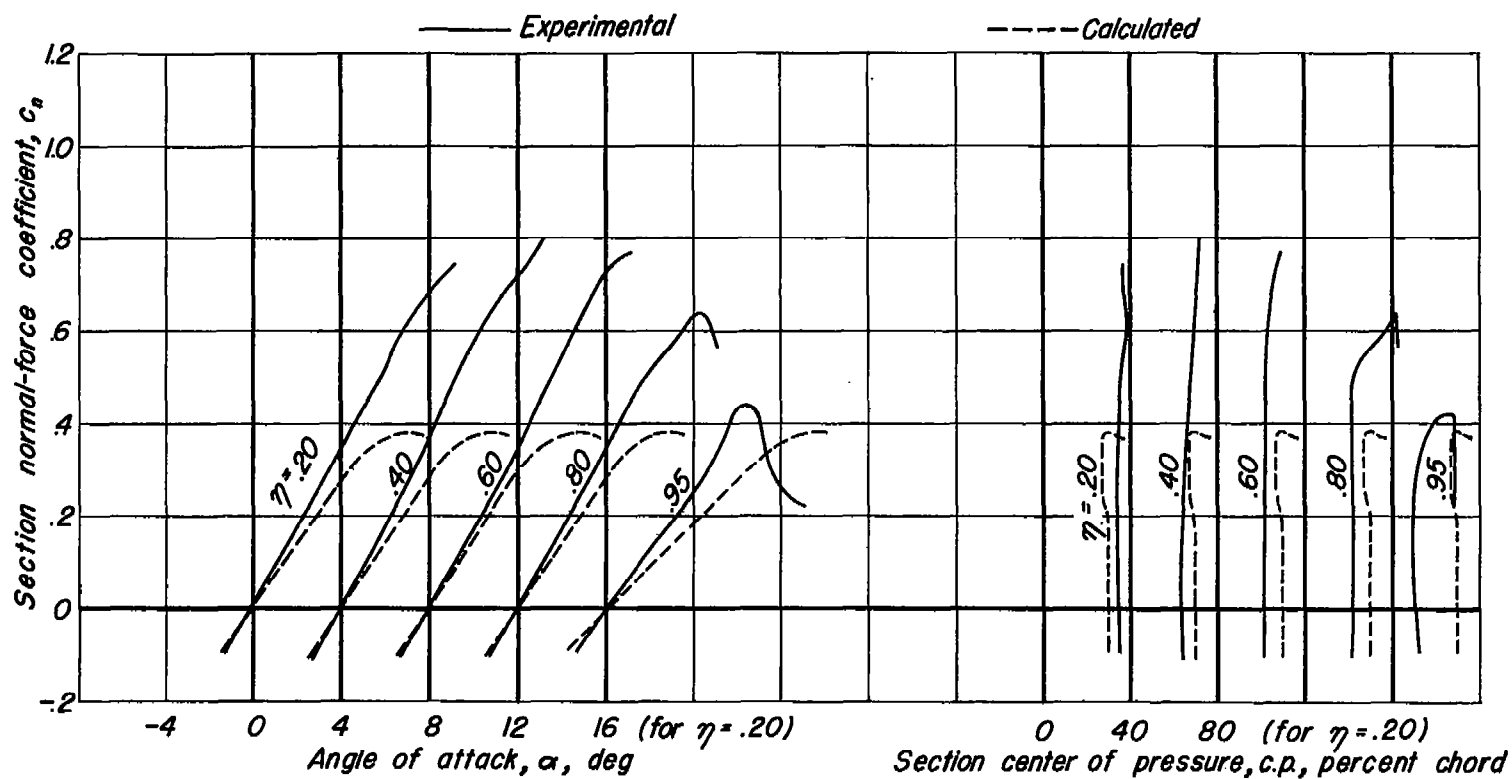
(e) $M = 0.85$

Figure 11.- Continued.



(f) $M = 0.90$

Figure 11.-Continued.

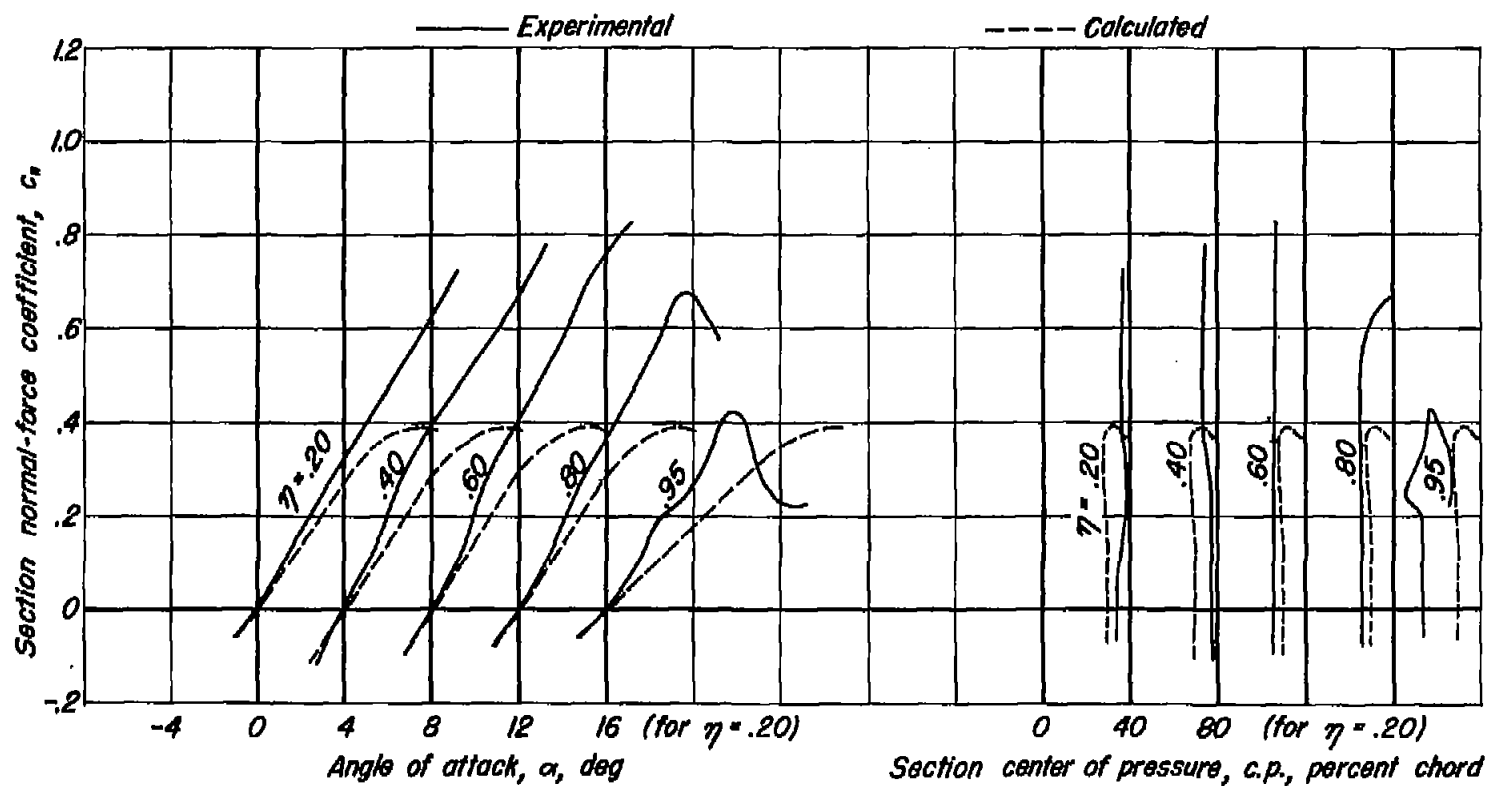
(g) $M = 0.95$

Figure 11.- Concluded.

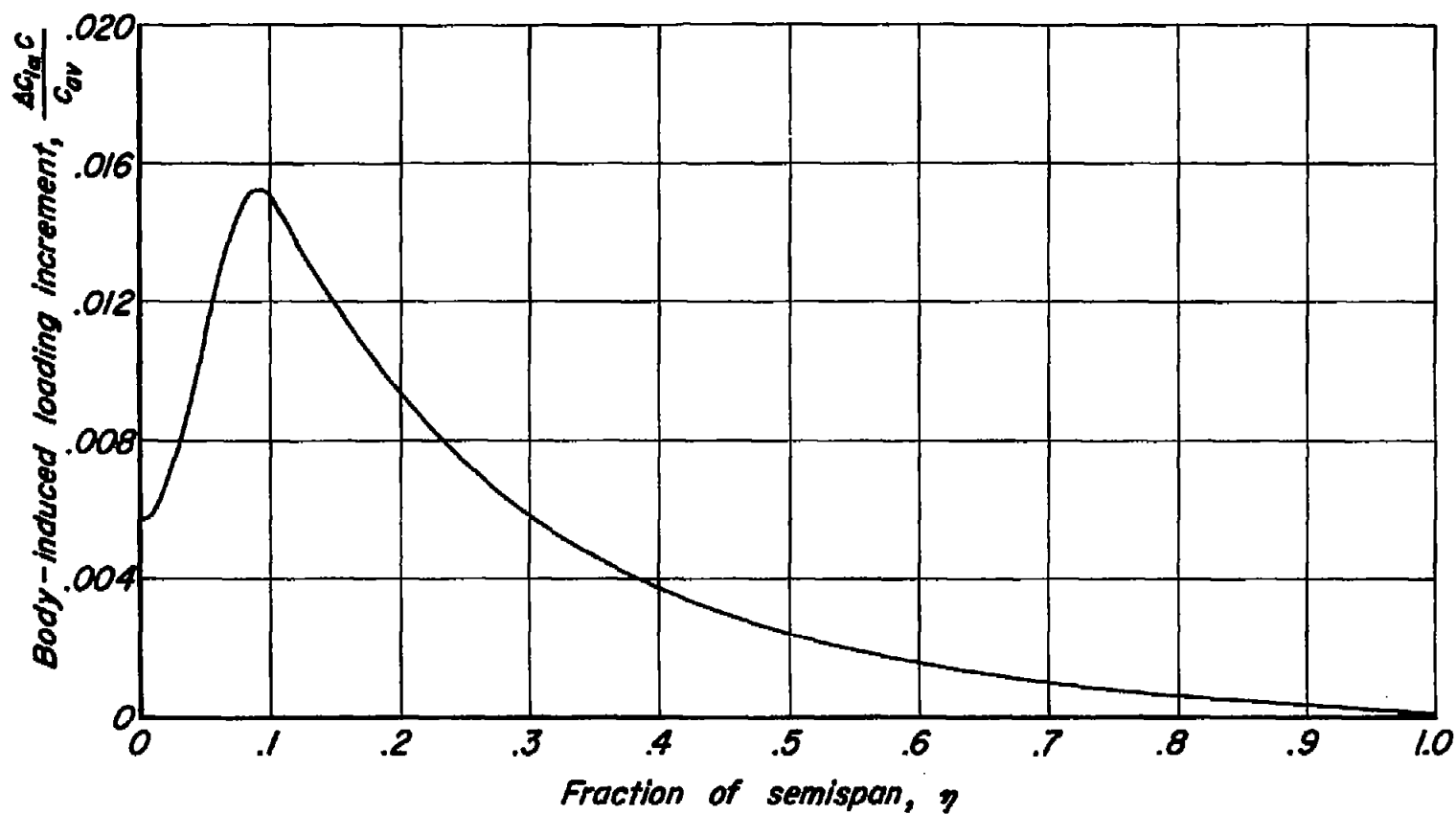
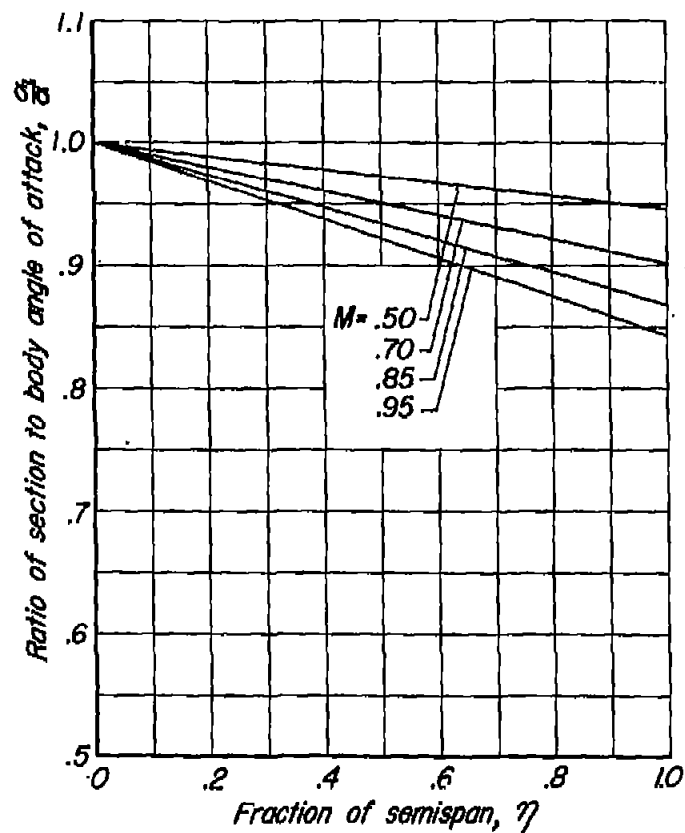
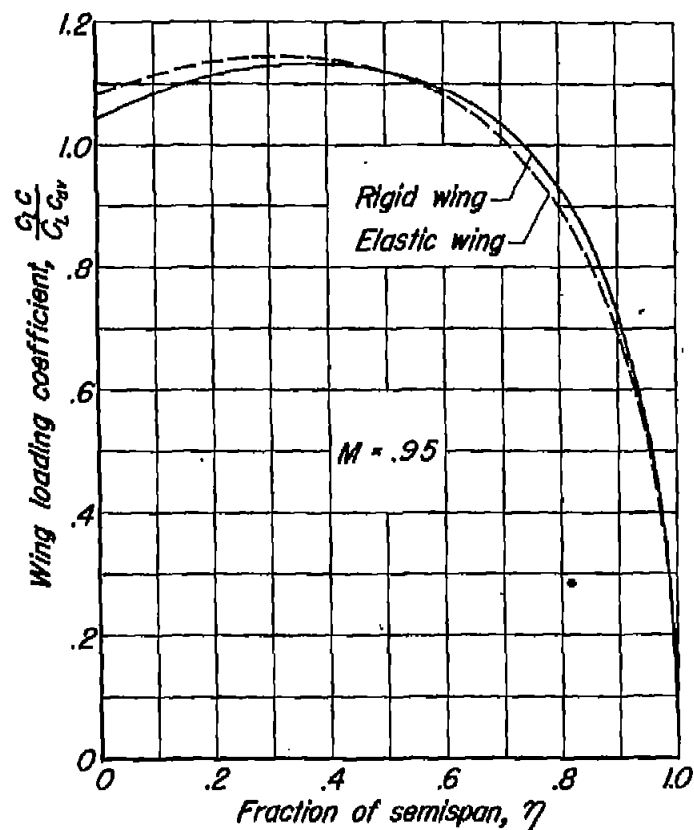


Figure 12.- Calculated increment of wing loading due to the presence of the body.



(a) Ratio of angles of attack.



(b) Span load distribution.

Figure 13.-Calculated effects of elastic deformation of the wing on the ratio of section to body angle of attack at various Mach numbers and on the span load distribution at a Mach number of 0.95.

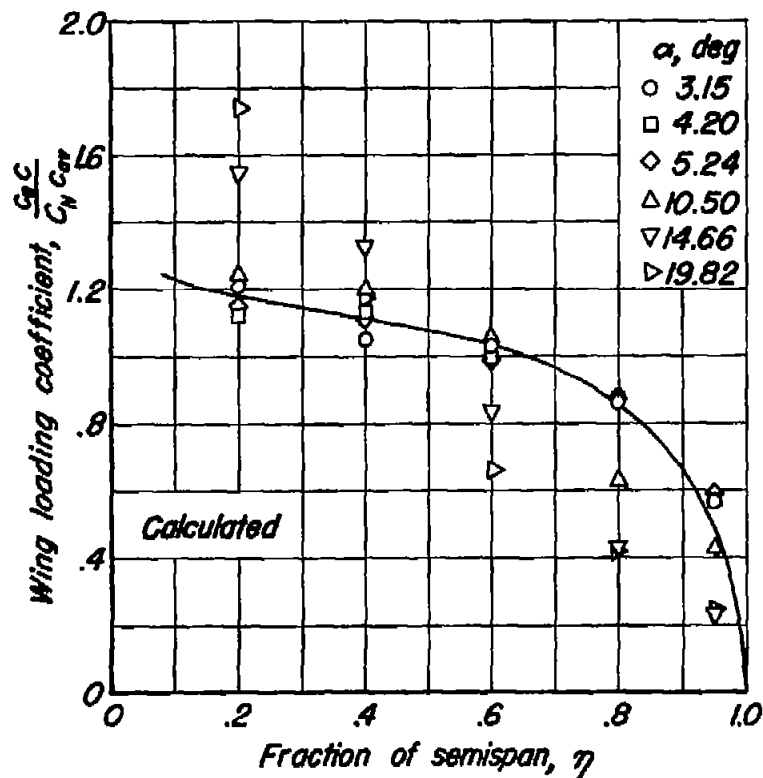
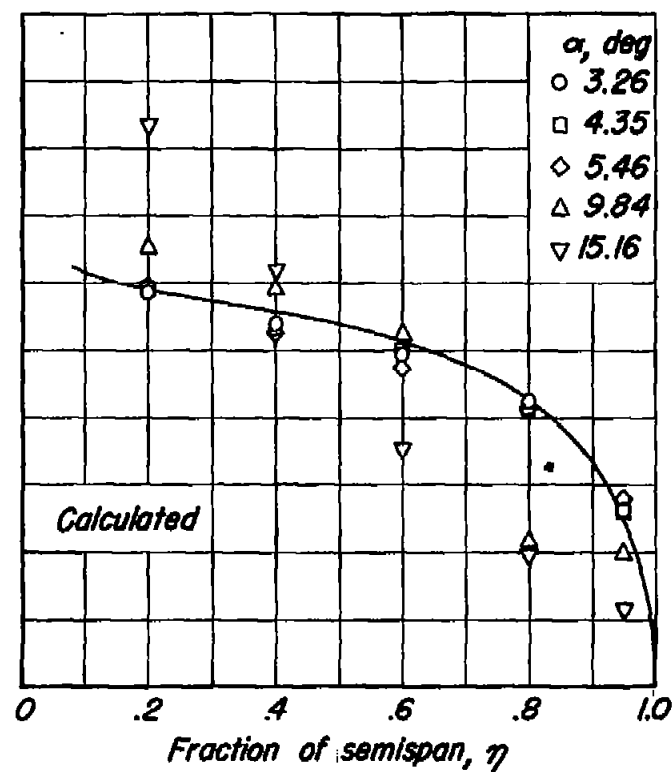
(a) $M = 0.50$ (b) $M = 0.70$

Figure 14.- Comparison between the experimental and calculated wing loading coefficients.

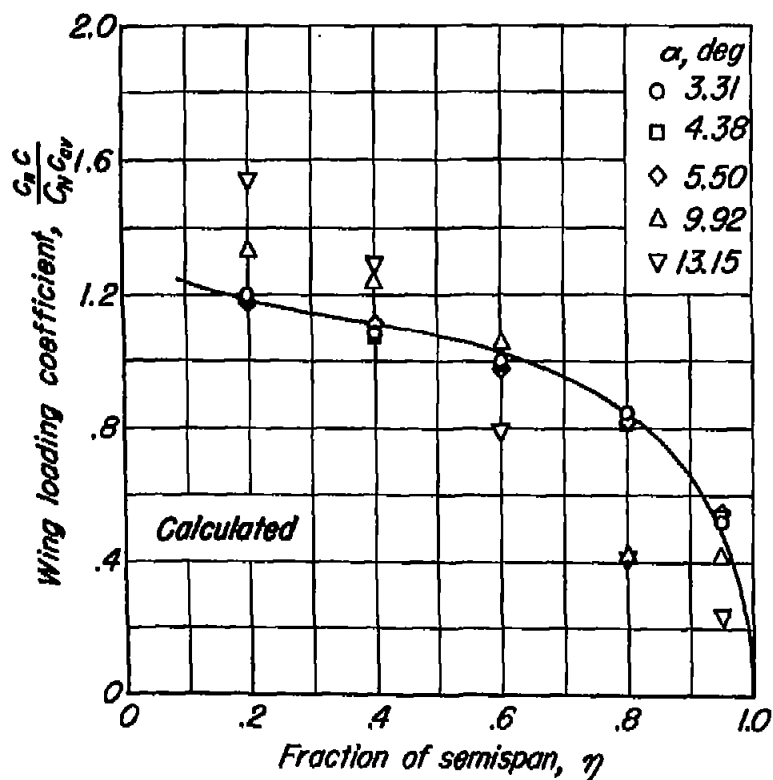
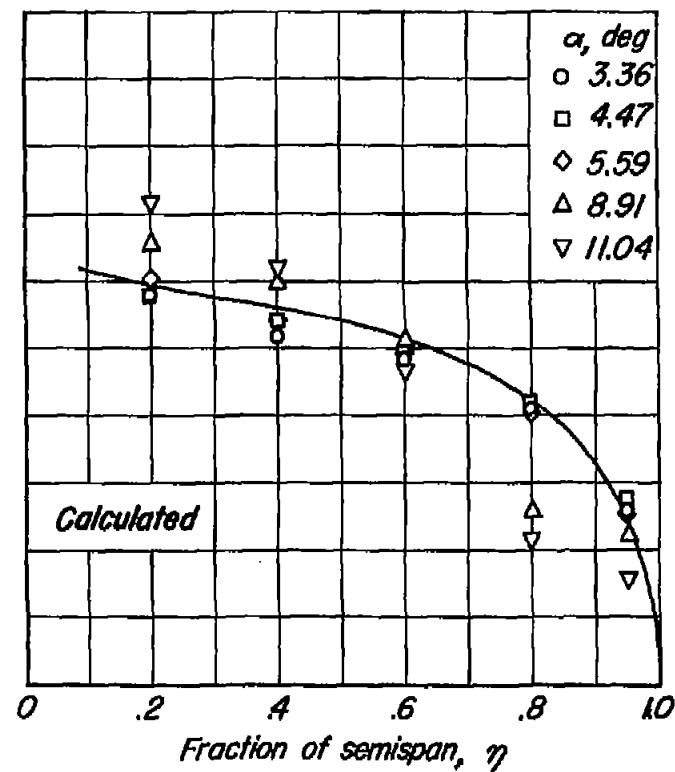
(c) $M = 0.75$ (d) $M = 0.80$

Figure 14.- Continued.

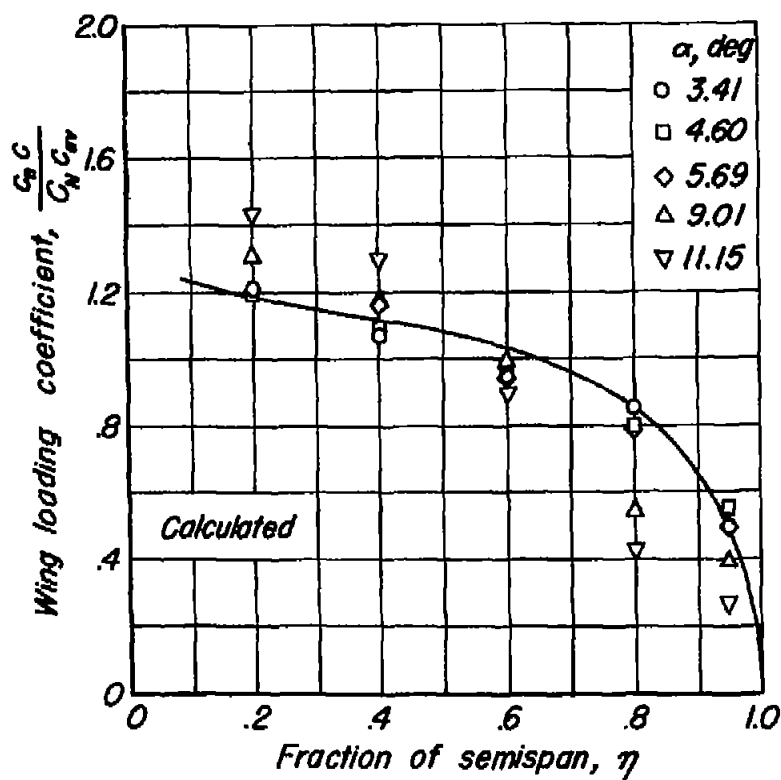
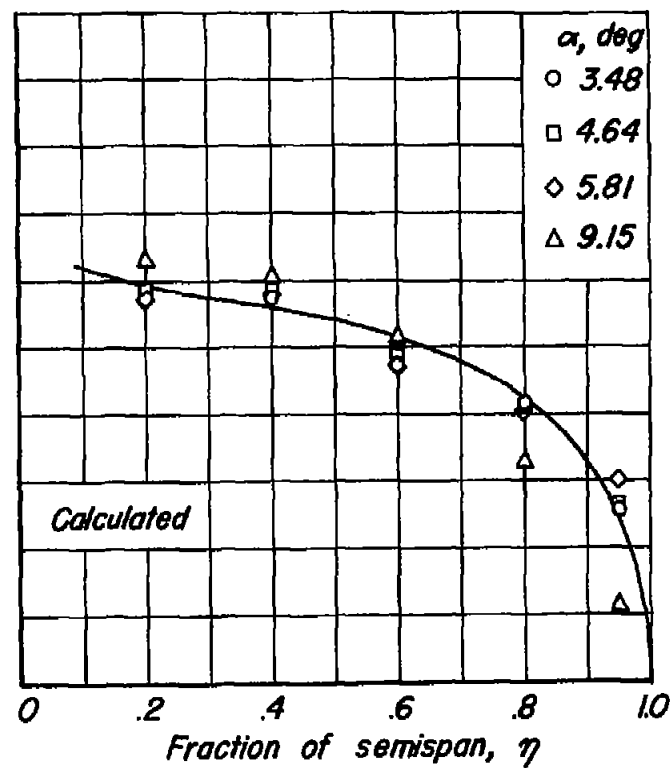
(e) $M = 0.85$ (f) $M = 0.90$

Figure 14.- Continued.

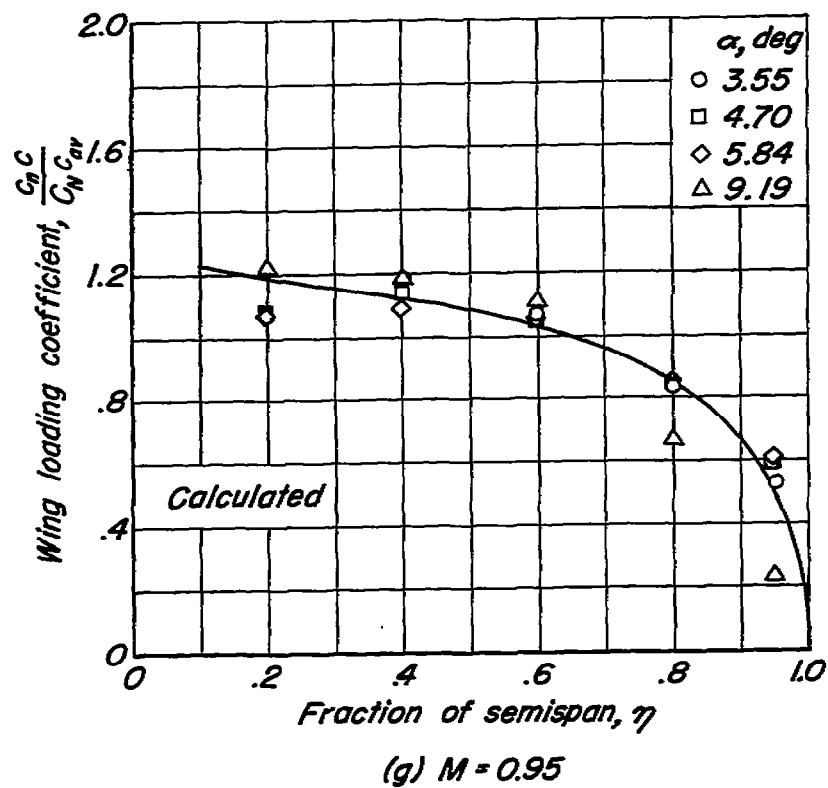
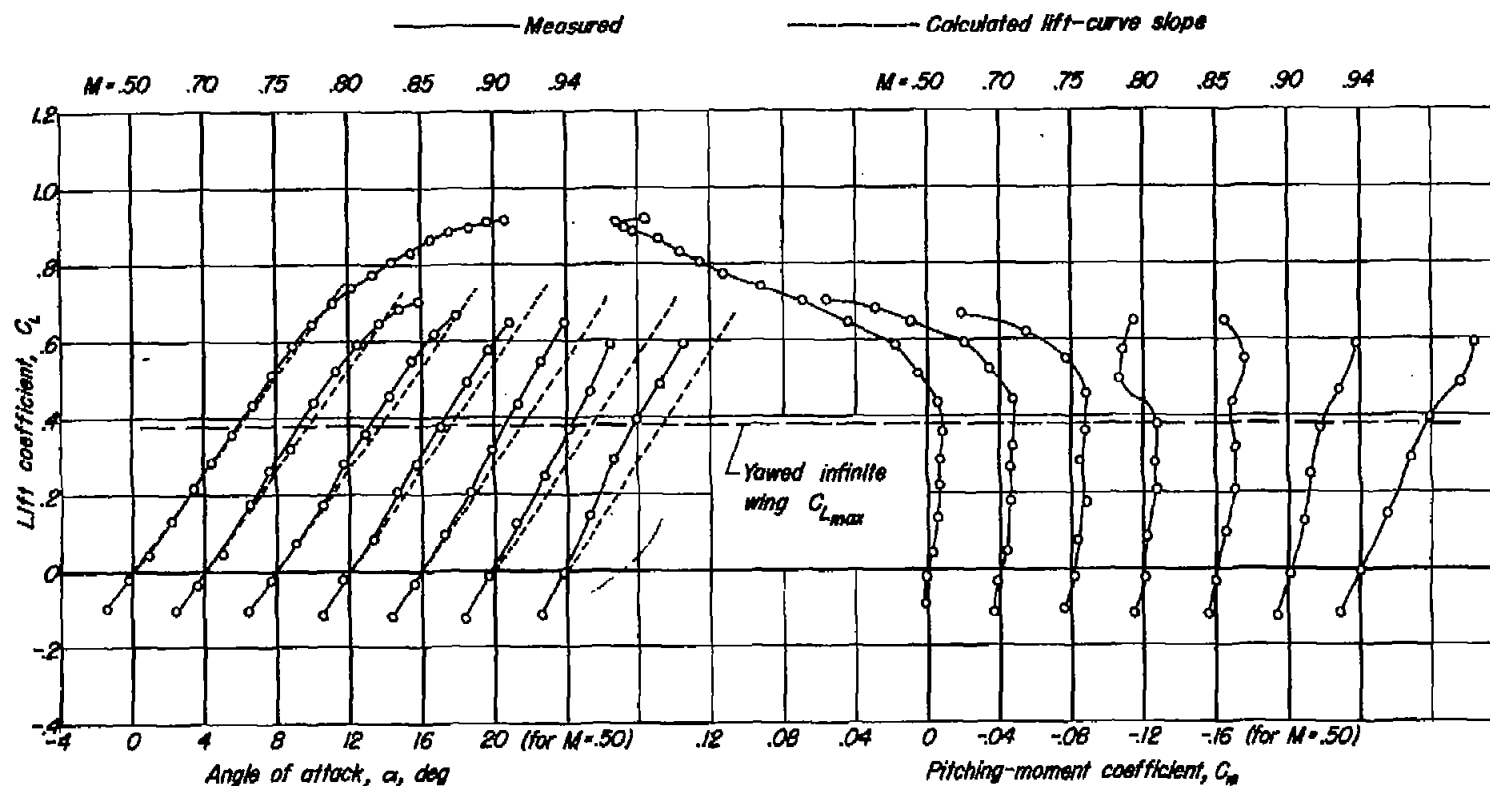


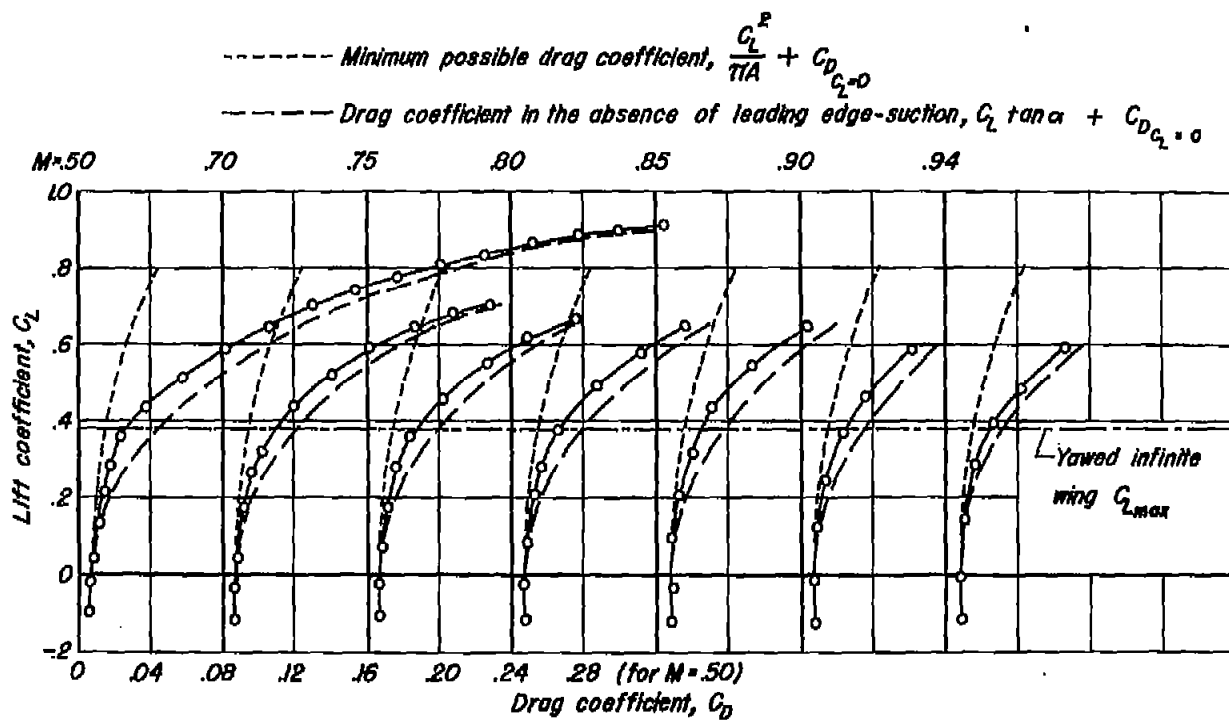
Figure 14.- Concluded.

CONFIDENTIAL



(a) Lift and pitching-moment characteristics.

Figure 15.- Aerodynamic characteristics of the wing-body combination from force-test measurements.



(b) Drag characteristics.
 Figure 15- Concluded.

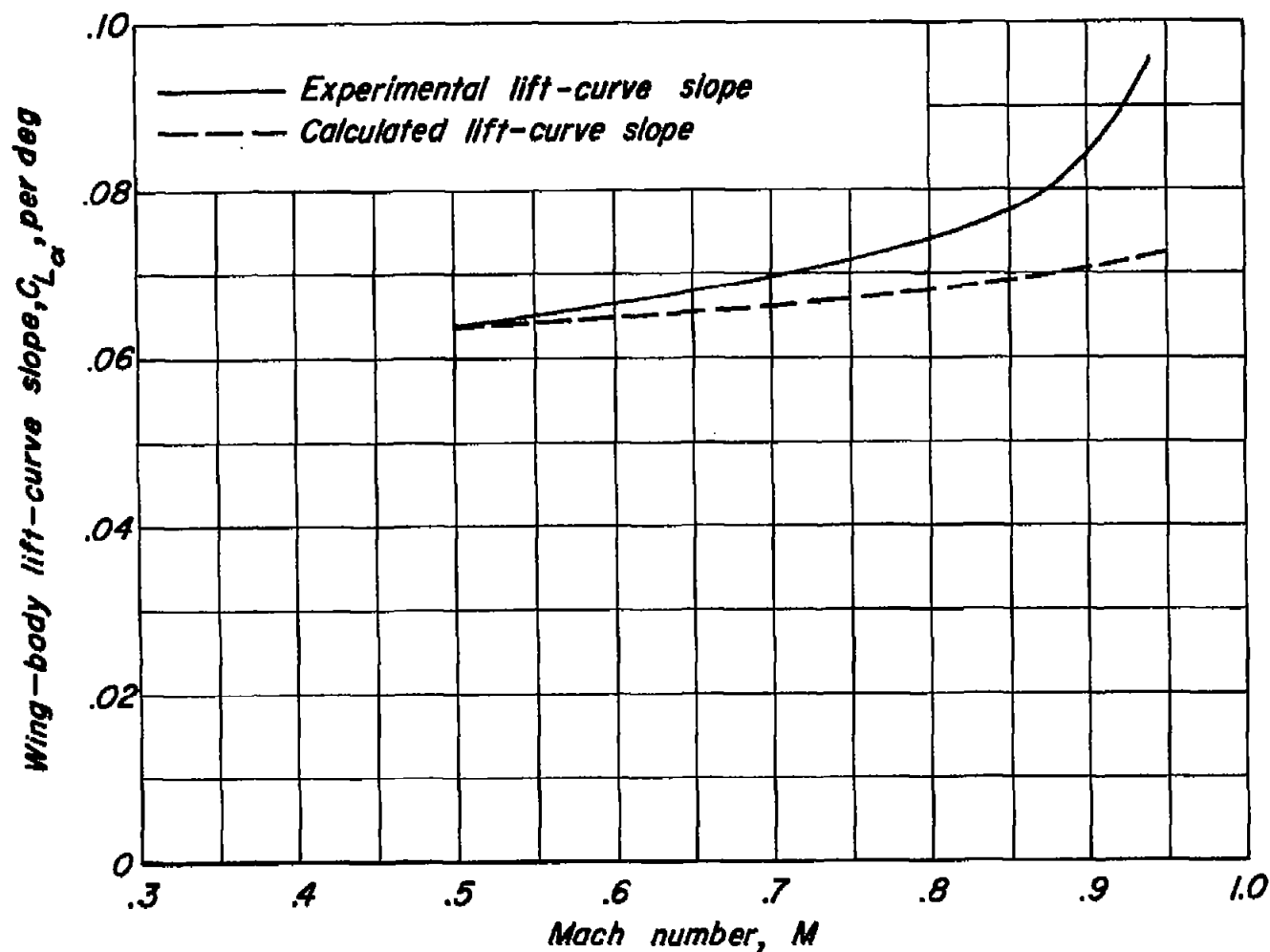


Figure 16.— Comparison of the variations with Mach number of the experimental lift-curve slope for the wing-body combination with the calculated lift-curve slope; $C_L=0$.

~~CONFIDENTIAL~~

